wbk Institute of Production Science

KIT Karlsruhe Institute of Technology

Symposium **Mechanical Surface Treatment 2019**

8th Workshop Machine Hammer Peening

Karlsruhe

22 and 23 October 2019

Symposium Mechanical Surface Treatment 2019

8th Workshop Machine Hammer Peening

22 and 23 October 2019, Karlsruhe

DOI: 10.5445/IR/1000099108

Contact

Prof. Dr.-Ing. habil. Volker Schulze
Director of Manufacturing and Materials Technology
wbk Institute of Production Science
Phone: +49 721 608-42440
Volker.Schulze@kit.edu

Publisher

wbk Institute of Production Science
Karlsruhe Institute of Technology
www.wbk.kit.edu

Authors

Prof. Dr.-Ing. habil. Volker Schulze
Dr.-Ing. Michael Gerstenmeyer
Patrick Neuenfeldt, M.Sc.

Preface

Dear colleagues,
ladies and gentlemen,

on behalf of the entire wbk Institute of Production Science, I would like to welcome you to this year's eights edition of the Machine Hammer Peening workshop in Karlsruhe. Launched in 2012 as the "Fachforum Festklopfen" in Darmstadt, the workshop, which alternates annually between the universities of Darmstadt, Vienna, Karlsruhe and Aachen, is enjoying increasing popularity.

At the same time this workshop is the 63rd meeting of the Working Group Mechanical Surface Treatments of the Deutsche Gesellschaft für Materialkunde (DGM). The group meets twice a year at German industrial and academic sites and discusses new aspects of all mechanical surface treatments starting with the technologies via the resulting surface states up to the improvements in the performance of the treated components in application.

Therefore the actual meeting is a kind of an experiment to bring together complementary but mutually interested groups from manufacturing technology and materials technology. This will enhance discussions which can be driven from both disciplines or viewpoints which have aims in common.

We are convinced that the technologies of mechanical surface treatments and especially the still new variants in the field of machine hammer peening have enormous potential in the field of finishing highly loaded machine components and tools and will continue to gain in importance in the future. The interaction of the DGM-group Mechanical Surface treatments running since a long time and the workshop Machine Hammer peening participants joins two really active groups and hopefully will glue.

With this in mind, I wish you an exciting and interesting workshop with many stimulating discussions.

Karlsruhe, 22 October 2019

Prof. Dr.-Ing. habil. Volker Schulze

Machine Hammer Peening (MHP)

Facing recent challenges

In the course of current and future technological and social trends, new fields of application are opening up for the MHP. In addition to shortening throughput in production, the MHP promises an improvement in the service life of dynamically highly stressed components and an increase in tool life. This results in an increase in productivity while simultaneously reducing costs. In addition, the MHP will gain in importance in the future in the field of finishing of additively manufactured components.

WMHP – An innovative exchange platform

The workshop focuses on the personal exchange and discussion between speakers, participants and scientists about research results, technology developments and successful applications. In addition, the workshop offers the opportunity to identify previously untapped potential of the MHP and to make it tangible for future research due to the bundling of competencies of different specialist areas.

To master machine hammer peening

By bringing together different technical expertise, the technologically complex interactions in machine hammer peening can be researched and discussed at the highest level. This enables sound scientific research under industrial boundary conditions.

DGM Technical Committee – Mechanical Surface Treatments

Mechanical surface treatments as shot peening and deep rolling are important procedures to work hardening of surface areas and to induce compressive residual stresses. Mostly the aim is the improvement of fatigue properties, wear resistance or corrosion resistance of components of mechanical engineering, automotive and aviation. Alternative processes as ultrasonic, laser or cavitation peening including modifications using prestressing or thermal treatments are also included in the committees work. The committee meets every half year at an industrial member or at university institutes.

Aims of the DGM Technical Committee

- Covering industrial and scientific topics in the area of mechanical surface treatments with the focus on the improvement of component properties and the further development of the processes
- Working on a science-based knowledge of correlations of process parameters of mechanical surface treatments, component states and component properties
- Initiating of research and development projects: Joint projects of universities, research institutes and industry
- Exchange of experiences between teams working in the field of mechanical surface treatments, and networking

Workshop History

Darmstadt, 11 October 2012

- Foundation event “Fachforum Festklopfen” (FFF)
- 15 participants

Vienna, 16 October 2013

- Continuation as Workshop Machine Hammer Peening (WMHP)
- First draft of terminology for MHP
- Development of a Wikipedia entry for MHP
- 23 participants

Aachen, 28 November 2014

- 3rd Workshop Machine Hammer Peening
- Revised terminology
- 30 participants

Karlsruhe, 24 November 2015

- 4th Workshop Machine Hammer Peening
- VDI guideline for MHP for a uniform nomenclature
- 36 participants

Darmstadt, 03 November 2016

- 5th Workshop Machine Hammer Peening
- Wikipedia entry for MHP online available
- Joint CIRP paper
- 43 participants

Vienna, 22 November 2017

- 6th Workshop Machine Hammer Peening
- 43 participants

Aachen, 12 and 13 November 2018

- 7th Workshop Machine Hammer Peening
- 29 participants

Lecture programme

Reception **1**

Prozesssicherheit bei der mechanischen Oberflächenbearbeitung **7**

FE Simulation of the HFMI Treatment – Previous and Upcoming Results **20**

Influence of mechanical surface treatments on propagation and opening behavior of physically short cracks in Inconel 718 **35**

Controlled Pneumatic Needle Peening – New Peening Technology for Aerospace Applications **49**

Experimental analysis of the surface integrity of stainless steel modified by robot based machine hammer peening **65**

Analyses of technical and true overlap in hammer peening operations **76**

Influence of the process parameters on the penetration behaviour of ceramic particles in Composite Peening **85**

Residual stress relaxation in HFMI-treated fillet welds after single overload peaks **100**

Interne Verfestigungsdomänen durch mechanische Oberflächenbehandlung während der additiven Fertigung **109**

Influence of MHP on the material structure of CrNi steels **122**

Influence of the hammer head geometry when machining higher strength materials by MHP **135**

Optimization of the stream finishing process for mechanical surface treatment by numerical and experimental process analysis **138**

Reception

Prof. Dr.-Ing. habil. Volker Schulze

wbk Institute of Production Science

Karlsruhe Institute of Technology


Karlsruhe Institute of Technology
wbk
Institute of Production Science
wbk INSTITUTE OF PRODUCTION SCIENCE
Karlsruhe, October 22th 2019
KIT – The Research University in the Helmholtz Association
www.wbk.kit.edu

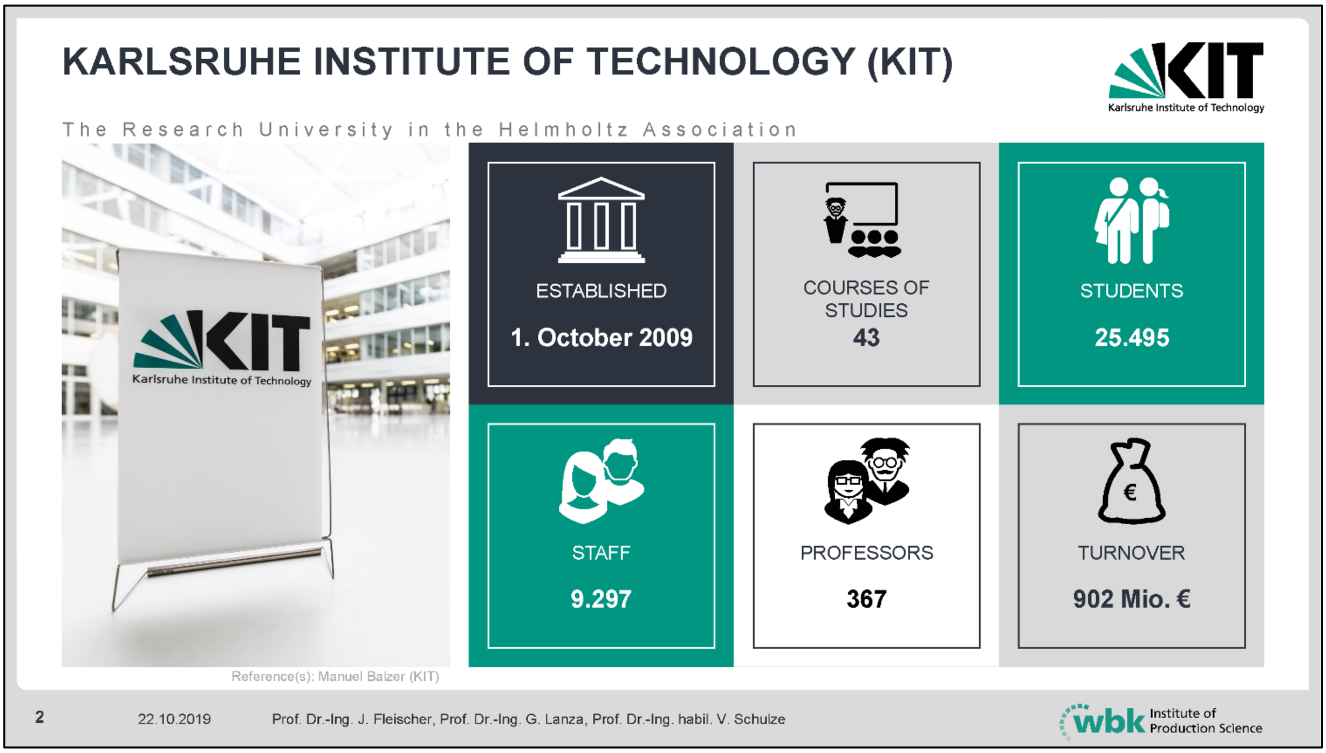
KARLSRUHE INSTITUTE OF TECHNOLOGY (KIT)
Karlsruhe Institute of Technology
The Research University in the Helmholtz Association
ESTABLISHED
1. October 2009
COURSES OF STUDIES
43
STUDENTS
25.495
STAFF
9.297
PROFESSORS
367
TURNOVER
902 Mio. €
Reference(s): Manuel Balzer (KIT)
2
22.10.2019
Prof. Dr.-Ing. J. Fleischer, Prof. Dr.-Ing. G. Lanza, Prof. Dr.-Ing. habil. V. Schulze
wbk Institute of Production Science


LOCATIONS
Institute of Production Science
Karlsruhe Institute of Technology
Ehrenhof Karlsruhe Germany
Manufacturing and materials technology
Campus Nord Eggenstein-Leopoldshafen Germany
Machines, equipment and process automation
Shanghai China
AMTC - Advanced Manufacturing Technology Center
Fasanengarten Karlsruhe Germany
Production systems Machines, equipment and process automation
Material Research Center for Energy Systems Karlsruhe Germany
Manufacturing and materials technology
Suzhou China
GAMI - Global Advanced Manufacturing Institute
3
22.10.2019
Prof. Dr.-Ing. J. Fleischer, Prof. Dr.-Ing. G. Lanza, Prof. Dr.-Ing. habil. V. Schulze
wbk Institute of Production Science

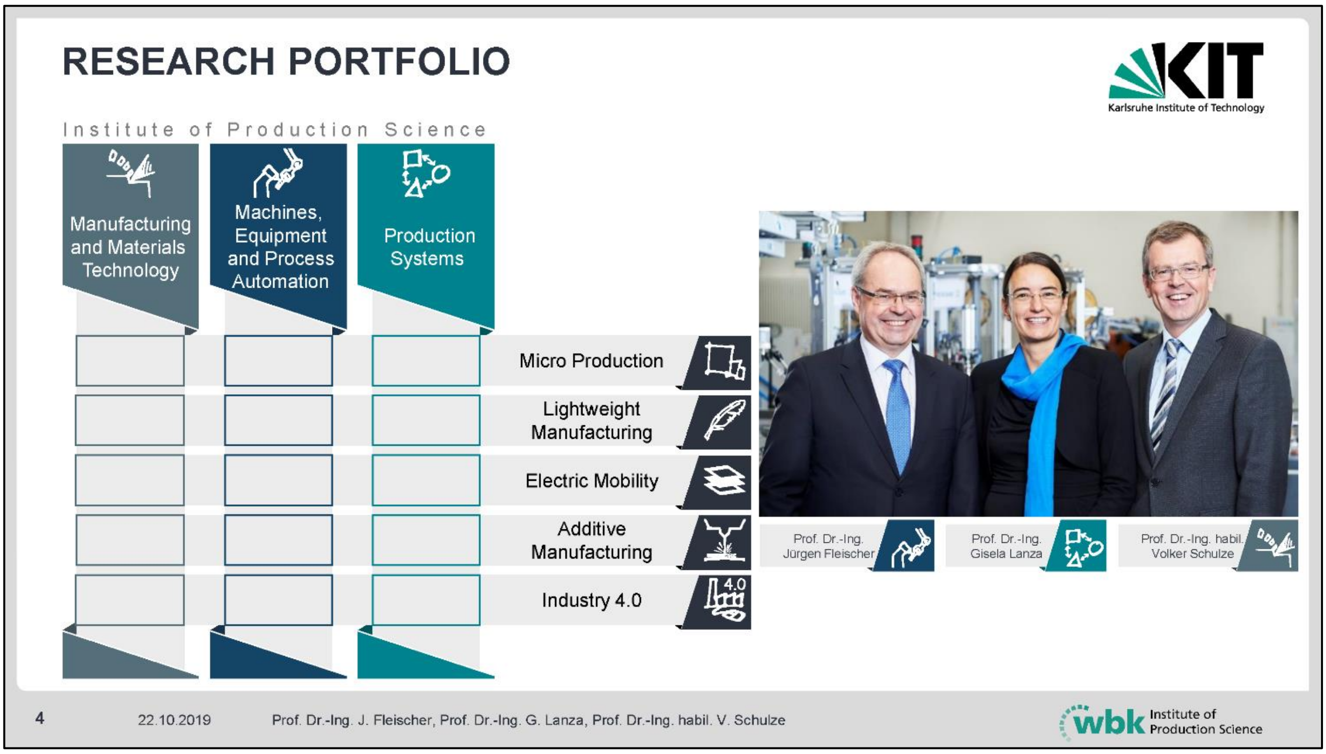
RESEARCH PORTFOLIO
Institute of Production Science
Karlsruhe Institute of Technology
Manufacturing and Materials Technology
Machines, Equipment and Process Automation
Production Systems
Micro Production
Lightweight Manufacturing
Electric Mobility
Additive Manufacturing
Industry 4.0
Prof. Dr.-Ing. Jürgen Fleischer
Prof. Dr.-Ing. Gisela Lanza
Prof. Dr.-Ing. habil. Volker Schulze
4
22.10.2019
Prof. Dr.-Ing. J. Fleischer, Prof. Dr.-Ing. G. Lanza, Prof. Dr.-Ing. habil. V. Schulze
wbk Institute of Production Science

MANUFACTURING AND MATERIALS TECHNOLOGY

Karlsruhe Institute of Technology

PRECISION MACHINING

- Turning, drilling, milling
- Stream Finishing
- Combined processes for process chain consolidation
- μ laser ablation und μ milling
- Simulation of manufacturing processes (chip formation, cooling strategies, particle flow)
- Surface Engineering: Load-adapted adjustment of surface layer conditions through optimized process control

GEAR ENGINEERING

- Soft- und hard machining for skiving
- Whirling and special processes for thread production and polygonal manufacturing
- Special kinematics for precision gearing
- Control of the process chain during broaching
- Optimized cooling lubricant strategy
- Kinematics simulation for die design and for analyzing local parameters

ADDITIVE MANUFACTURING

- Analysis and optimization of additive manufacturing processes
- Laser Beam Melting (LBM)
- Lithography-based Ceramic Manufacturing (LCM)
- Development of metal powders for high-performance components
- Chipping and mechanical surface treatment of additive manufactured parts
- Multi-material processing
- Digital process chain analysis

5 22.10.2019 Prof. Dr.-Ing. J. Fleischer, Prof. Dr.-Ing. G. Lanza, Prof. Dr.-Ing. habil. V. Schulze

wbk Institute of Production Science

MACHINES, EQUIPMENT AND PROCESS AUTOMATION

Karlsruhe Institute of Technology

MACHINE TOOLS AND MECHATRONICS

- Intelligent mechatronic components for production machines
- Condition Monitoring and predictive maintenance
- Simulation and optimization of machines and components

LIGHTWEIGHT MANUFACTURING

- Development of innovative, hybrid manufacturing processes
- Joining technologies for hybrid parts
- Intelligent tools for fibre composite manufacturing
- Intelligent, sensor based gripping technologies
- Flexible, robot based manufacturing processes for lightweight construction applications

ELECTRIC MOBILITY

- Gripping, handling and mounting systems for battery cell, -module, electric motor and fuel cells
- Process and Prototype development, simulation and evaluation of immature manufacturing processes
- Process control and optimization for energy storage and electric motor production

6 22.10.2019 Prof. Dr.-Ing. J. Fleischer, Prof. Dr.-Ing. G. Lanza, Prof. Dr.-Ing. habil. V. Schulze

wbk Institute of Production Science

PRODUCTION SYSTEMS

Karlsruhe Institute of Technology

GLOBAL PRODUCTION STRATEGIES

- Strategic planning of production networks
- Site-specific production using Industry 4.0
- Information and quality management in supply chain networks
- Order-based production and logistics planning in networks

PRODUCTION SYSTEM PLANNING

- Adaptive production systems
- Industry 4.0 methods
- Digitalization strategies
- Machine learning and data mining
- Agile factory planning
- Robust, intelligent production control
- Cost evaluation and simulative validation
- Technology planning

QUALITY ASSURANCE

- In-line measurement technology for immature processes
- Soft sensors for intelligent data analysis
- Function-oriented measurements
- Autonomous measurement technology
- Measurement uncertainty evaluation
- Process control based on quality data

7 22.10.2019 Prof. Dr.-Ing. J. Fleischer, Prof. Dr.-Ing. G. Lanza, Prof. Dr.-Ing. habil. V. Schulze

wbk Institute of Production Science

GAMI

Karlsruhe Institute of Technology

Global Advanced Manufacturing Institute

The Global Advanced Manufacturing Institute (GAMI) tries to deepen the understanding of global production structures according to the three KIT pillars research, innovation and teaching and to develop new, robust and controlled production networks for industrial enterprises for the local framework conditions.

FOUNDED	LOCATION	ENGINEERS	ADMINISTRATION	STUDENTS
2008	Suzhou	20	4	5

Global Advanced Manufacturing Institute

Applied Research	Industry Consulting for German Firms	Continuing Education / Training / Coaching

8 22.10.2019 Prof. Dr.-Ing. J. Fleischer, Prof. Dr.-Ing. G. Lanza, Prof. Dr.-Ing. habil. V. Schulze

wbk Institute of Production Science


AMTC
Karlsruhe Institute of Technology
Advanced Manufacturing Technology Center
Founded as a cooperation of the Chinese-German University College (CDHK) with the wbk (KIT) and the College of Mechanical Engineering (Tongji University), the AMTC offers practical education and training for engineers working in China in production engineering, contract research and development for manufacturing companies in China as well as basic research in the field of automated manufacturing.
FOUNDED 2012
LOCATION Shanghai
ENGINEERS 3
ADMINISTRATION 4
STUDENTS 20
Advanced Manufacturing Technology Center
Education
Research
Technological Exchange
9
22.10.2019
Prof. Dr.-Ing. J. Fleischer, Prof. Dr.-Ing. G. Lanza, Prof. Dr.-Ing. habil. V. Schulze
wbk Institute of Production Science

Prozesssicherheit bei der mechanischen Oberflächenbearbeitung

Dr.-Ing. Oliver Maiß

Alfred Ostertag

Ecoroll AG Werkzeugtechnik


ECOROLL
Prozesssicherheit bei der mechanischen Oberflächenbearbeitung
Systeme der Prozessüberwachung beim Walzen und Hämmern
Dr.-Ing. Oliver Maiß, Alfred Ostertag
Karlsruhe, 22.10.2019
www.ecoroll.de

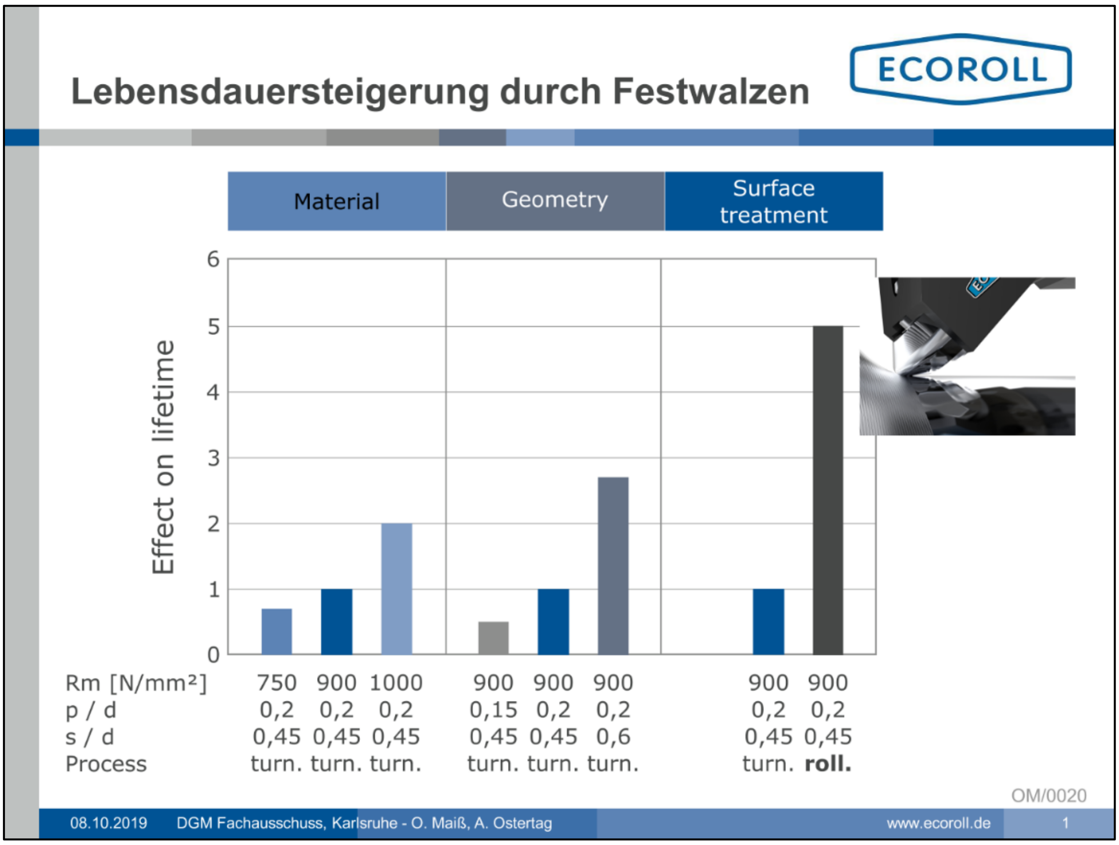
Lebensdauersteigerung durch Festwalzen
ECOROLL
Material
Geometry
Surface treatment
Effect on lifetime
0
1
2
3
4
5
6
Rm [N/mm²] 750 900 1000 900 900 900 900 900
p / d 0,2 0,2 0,2 0,15 0,2 0,2 0,2 0,2
s / d 0,45 0,45 0,45 0,45 0,45 0,6 0,45 0,45
Process turn. turn. turn. turn. turn. turn. turn. roll.
OM/0020
08.10.2019 DGM Fachausschuss, Karlsruhe - O. Maiß, A. Ostertag
www.ecoroll.de
1


Effekte des Glatt- und Festwalzens
ECOROLL
Oberfläche
Mikrostruktur
Textur
Härte
Eigen-
spannungen
Randzone
Eigenspannungen sind Spannungen im inneren eines Bauteils, die auch vorliegen, wenn keine äußeren Kräfte, Momente oder Temperaturgradienten anliegen.
OM/0031
08.10.2019
DGM Fachausschuss, Karlsruhe - O. Maiß, A. Ostertag
www.ecoroll.de
2


Motivation
ECOROLL
Prozess zur Festlegung von „richtigen“ Prozesseinstellgrößen:
Versuche
ESP-
Messung
Lebens-
dauertests
Parameter-
Freeze
Lebensdauertest nicht ausreichend
Wie kann die Eigenspannung in der QS erfasst werden?
08.10.2019
DGM Fachausschuss, Karlsruhe - O. Maiß, A. Ostertag
www.ecoroll.de
3


Agenda
ECOROLL
3
Überwachung der Schlagenergie beim MHP
2
Prozessüberwachung beim Walzen mit hydrostatischen Walzwerkzeugen
1
Digitale Walzkraftmessung für mechanische Walzwerkzeuge
08.10.2019
DGM Fachausschuss, Karlsruhe - O. Maiß, A. Ostertag
www.ecoroll.de
4


Agenda
ECOROLL
3
Überwachung der Schlagenergie beim MHP
2
Prozessüberwachung beim Walzen mit hydrostatischen Walzwerkzeugen
1
Digitale Walzkraftmessung für mechanische Walzwerkzeuge
08.10.2019
DGM Fachausschuss, Karlsruhe - O. Maiß, A. Ostertag
www.ecoroll.de
5

Bestimmung der Walzkraft im Prozess

ECOROLL

Originalbetriebsanleitung
Betriebsanleitung Nr. 171001/2
Einrollen-Glattwalzwerkzeug EG5-40M

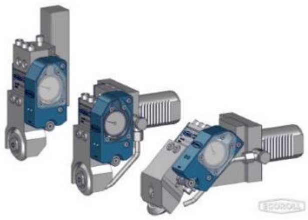

Das ECOROLL Einrollen Glattwalzwerkzeug EG5-40M entspricht dem Stand der Technik und den anerkannten sicherheitstechnischen Regeln. Dennoch können bei seiner Verwendung Gefahren für Leib und Leben des Benutzers oder Dritter bzw. Beeinträchtigungen des Werkzeugs und anderer Sachwerte entstehen.

Werkzeug nur in technisch einwandfreiem Zustand sowie bestimmungsgemäß, sicherheits- und gefahrenbewusst unter Beachtung der Betriebsanleitung benutzen! Insbesondere Störungen, die die Sicherheit beeinträchtigen können, umgehend beseitigen!

Werkzeuge nur mit Original ECOROLL Teilen oder von ECOROLL zugelassenen Teilen verwenden! Bei Missachtung kann es zum Erlöschen der Herstellergarantie kommen.

ECOROLL AG Werkzeugtechnik
Postfach 31 42, D-29231 Celle
Hans-Heinrich-Warnke-Straße 8, D-29227 Celle
Tel. +49 5141 9865-0
Fax +49 5141 881440
Web www.ecoroll.de
E-Mail mail@ecoroll.de

ECOROLL Corporation Tool Technology
502 Techne Center Drive Suite C
Milford, OH 45150
USA
Tel +1 513 248 4700
Fax +1 513 248 4265
Web www.ecoroll.com
Email mail@ecoroll.com

Betriebsanleitung Nr. 171001/2 EG5-40M | © ECOROLL AG/ECOROLL Corp. Technische Änderungen vorbehalten | Druckdatum: 26.04.2019 Erstellt am: 01.03.2002 Seite 1/22

ECOROLL

Fehler! Verweisquelle konnte nicht gefunden werden. zeigt die mittelbaren Maße für die Glattwalzkraft, die aus Tabelle 1 in Abhängigkeit vom Werkstückdurchmesser und der Werkstofffestigkeit entnommen wurden. Die Federcharakteristik wurde für ein spezifisches EG5-40M-Werkzeug gemessen, für andere Werkzeuge können die Werte bis zu ± 20% abweichen.

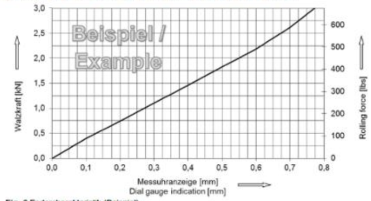

Fig. 6 Federcharakteristik (Beispiel)

Falls erforderlich, können zur Optimierung des Walzergebnisses folgende Parameter verändert werden:

Rautiefe verringern	Rautiefe erhöhen
• Vorspannung erhöhen • Vorschub verringern • Zweiten Durchgang mit gleicher Einstellung walzen	• Vorspannung reduzieren • Vorschub erhöhen • Drehzahl erhöhen

Tabelle 2 Optimierung des Walzergebnisses

Die Maßnahmen zur Erhöhung der Rautiefe bis zum zul... wünschte Restrautiefe als auch Zeiteinsparungen ...

Federkennlinie in Betriebsanleitung

Betriebsanleitung Nr. 171001/2 EG5-40M | © ECOROLL AG/ECOROLL Corp. Technische Änderungen vorbehalten | Druckdatum: 26.04.2019 Erstellt am: 01.03.2002 Seite 10/22

08.10.2019 DGM Fachausschuss, Karlsruhe - O. Maiß, A. Ostertag www.ecoroll.de 7

Prozessfehler bei mechanischen Walzwerkzeugen

ECOROLL

- Zustellfehler beim Walzen
- Veränderung der Federkonstanten durch Kollision
- Geometrieabweichung bei Vorbearbeitung
- Zerspanwerkzeug fehlerhaft eingemessen

08.10.2019 DGM Fachausschuss, Karlsruhe - O. Maiß, A. Ostertag www.ecoroll.de 8

Digitale Messuhr

ECOROLL

EMO Hannover 16-21·9·2019

08.10.2019 DGM Fachausschuss, Karlsruhe - O. Maiß, A. Ostertag www.ecoroll.de 9

Agenda

ECOROLL

3 **Überwachung der Schlagenergie beim MHP**

2 **Prozessüberwachung beim Walzen mit hydrostatischen Walzwerkzeugen**

1 **Digitale Walzkraftmessung für mechanische Walzwerkzeuge**

08.10.2019 DGM Fachausschuss, Karlsruhe - O. Maiß, A. Ostertag www.ecoroll.de 10

Verfahren - 3D-Walzen von Freiformflächen

ECOROLL

Das Nachführsystem der HG-Werkzeuge ermöglicht das Glatt- und Festwalzen von Freiformflächen

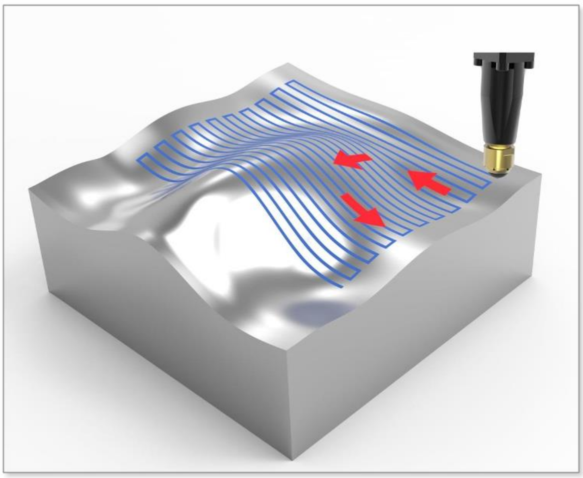

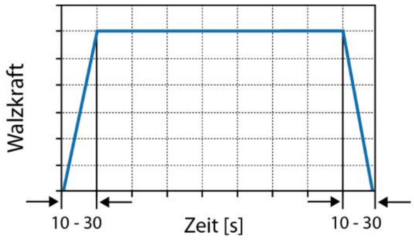

08.10.2019 DGM Fachausschuss, Karlsruhe - O. Maiß, A. Ostertag www.ecoroll.de 11

Hydrostatisch gelagerte Werkzeuge

ECOROLL

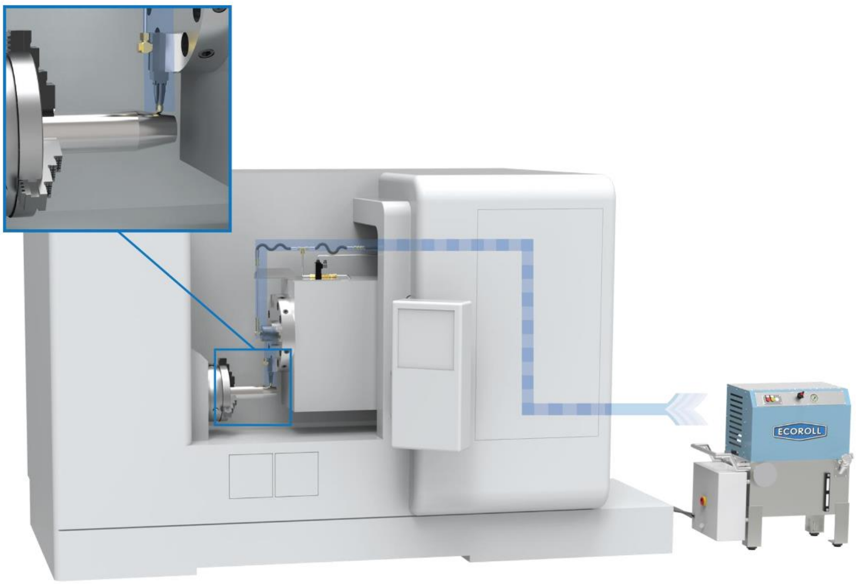

08.10.2019 DGM Fachausschuss, Karlsruhe - O. Maiß, A. Ostertag www.ecoroll.de 12

Prozessfehler beim Walzen mit hydrostatischen Werkzeugen

ECOROLL

- Drossel verstopft
- Druckeinstellung durch Bediener fehlerhaft
- Aggregat ist defekt

08.10.2019 DGM Fachausschuss, Karlsruhe - O. Maiß, A. Ostertag www.ecoroll.de 13

Prozessüberwachung mit ToolScope

ECOROLL

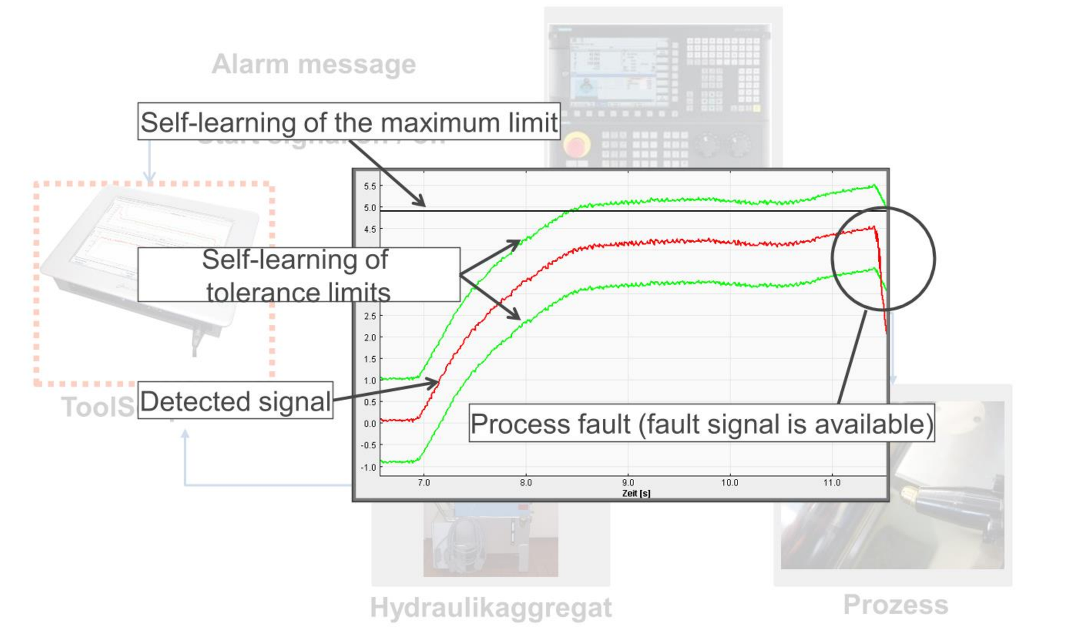

08.10.2019 DGM Fachausschuss, Karlsruhe - O. Maiß, A. Ostertag www.ecoroll.de 14

Agenda

ECOROLL

3 Überwachung der Schlagenergie beim MHP

2 Prozessüberwachung beim Walzen mit hydrostatischen Walzwerkzeugen

1 Digitale Walzkraftmessung für mechanische Walzwerkzeuge

08.10.2019 DGM Fachausschuss, Karlsruhe - O. Maiß, A. Ostertag www.ecoroll.de 15

Analyse des Schlagvorganges

ECOROLL

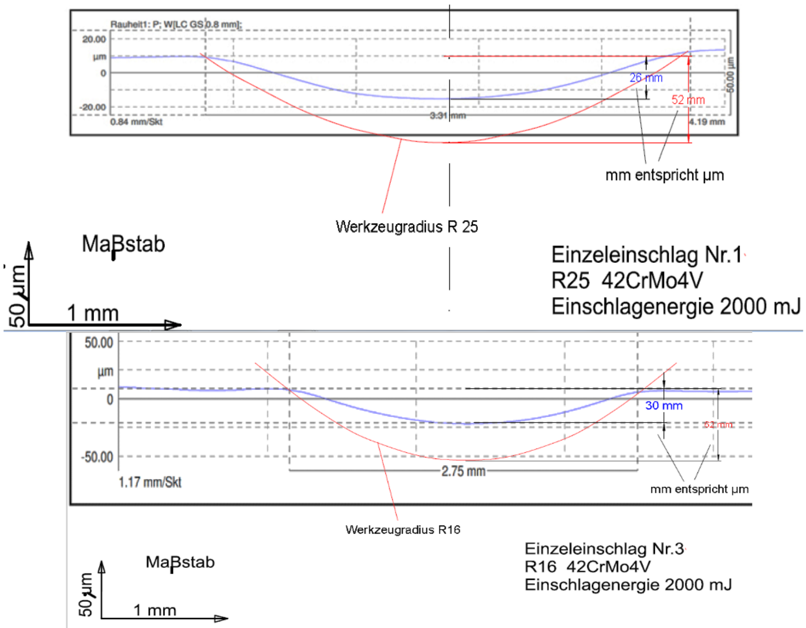

Einzeleinschlag Nr.1
R25 42CrMo4V
Einschlagenergie 2000 mJ

Einzeleinschlag Nr.3
R16 42CrMo4V
Einschlagenergie 2000 mJ

08.10.2019 DGM Fachausschuss, Karlsruhe - O. Maiß, A. Ostertag www.ecoroll.de 16

Hämmerwerkzeuge ECOpeen (Konzept)

ECOROLL

Schlagsystem:
Mechanisch-pneumatisch,
Bekannt aus marktgängigen Bohrhämmern
Rückstoßfrei!

Rückhub

Schlag

08.10.2019 DGM Fachausschuss, Karlsruhe - O. Maiß, A. Ostertag www.ecoroll.de 17

Schlagenergie - Schlagkraft

ECOROLL

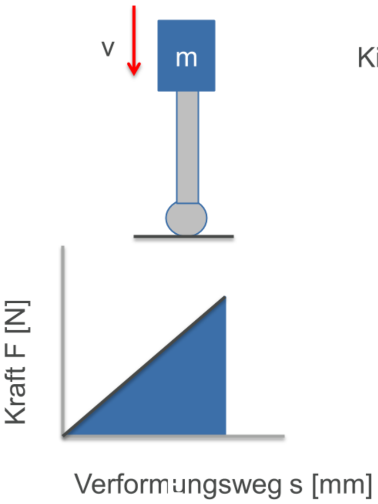

Kinetische Energie (Schlagenergie)

$$E_{kin} = \frac{1}{2}\, m\, v^2$$

Umformenergie

$$E_U = \frac{1}{2} F\, s$$

Schlagkraft

$$F = \frac{2EU}{s}$$

Schlussfolgerung:
- Schlagkraft ist abhängig von Schlagenergie und Verformungsweg.
- Ist als Leistungsangabe von Hämmerwerkzeugen ungeeignet.

www.ecoroll.de

Schlagenergie – Kennfeld ECOpeen A

ECOROLL

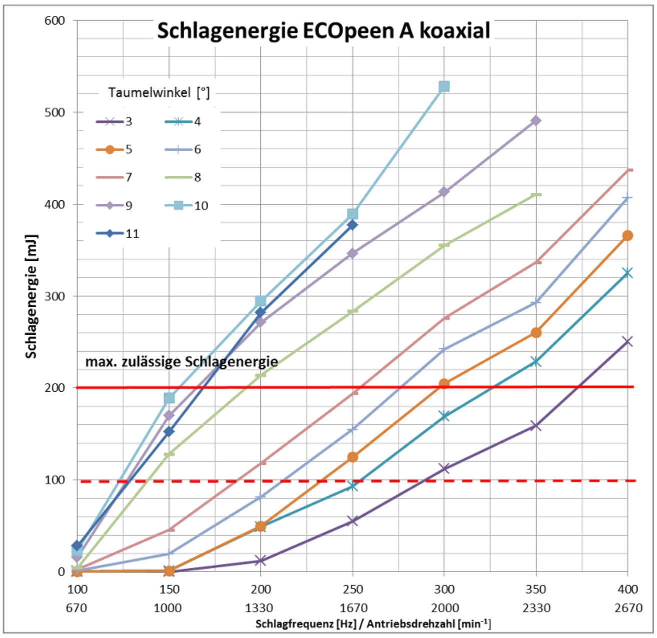

08.10.2019 DGM Fachausschuss, Karlsruhe - O. Maiß, A. Ostertag www.ecoroll.de 19

Steuerung der Schlagenergie

ECOROLL

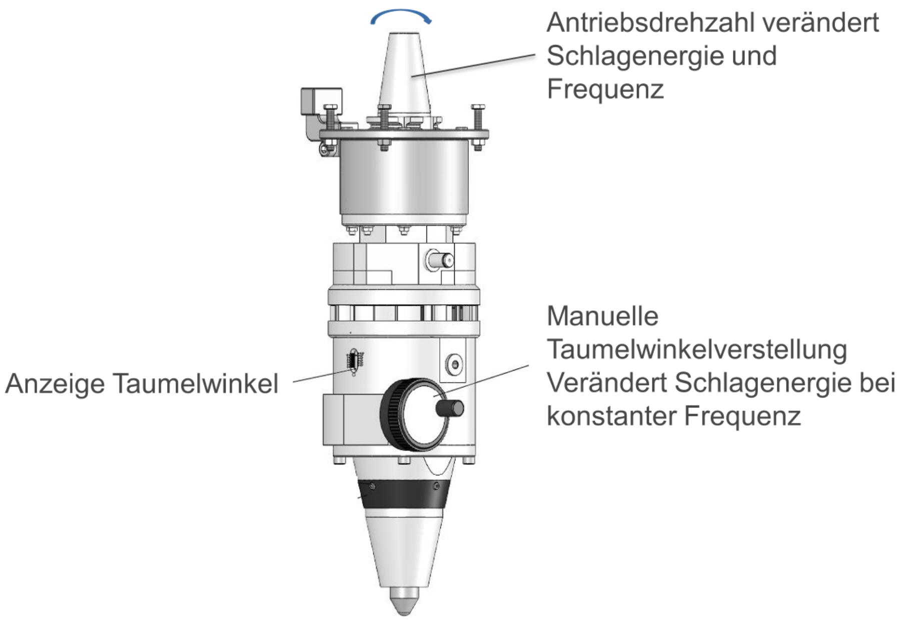

08.10.2019 DGM Fachausschuss, Karlsruhe - O. Maiß, A. Ostertag www.ecoroll.de 20

Messung der Schlagenergie

ECOROLL

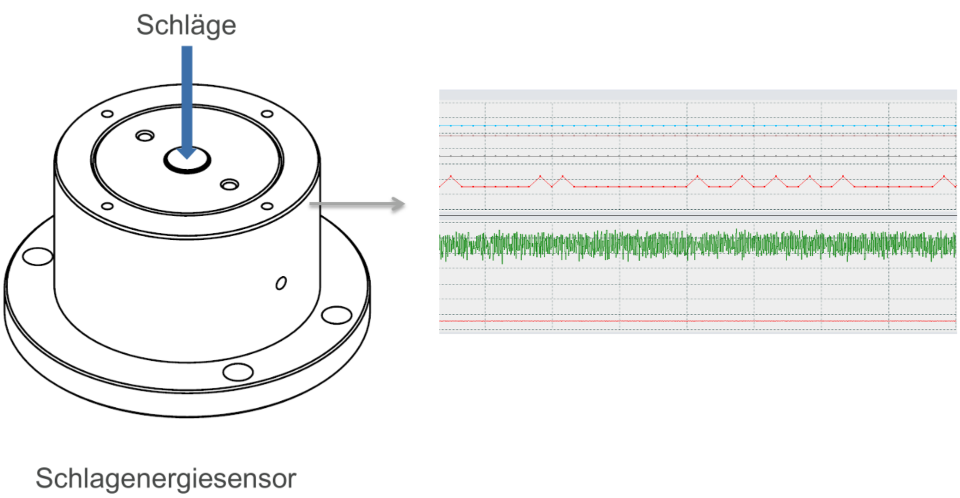

08.10.2019 DGM Fachausschuss, Karlsruhe - O. Maiß, A. Ostertag www.ecoroll.de 21

Verifizierung der Schlagenergie

ECOROLL

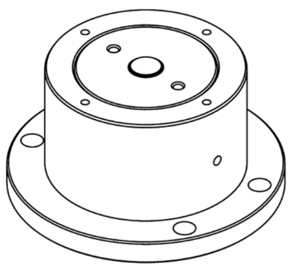

- Einbau des Schlagenergiesensors in den Arbeitsraum der Maschine.
- Zyklisches Anfahren des Sensors für Kontrollmessungen.
- Bei Abweichung Korrektur der Taumelwinkel-Eistellung oder Antriebsdrehzahl.

08.10.2019 DGM Fachausschuss, Karlsruhe - O. Maiß, A. Ostertag www.ecoroll.de 22

Vielen Dank für Ihre Aufmerksamkeit

ECOROLL

ECOROLL AG Werkzeugtechnik
Hans-Heinrich-Warnke-Str. 8
29227 Celle
www.ecoroll.de

Dr.-Ing. Oliver Maiß
Leiter Konstruktion
Tel.: 05141 / 9865-51
Mail: oliver.maiss@ecoroll.de

Alfred Ostertag
Berater
Tel.: 05141 / 9865-51
Mail: alfred.ostertag@ecoroll.de

www.ecoroll.de

FE Simulation of the HFMI Treatment – Previous and Upcoming Results

Stefanos Gkatzogiannis

Steel & Lightweight Structures

Karlsruhe Institute of Technology

Karlsruher Institut für Technologie

VERSUCHSANSTALT FÜR STAHL, HOLZ & STEINE

FE Simulation of the HFMI Treatment - Previous and Upcoming Results

Stefanos Gkatzogiannis, Peter Knoedel, Thomas Ummenhofer

Karlsruhe Institute for Technology
Steel & Lightweight Structures
Research Center for Steel, Timber & Masonry
Germany

Agenda

Karlsruher Institut für Technologie

1. What is HFMI? – Application in Practice
2. Simulation of HFMI – Necessity and Main Aspects
3. Simulation of HFMI – Modelling of the Pin Motion
4. Simulation of HFMI – Calibration based on Drop Tests
5. Summary and Future Results

Stefanos Gkatzogiannis, 8th Workshop Machine Hammer Peening – 22 and 23 October, Karlsruhe Institute of Technology, Germany 2

Problem Statement

The HFMI post-weld treatment process

Stefanos Gkatzogiannis, 8th Workshop Machine Hammer Peening – 22 and 23 October, Karlsruhe Institute of Technology, Germany **3**

The HFMI Post Weld Treatment

The High Frequency Mechanical Impact or HFMI [Marquis, 2016] treatment is a post-weld mechanical treatment method applied for the increase of fatigue life of welded structures.

An appropriate device carrying a pin of hardened steel runs along the weld toe, deforms it by hammering and introduces compressive residual stresses at the surface layer, which counterbalance the welding tensile ones. Therewith, a significant increase of the weldment's fatigue life is achieved.

There are two manufacturers of HFMI devices in Germany: HIFIT and PITEC.

HIFIT

PITEC

HIFIT treatment of a fillet weld

Stefanos Gkatzogiannis, 8th Workshop Machine Hammer Peening – 22 and 23 October, Karlsruhe Institute of Technology, Germany **4**

The HFMI Post V

The High Frequency Mechanica
treatment is a post-weld mecha
increase of fatigue life of welde

An appropriate device carrying
toe, deforms it by hammering a
at the surface layer, which coun
Therewith, a significant increase

There are two manufacturers o
HIFIT and PITEC.

HIFIT

reatment of a fillet weld

Stefanos Gkatzogiannis, 8th Workshop Machine Hammer Peening – 22 and 23 October, Karlsruhe Institute of Technology, Germany 5

The HFMI Post Weld Treatment – Experimental Validation

- The method has been thoroughly investigated experimentally and is proven to increase the fatigue resistance in the high cycle regime of welded joints by even more than 100%.

- A thorough review of experimental work up to 2013 is given in [Yildirim, 2013].

- The KIT Steel and Lightweight Structures Institute has as well carried numerous experimental investigations on HFMI efficiency. Some of them are:
    - The *REFRESH* project [Ummenhofer, 2009]
    - The *DASt Richtlinie* project [Kuhlman, 2018]
    - The *HFH-Korrosion* project [Ummenhofer, 2018]

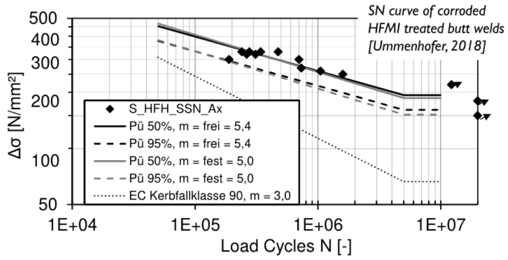

SN curve of corroded HFMI treated butt welds [Ummenhofer, 2018]

FAT class improvement factors for the HFMI treated specimens [Ummenhofer, 2013]

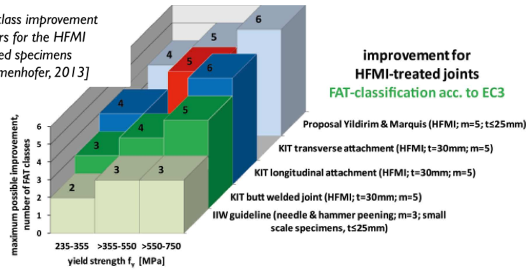

Stefanos Gkatzogiannis, 8th Workshop Machine Hammer Peening – 22 and 23 October, Karlsruhe Institute of Technology, Germany 6

The HFMI Post Weld Treatment in Civil Engineering

Karlsruher Institut für Technologie

- The method is applicable in both mechanical and structural civil engineering fields. Its application is regulated according to:
  - IIW recommendations [Marquis, 2016]
  - A new DASt guideline is now active for application as well in structural engineering [DASt, 2019]
- Possible Fields of application in Structural Engineering:
  - Steel and composite bridges
  - Welded Details of Towers and Jacket Structures like in Offshore Wind Energy Turbines
  - Cranes

and eventually every fatigue loaded structural welded detail.

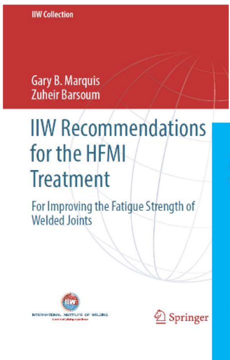

Stefanos Gkatzogiannis, 8th Workshop Machine Hammer Peening – 22 and 23 October, Karlsruhe Institute of Technology, Germany **7**

The HFMI Post Weld Treatment – Practical Aspects

Karlsruher Institut für Technologie

- The two guidelines cover mostly practical aspects:
  - Application of the HFMI treatment including angle and working speed
  - Quality control based on groove geometry and surface quality
  - Fatigue design of HFMI treated weldments based on FAT classes and the approaches of nominal and hot-spot stress taking into consideration size effects etc.

Table 2 Sample treatment procedure parameters for two HFMI tools

Parameter	HFMI tool	
	High frequency impact treatment (HiFIT) [22]	Ultrasonic impact treatment (UIT) [21, 23]
Power source	Pneumatic	Ultrasonic magnetostrictive
Number of indenters	1	1–4
Angle of the axis of the indenters with respect to the plate surface, ϕ (see Fig. 6)	60°–80°	30°–60° [21] 40°–80° [23]
Angle of the axis of the indenters with respect to the direction of travel, ψ (see Fig. 6)	70°–90°	90° (all pins should contact the weld toe)
Working speed	3–5 mm/s	5–10 mm/s [21] 5–25 mm/s [23]
Other		The self-weight of the tool is sufficient [21, 23] Minimum of 5 passes [23]

Application parameters according to [Marquis, 2016]

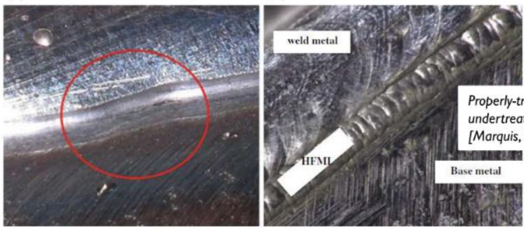

Properly-treated and undertreated weld toes [Marquis, 2016]

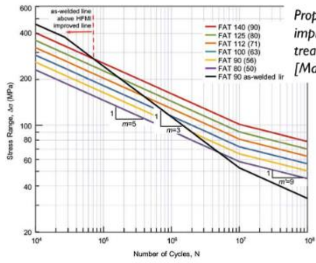

Proposed fat class improvement for the HFMI treated weldments [Marquis, 2016]

Stefanos Gkatzogiannis, 8th Workshop Machine Hammer Peening – 22 and 23 October, Karlsruhe Institute of Technology, Germany **8**

KIT
Karlsruher Institut für Technologie

Simulation of HFMI

Stefanos Gkatzogiannis, 8th Workshop Machine Hammer Peening – 22 and 23 October, Karlsruhe Institute of Technology, Germany 9

Simulation of the HFMI Treatment

KIT
Karlsruher Institut für Technologie

- The validation of a simulation model that predicts the introduced residual stresses can enable a less conservative design and offer a better overview of the method through sensitivity analyses
- Coupling with fracture mechanics is possible, in order to predict with even better accuracy the fatigue life of a component
- Several simulation models have been proposed in the past neglecting though in most cases significant aspects of the problem
- Same physical problem with the indentation of a semi-infinite plate with a spherical indenter under significant initial velocity (non static case)

HFMI simulation is a multi-parameter analysis

Main aspects of the FE simulation of HFMI

1 Pin Movement
- impact speed / intensity
- frequency

2 Contact Definition
- contact model
- friction coefficients

3 Material Behaviour
- strain rate dependent material behaviour in the HAZ
- material model

4 Application Setup
- application angle
- travelling speed

Stefanos Gkatzogiannis, 8th Workshop Machine Hammer Peening – 22 and 23 October, Karlsruhe Institute of Technology, Germany 10

HFMI Simulation – Material Behavior

Karlsruher Institut für Technologie

Reversed plasticity

During spherical indentation, underneath the treatment surface, compressive stresses are introduced which are counterbalanced by outer tensile ones. During continuous treatment along a line, reversal of the plastic strains' and residual stresses' sign takes place.

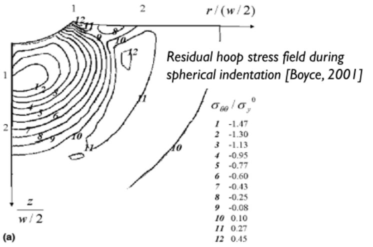
Residual hoop stress field during spherical indentation [Boyce, 2001]

Strain rate dependency

During HFMI strain rates of up to 400 s^{-1} are referred. Previous analyses have proven that yield stress is predominant for the introduced residual stresses. Its strain rate dependency under the present strain rate has to be considered.

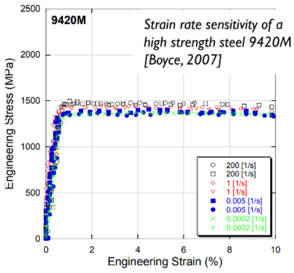

Strain rate sensitivity of a high strength steel 9420M [Boyce, 2007]

Compression / Tension

Previous investigations [Cadoni, 2018] have shown that the strain rate sensitivity of structural steel significantly deviates in tension and compression.

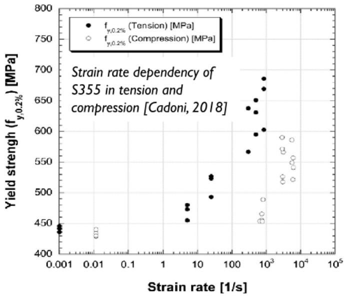

Strain rate dependency of S355 in tension and compression [Cadoni, 2018]

HFMI simulation – Specimens of Parent Material

Karlsruher Institut für Technologie

Specimens of parent material

- Specimens of parent material S355 simulated and measured in a previous study [Foehrenbach, 2016] were simulated as a first step for the validation of the method

Highlights of the Simulation

- Simulation is carried out with LS Dyna [LS-Dyna, 2016]
- Coulomb-friction is applied: coefficients in previous studies and from textbook knowledge deviate from each other significantly, 0.30 to 0.15 is currently applied
- Bilinear material model, with kinematic, isotropic and mixed hardening is applied
- Strain-rate dependency is taken into consideration with the Cowper-Symonds model
- Rigid body properties (mass, inertia) attributed to the HFMI Pin

investigated component – dimensions in mm

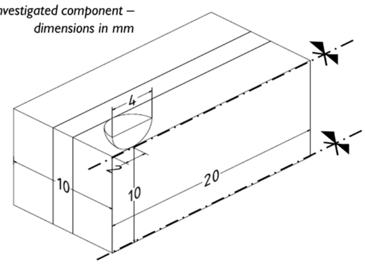

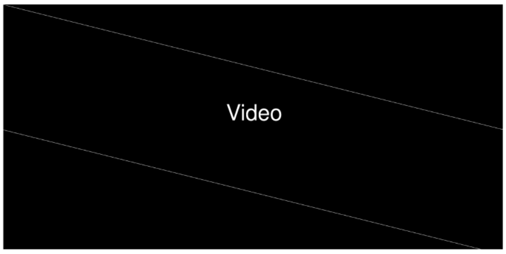

The Cowper Symonds material model

$$\dot{\varepsilon}_{pl} = D \cdot \left(\frac{\sigma_y{}'}{\sigma_y} - 1\right)^q$$

Simulation of HFMI

Modelling the Pin Motion

Stefanos Gkatzogiannis, 8th Workshop Machine Hammer Peening – 22 and 23 October, Karlsruhe Institute of Technology, Germany **13**

HFMI Simulation – Modelling the Pin Motion

Two methods can be applied for modelling the pin vertical motion, a displacement- and a force-based

Displacement-based

- (+) more straightforward to simulate
- (+) measurement of the trace
- (−) unrealistic strain rate evolution – erroneous coupling with strain rate dependent material

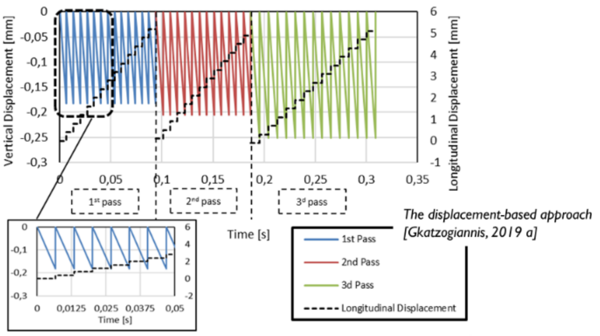

The displacement-based approach [Gkatzogiannis, 2019 a]

Force-based

- (+) calibration of the model through trial and error is needed
- (+) realistic strain rate evolution
- (−) measurement of contact force or impact velocity

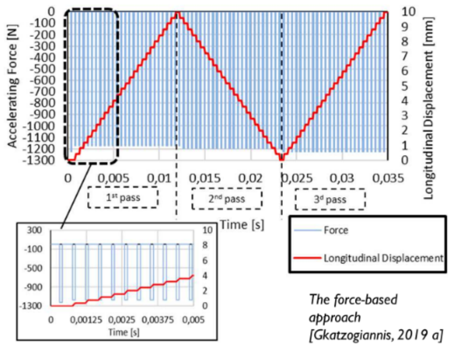

The force-based approach [Gkatzogiannis, 2019 a]

Stefanos Gkatzogiannis, 8th Workshop Machine Hammer Peening – 22 and 23 October, Karlsruhe Institute of Technology, Germany **14**

Karlsruher Institut für Technologie

Drop Tests

Calibration of Material Behavior Through Drop Tests

Stefanos Gkatzogiannis, 8th Workshop Machine Hammer Peening – 22 and 23 October, Karlsruhe Institute of Technology, Germany 15

Drop Tests

Karlsruher Institut für Technologie

- A series of drop tests was carried out in order to reproduce a single HFMI impact in the laboratory under known impact velocity and force (mass)
- Goal was the evaluation of the dynamic yield stress under the present deformation mode
- FE analyses would provide the strain rate for each impact
- Analytical calculations based on measurements of the trace or the rebound velocity would be applied for the calculation of the dynamic yield stress
- 1st step validation through comparison with high strain rate tensile tests [HFH-Simulation], literature – 2nd step validation through application of the calibrated material model in a HFMI Simulation and comparison with RS

The evaluation of the drop tests

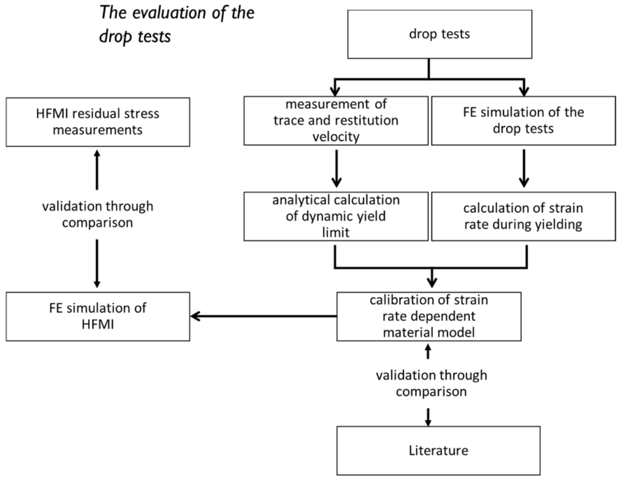

Stefanos Gkatzogiannis, 8th Workshop Machine Hammer Peening – 22 and 23 October, Karlsruhe Institute of Technology, Germany 16

Drop Tests

Test setup for the drop tests

- A wooden bearing structure carries 4 rails – an impact assembly runs across the rails, the pin on its bottom hits the target
- Satisfactory accuracy:
  - impact velocities in the range of the measured for HIFIT and PITEC achieved (2 m/s – 5 m/s),
  - maximum rotation of ± 1°
  - adequate tolerance, no breaking down of the free fall
  - rebound velocity measured with video camera 120 fps, accuracy of ± 0.001 m/s

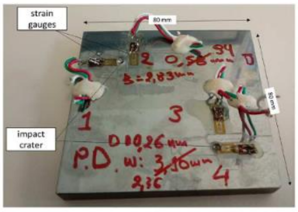

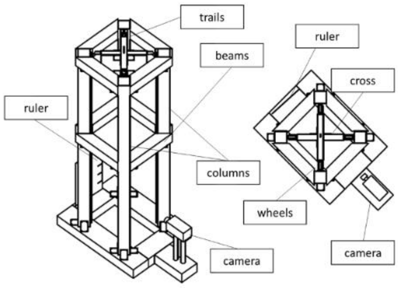

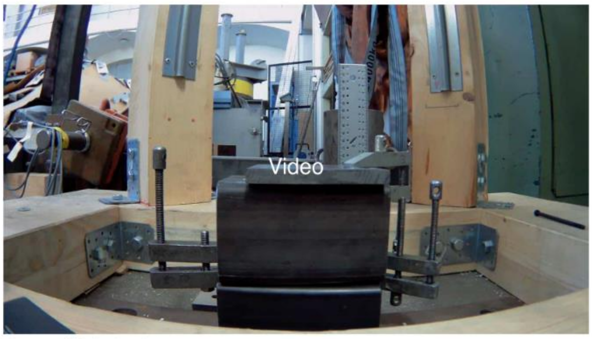

Stefanos Gkatzogiannis, 8th Workshop Machine Hammer Peening – 22 and 23 October, Karlsruhe Institute of Technology, Germany **17**

Drop Tests

Results

- Determination of the strain rate with FE simulation of the experiment:
  - strain rate independent elastic-plastic behavior
  - strain rates too high especially at initiation of contact (singularities)
  - split Hopkinson bar impact velocities of 9, 18 and 27 m/s lead to strain rates of 900 to 7000 s^{-1} [Cadoni, 2018]
- Analytical calculation of the dynamic yield stress based on trace measurement analogous to cylindrical indentation [Lim, 1998]: not possible for present impact velocities and a spherical indenter
- Analytical calculation of the dynamic yield stress based on rebound velocity [Tabor, 1948 - Johnson, 1985]:
  - measurement of rebound velocity was successful
  - satisfactory results for S355 - unsatisfactory results for S690, S960
- Factors of the method producing errors are:
  - the assumption of strain rate independent material behavior in the FE simulation of the experiment
  - the formula for calculating yield strength based on rebound velocity far too empirical

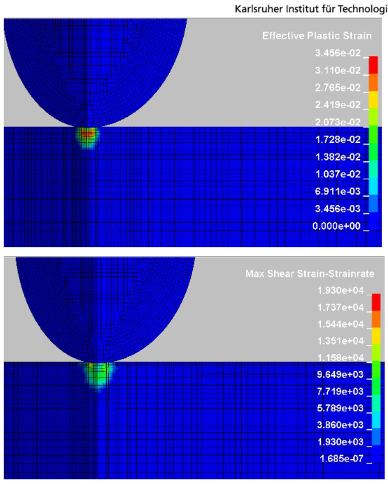

Introduction of the plastic strain spherical zone underneath the impact surface - (a) Von Mises strain rate - (b) maximum shear strain rate

Stefanos Gkatzogiannis, 8th Workshop Machine Hammer Peening – 22 and 23 October, Karlsruhe Institute of Technology, Germany **18**

Drop Tests

Dynamic yield stress of S355

Results

- Determination o
  - strain rate
  - strain rates
  - split Hopk 900 to 700
- Analytical calcula analogous to cyl velocities and a
- Analytical calcula 1948 - Johnson,
  - measurem
  - satisfactory
- Factors of the m
  - the assump of the exp
  - the formul empirical

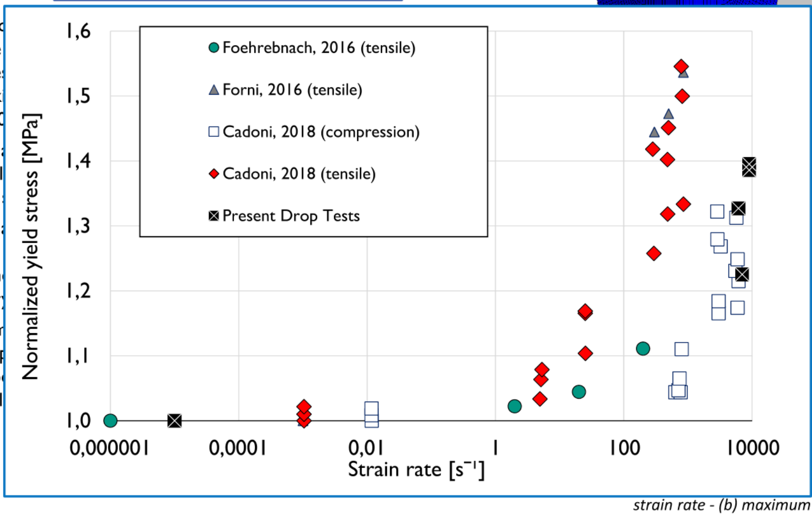

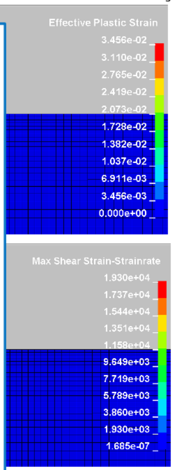

strain spherical zone
rface - (a) Von Mises
strain rate - (b) maximum shear strain rate

Stefanos Gkatzogiannis, 8th Workshop Machine Hammer Peening – 22 and 23 October, Karlsruhe Institute of Technology, Germany **19**

Results

Stefanos Gkatzogiannis, 8th Workshop Machine Hammer Peening – 22 and 23 October, Karlsruhe Institute of Technology, Germany **20**

HFMI Simulation - Results

Results referenced as [Schubnell, 2019] are the same ones from [Foehrenbach, 2016]

Karlsruher Institut für Technologie

Results with the displacement-based (DB) method

- Two models were simulated, a strain rate independent (RI) and a dependent (RD)
- Simulated RS results follow qualitatively the pattern of the measured transverse RS – nevertheless, the peak lies significantly deeper in the simulatiom
- In the case of the longitudinal RS, the model does not predict the RS profile not even qualitatively, especially near the surface

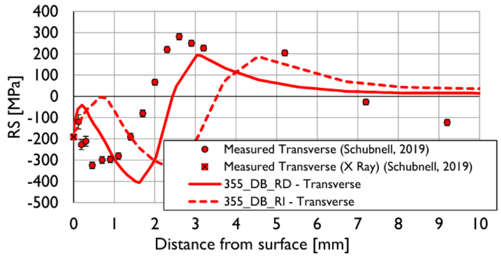

- The introduction of the strain rate dependency seems to improve the agreement between measurements and simulation, nevertheless its use with a displacement base approach is questionable and has no potential for further improvement (measurement restrictions)

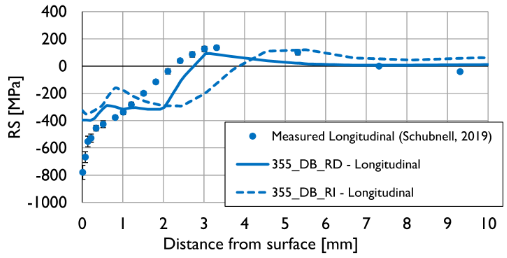

Stefanos Gkatzogiannis, 8th Workshop Machine Hammer Peening – 22 and 23 October, Karlsruhe Institute of Technology, Germany 21

HFMI Simulation - Results

Results referenced as [Schubnell, 2019] are the same ones from [Foehrenbach, 2016]

Karlsruher Institut für Technologie

Results with the force-based (FB) method

- Four different models were simulated
- Simulated RS results follow qualitatively and quantitatively the pattern of the measured RS, both for the transverse and the longitudinal case
- In the case of the transverse RS, all models provide similar agreement with the measured stresses

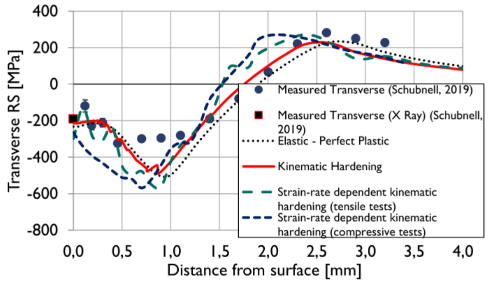

- Against initial expectations the compressive strain rate dependent model is less accurate – input data is to be accounted for [Gkatzogiannis, 2019 a]
- In the case of the longitudinal RS, the strain rate independent models seem to underestimate the RS near the surface
- The overall evaluation of the results strain rate dependency is predominant for S355

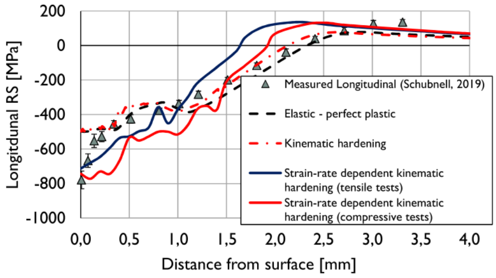

Stefanos Gkatzogiannis, 8th Workshop Machine Hammer Peening – 22 and 23 October, Karlsruhe Institute of Technology, Germany 22

Karlsruher Institut für Technologie

Summary and Upcoming Results

Stefanos Gkatzogiannis, 8th Workshop Machine Hammer Peening – 22 and 23 October, Karlsruhe Institute of Technology, Germany **23**

Karlsruher Institut für Technologie

HFMI Simulation – Summary of Previous Results and Open Questions

Two main aspects of the HFMI Simulation were investigated by modelling specimens of parent material:

- Modelling the movement of the HFMI Pin:
  - Two different approaches for simulating the predominant vertical motion of the pin were applied: a displacement- and a force-based
  - Introduction of strain rate dependency into the simulation improves significantly the agreement between simulated and measured RS, however introduction to the displacement-based simulation is questionable
  - Force-based approach provides better agreement with the measured profiles and allows for the consideration of a strain rate dependent behaviour
- Calibration of Material behaviour based on the Dropt Tests:
  - Cowper Symonds strain rate dependent material model was calibrated based on the results of the drop tests
  - Compressive results by [Cadoni, 2018] were taken into consideration as well to increase the sample
  - Simulation of HFMI using the calibrated, strain rate dependent material model, presents much better agreement with the measured RS than the strain rate independent plasticity models

Open Questions

- Real scale welded components – numerical capacity problems arise [Gkatzogiannis, 2019 b]
- Influence of WRS – coupling with welding simulation [Gkatzogiannis, 2019 b]
- Coupling with fracture mechanics investigations

Stefanos Gkatzogiannis, 8th Workshop Machine Hammer Peening – 22 and 23 October, Karlsruhe Institute of Technology, Germany **24**


HFMI Simulation – Upcoming Results
Karlsruher Institut für Technologie
• Dissertation [Gkatzogiannis, 2019 b]
• Ongoing research project ends in December, 2019:
Schubnell J., Gkatzogiannis S., Farajian M., Knoedel P., Ummenhofer T: IGF-Vorhaben Nr. 19227 N – Rechnergestütztes Bewertungstool zum Nachweis der Lebensdauerverlängerung von mit dem Hochfrequenz-Hämmerverfahren (HFMI) behandelten Schweißverbindungen aus hochfesten Stählen
Research partners:
Fraunhofer IWM
VERSUCHSANSTALT FÜR STAHL, HOLZ & STEINE
Funded by:
DVS
Bundesministerium für Wirtschaft und Energie
AiF
Industrial partners:
BILFINGER
CCTH
VOLVO Construction Equipment
KREBS+KIEFER
RAMBØLL
IMS
get it right®
HiFIT
aerodyn
SCHACHTBAU NORDHAUSEN
BOMBARDIER
Schuler Ingenieurbüro für Bautechnik Karlsruhe
ipu
MAURER SÖHNE forces in motion
tkb. Technologiekontor Bremerhaven
SENVION
PITEC
voestalpine EINEN SCHRITT VORAUS.
Stefanos Gkatzogiannis, 8th Workshop Machine Hammer Peening – 22 and 23 October, Karlsruhe Institute of Technology, Germany
25

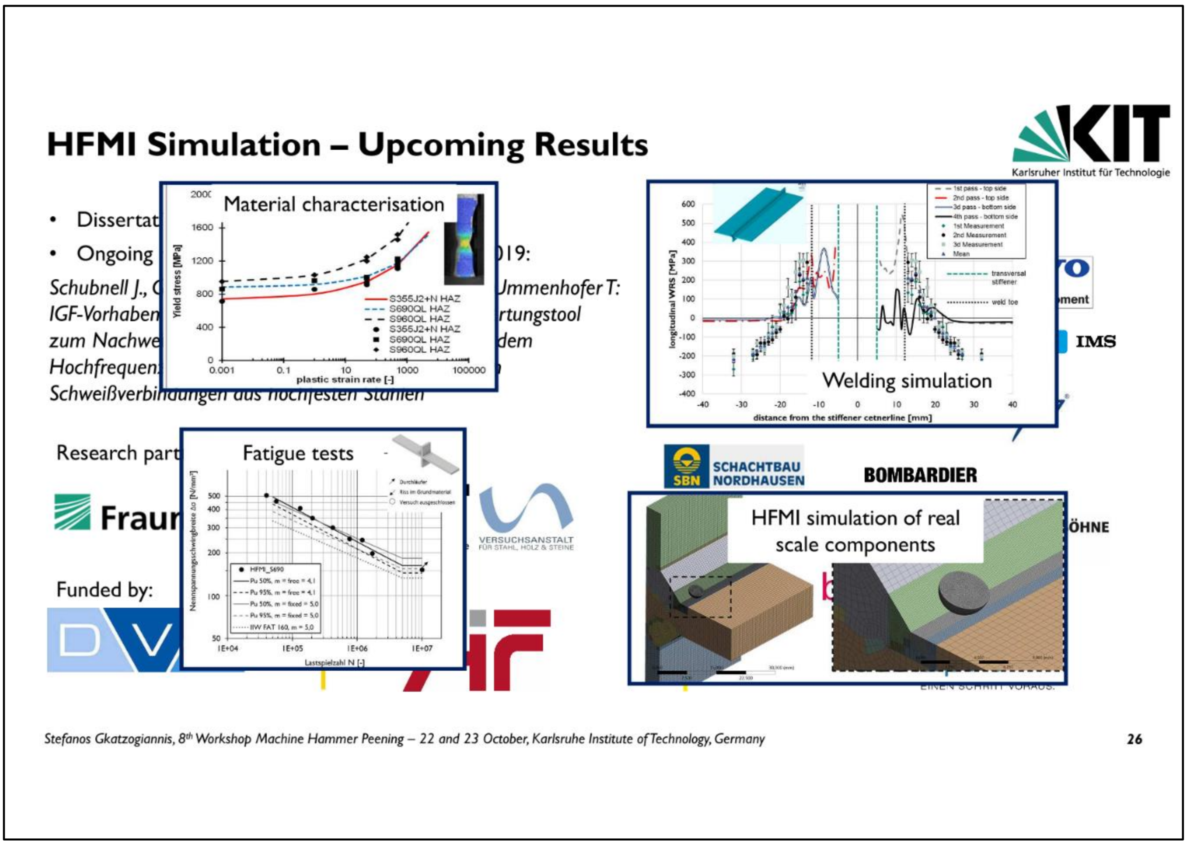
HFMI Simulation – Upcoming Results
Karlsruher Institut für Technologie
Material characterisation
Yield stress [MPa]
plastic strain rate [-]
S355J2+N HAZ
S690QL HAZ
S960QL HAZ
Welding simulation
longitudinal WRS [MPa]
distance from the stiffener cetnerline [mm]
Fatigue tests
Lastspielzahl N [-]
HFMI simulation of real scale components
SCHACHTBAU NORDHAUSEN
BOMBARDIER
Stefanos Gkatzogiannis, 8th Workshop Machine Hammer Peening – 22 and 23 October, Karlsruhe Institute of Technology, Germany
26

Thank you very much for your attention!

Karlsruher Institut für Technologie

References

[Boyce, 2001]	Boyce B. L., Chen X., Hutchinson J. W., Ritchie R. O.; The Residual Stress State due to a Spherical Hard-Body Impact, Mechanics of Materials 33, pp. 441-454, 2001.
[Boyce, 2007]	Boyce B. L., Crenshaw T. B., Dilmore M. F.; The Strain-Rate Sensitivity of High-Strength High-Toughness Steels, SANDIA REPORT, SAND2007-0036, Unlimited Release, January 2007.
[Cadoni, 2018]	Cadoni E., Forni D., Gieleta R., Kruszka L.; Tensile and Compressive Behaviour of S355 Mild Steel in a Wide Range of Strain Rates; The Eu-ropean Physical Journal Special Topics 227, pp. 29-43, 2018.
[DASt, 2019]	DASt – Richtlinie 026; Ermüdungsverbesserung bei Andwendung höherfrequenter Hämmerverfahren, 2019.
[Foehrenbach, 2016]	Foehrenbach J., Hardenacke V., Farajian M.; High Frequency Mechanical Impact Treatment (HFMI) for the Fatigue Improvement: Numerical and Experimental Investigations to describe the Condition in the Surface Layer, Welding in the World 60 (4), pp. 749–755, 2016.
[Forni, 2016]	Forni D., Chiaia B., Cadoni E.; Strain Rate Behaviour in Tension of S355 Steel: Base for Progressive Collapse Analysis, Engineering Structures 119, pp. 167-173, 2016.
[Gkatzogiannis, 2019]	Gkatzogiannis S., Knoedel P., Ummenhofer T.; Calibration of HFMI Simulation based on Drop Tests, EUROMAT 19, 1-6 September, Stockholm, 2019.
[Gkatzogiannis, 2019 b]	Gkatzogiannis S.; Finite Element Simulation of Residual Stresses from Welding and High Frequency Hammer Peening, Doctoral Dissertation, Karlsruhe Institute of Technology, Steel- and Lightweight Structures, to be submitted in 2019.
[Kuhlman, 2018]	Kuhlman U., Breunig S., Ummenhofer T., Weidner P.; Entwicklung einer DASt-Richtlinie für höherfrequente Hämmerverfahren - Zusammenfassung der durchgeführten Untersuchungen und Vorschlag eines DASt-Richtlinien-Entwurfs, Stahlbau 87 (10), pp. 967-983, 2018.
[LS Dyna, 2016]	LS-DYNA, Theory Manual, Livermore Software Technology Corporation (LSTC), Livermore California 2016.
[Marquis, 2016]	Marquis G. B., Barsoum Z.; IIW Recommendations for the HFMI Treatment – For Improving the Fatigue Strength of Welded Joints, 1st Edition, Springer Singapore (IIW Collection), Singapore 2016.
[Ummenhofer, 2009]	Ummenhofer T.; REFRESH: Lebensdauerverlängerung bestehender und neuer geschweißter Stahlkonstruktionen, Abschlussbericht D 761, KIT Stahl- und Leichtbau, Versuchsanstalt für Stahl, Holz und Steine, Karlsruhe, 2009.
[Ummenhofer, 2013]	Ummenhofer T., Weidner P.; Improvement Factors for the Design of Welded Joints subjected to High Frequency Mechanical Impact Treatment, Steel Construction 6 (3), pp. 191-199, 2013.
[Ummenhofer, 2018]	Ummenhofer T., Engelhardt I., Knoedel P., Gkatzogiannis S., Weinert J., Loeschner D.; Erhöhung der Ermüdungsfestigkeit von Offshore-Windenergieanlagen durch Schweißnahtnachbehandlung unter Be-rücksichtigung des Korrosionseinflusses, Schlussbericht, DVS 09069 – IGF 18457 N, KIT Stahl- und Leichtbau, Versuchsanstalt für Stahl, Holz und Steine, Karlsruhe und Hochschule für angewandte Wissenschaf-ten München, Labor für Stahl- und Leichtmetallbau, Germany, 2018.
[Yildirim, 2013]	Yildirim H. C., Marquis G. B.; Overview of Fatigue Data for High Frequency Mechanical Impact Treated Welded Joints, Weld World 56 (7-8), pp. 82-96, 2013.

Stefanos Gkatzogiannis, 8th Workshop Machine Hammer Peening – 22 and 23 October, Karlsruhe Institute of Technology, Germany **27**

Influence of mechanical surface treatments on propagation and opening behavior of physically short cracks in Inconel 718

Alexander Klumpp

IAM-WK – Institute for Applied Materials

Karlsruhe Institute of Technology

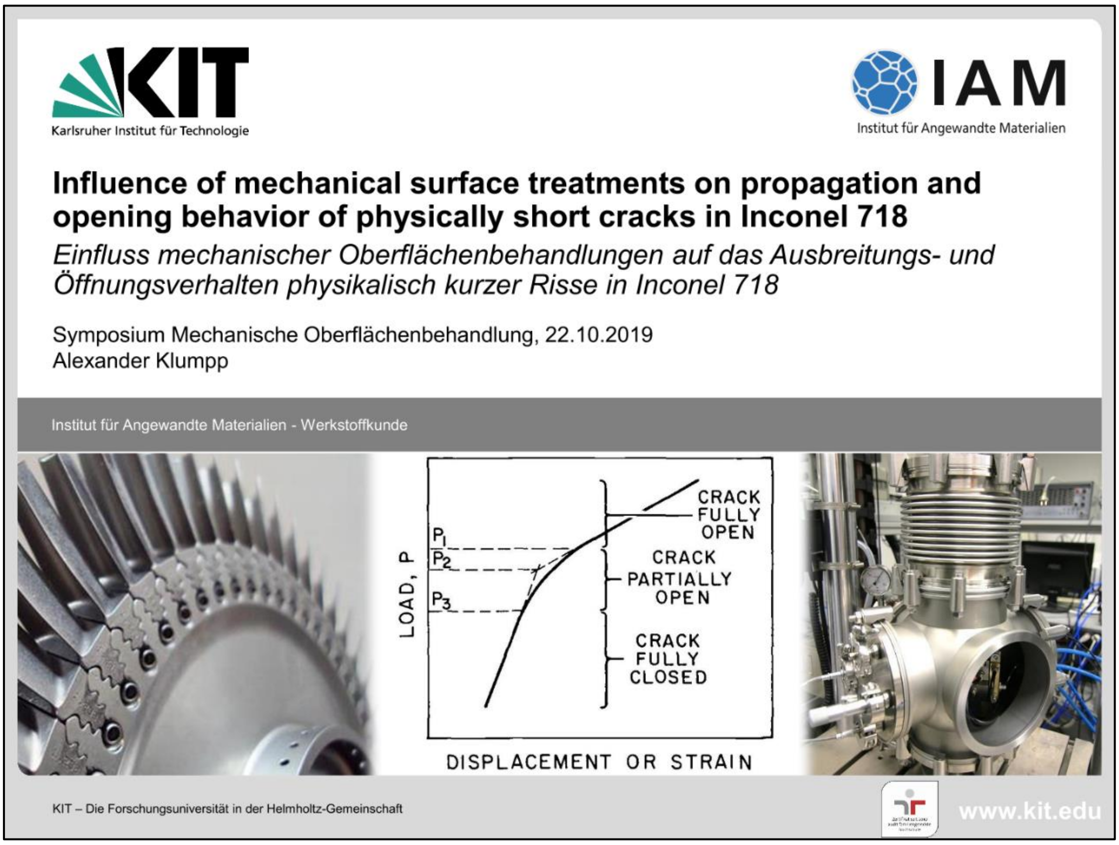
KIT
Karlsruher Institut für Technologie
IAM
Institut für Angewandte Materialien
Influence of mechanical surface treatments on propagation and opening behavior of physically short cracks in Inconel 718
Einfluss mechanischer Oberflächenbehandlungen auf das Ausbreitungs- und Öffnungsverhalten physikalisch kurzer Risse in Inconel 718
Symposium Mechanische Oberflächenbehandlung, 22.10.2019
Alexander Klumpp
Institut für Angewandte Materialien - Werkstoffkunde
LOAD, P
P1
P2
P3
CRACK FULLY OPEN
CRACK PARTIALLY OPEN
CRACK FULLY CLOSED
DISPLACEMENT OR STRAIN
KIT – Die Forschungsuniversität in der Helmholtz-Gemeinschaft
www.kit.edu

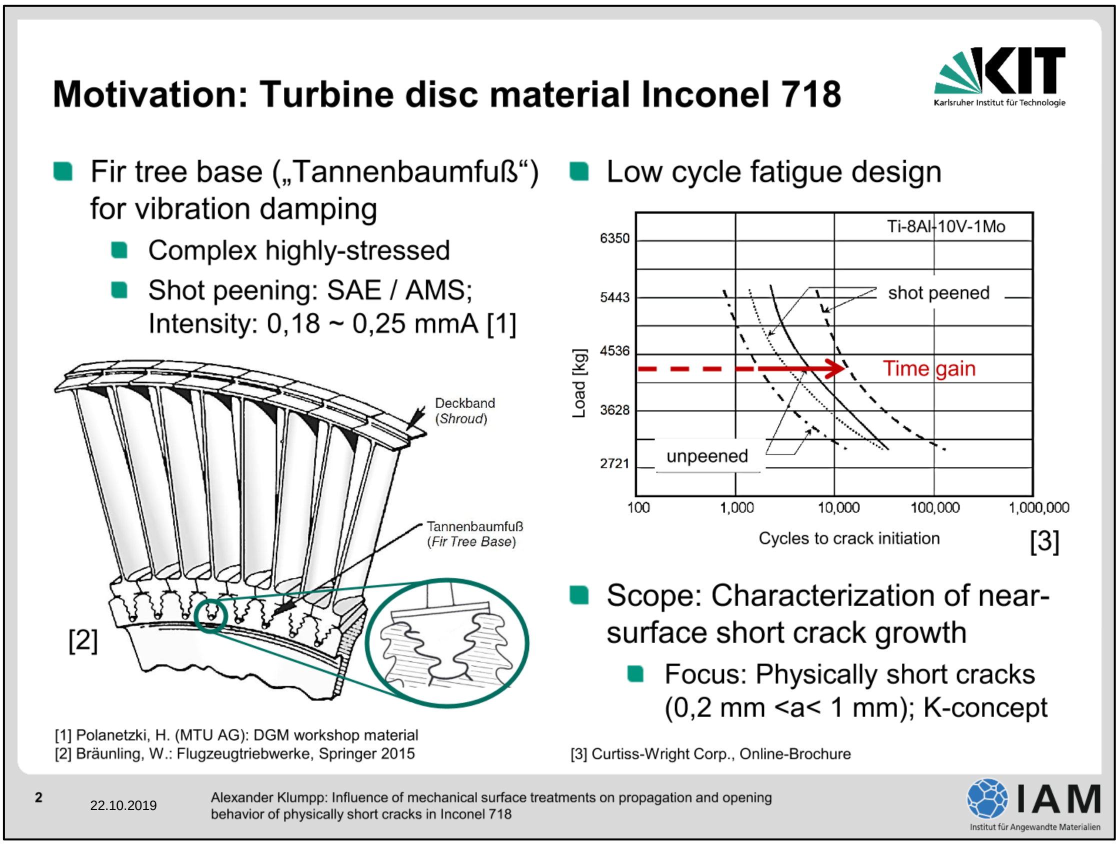
Motivation: Turbine disc material Inconel 718
KIT
Karlsruher Institut für Technologie
Fir tree base („Tannenbaumfuß") for vibration damping
Complex highly-stressed
Shot peening: SAE / AMS; Intensity: 0,18 ~ 0,25 mmA [1]
Deckband (Shroud)
Tannenbaumfuß (Fir Tree Base)
[2]
Low cycle fatigue design
Ti-8Al-1V-1Mo
6350
5443
4536
3628
2721
Load [kg]
shot peened
Time gain
unpeened
100
1,000
10,000
100,000
1,000,000
Cycles to crack initiation
[3]
Scope: Characterization of near-surface short crack growth
Focus: Physically short cracks (0,2 mm <a< 1 mm); K-concept
[1] Polanetzki, H. (MTU AG): DGM workshop material
[2] Bräunling, W.: Flugzeugtriebwerke, Springer 2015
[3] Curtiss-Wright Corp., Online-Brochure
2
22.10.2019
Alexander Klumpp: Influence of mechanical surface treatments on propagation and opening behavior of physically short cracks in Inconel 718
IAM
Institut für Angewandte Materialien

Motivation: Recent developments in machine hammer peening (MHP)

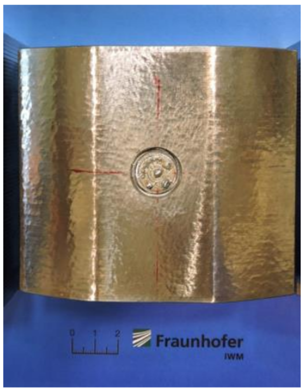

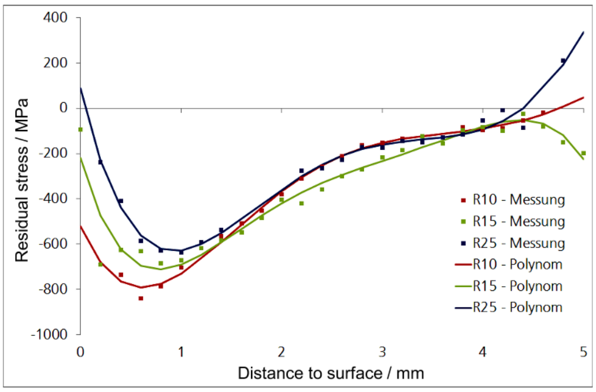

ECOROLL AG / Fraunhofer IWM

- Studies regarding residual stress evolution in Inconel 718:
  - Mechanical MHP system type „EcoPeen“
  - Several millimeters of residual stress penetration depth are feasible
  - → Investigation of crack behavior after shot peening and other mechanical surface treatments

3 22.10.2019 Alexander Klumpp: Influence of mechanical surface treatments on propagation and opening behavior of physically short cracks in Inconel 718

Outline

- Basics of fracture mechanics
- Material and mechanical surface treatments
- Experimental setup for characterization of short crack propagation and opening
- Results and discussion
- Conclusion

4 22.10.2019 Alexander Klumpp: Influence of mechanical surface treatments on propagation and opening behavior of physically short cracks in Inconel 718

K-concept and „intrinsic“ approach

- Stress intensity K_I / K / K_{nom} for characterization of mechanical crack load in mode I

$$K_{nom} = \sigma\sqrt{\pi a}Y \text{ (static load)}$$

$$\Delta K_{nom} = \Delta\sigma\sqrt{\pi a}Y = K_{max} - K_{min}$$
$$R_{nom} = \frac{K_{min}}{K_{max}} \text{ (cyclic fatigue load)}$$

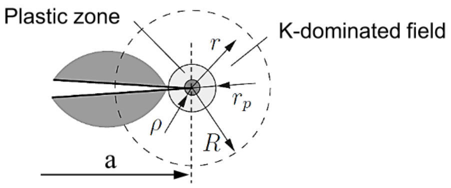

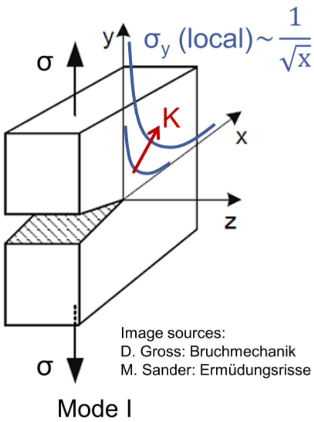

Image sources:
D. Gross: Bruchmechanik
M. Sander: Ermüdungsrisse

- Cyclic fatigue crack growth governed by the material's „intrinsic“ resistance (Ritchie, 1988)
  → Against formation of new surfaces

Literature: Ritchie, R. O. (1988). Mechanisms of fatigue crack propagation in metals, ceramics and composites: role of crack tip shielding. *Materials Science and Engineering: A*, *103*(1), 15-28.

5 22.10.2019 Alexander Klumpp: Influence of mechanical surface treatments on propagation and opening behavior of physically short cracks in Inconel 718

Closure-based („extrinsic“) concept

- Paris diagram (1961) for long crack propagation

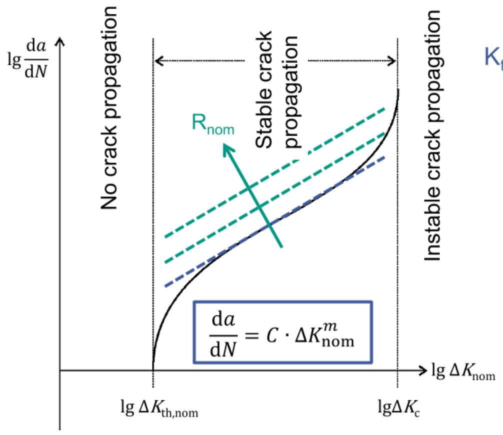

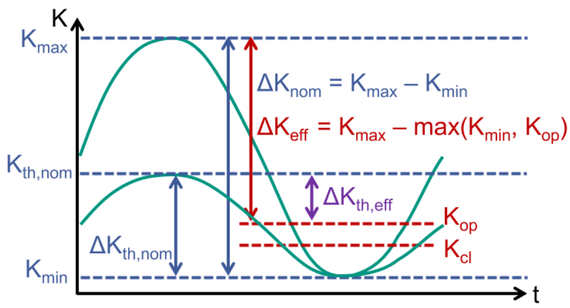

- Crack closure effect (Elber, 1971)
  - E.g. due to plasticity, roughness, compressive residual stresses

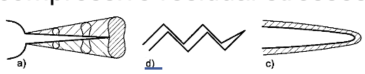

- Effective threshold $\Delta K_{th,eff}$
  → Dependent on work hardening
- *Further effects of residual stresses?*

6 22.10.2019 Alexander Klumpp: Influence of mechanical surface treatments on propagation and opening behavior of physically short cracks in Inconel 718

Effects of residual stresses

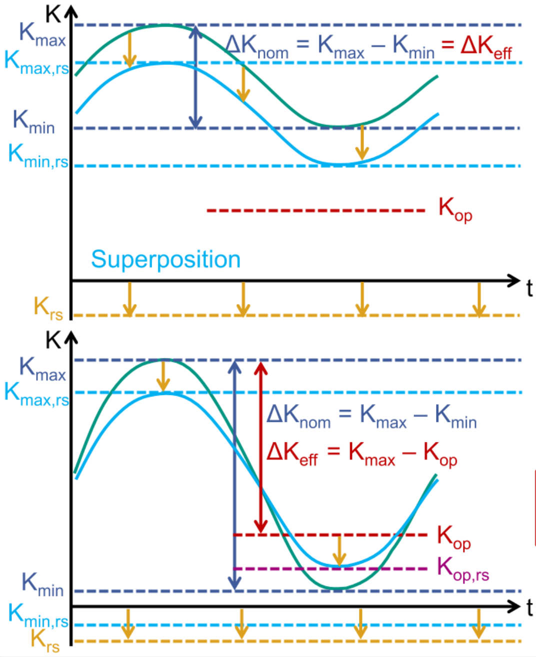

- „Residual stress intensity“ K_{rs}
  - Weight function / numerical determination (FE)
- No closure, buth with res. stress
  - Local load ratio (R_{eff}) affected, but not ΔK_{eff}

$$\Delta K_{\text{eff}} = \Delta K_{\text{nom}} \qquad R_{\text{eff}} = \frac{K_{\text{min,rs}}}{K_{\text{max,rs}}} \neq R_{\text{nom}}$$

- Closure effect with res. stress
  - Both ΔK_{eff} and R_{eff} are affected

$$\Delta K_{\text{eff}} = K_{\text{max}} - K_{\text{op}} \neq \Delta K_{\text{nom}} \qquad R_{\text{eff}} = \frac{K_{\text{op,rs}}}{K_{\text{max,rs}}} \neq R_{\text{nom}}$$

→ Numerical and experimental methods are required!

7 22.10.2019 Alexander Klumpp: Influence of mechanical surface treatments on propagation and opening behavior of physically short cracks in Inconel 718

Material: Alloy „Inconel“ 718

Chemical compositon (mass %)									
Ni	Fe	Cr	Mo	Ti	Nb	Al	Co	Mn	C
Basis	18,80	18,40	2,91	0,99	5,28	0,58	0,24	0,07	0,03

- Heat treatment: ASTM B637
  - γ‘‘-precipitation hardening with two step tempering:
    955 °C (1h)
    720 °C (8h)
    620 °C (8h)
  - Mean γ-grain size: app. 19 µm

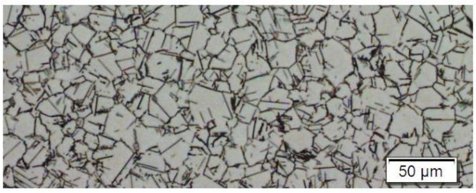

- Micro hardness: app. 460 HV 0,1
- Tests at 20 °C and 550 °C
  - Mechanical properties [1]

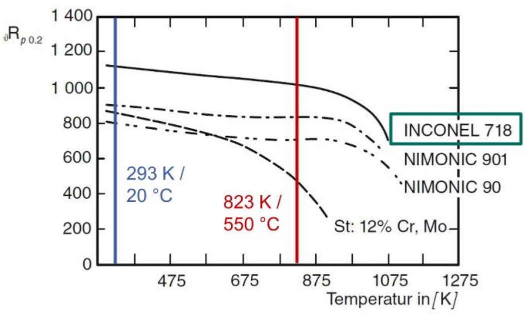

[1] Bräunling, W.: Flugzeugtriebwerke, Springer 2015

8 22.10.2019 Alexander Klumpp: Influence of mechanical surface treatments on propagation and opening behavior of physically short cracks in Inconel 718

Mechanical surface treatments (Support by OSK Kiefer, Malsch)

- Goal: Variation of profiles of residual stresses and work hardening (Measure: Micro hardness)
- Application of:

Shot peening: Cut wire G3 Ø 0,8 / S170; 0.21 ~ 0.76 mmA intensity; 100 ~ 300 % coverage

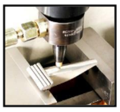

Deep rolling: hard metal Ø 6.35; 200 ~ 250 bar pressure; 0.03 ~ 0.04 mm stepover distance

(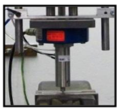 Piezo peening: Hard metal Ø 5; 36 µm stroke; 500 impacts/s; 0.25 mm stepover distance)

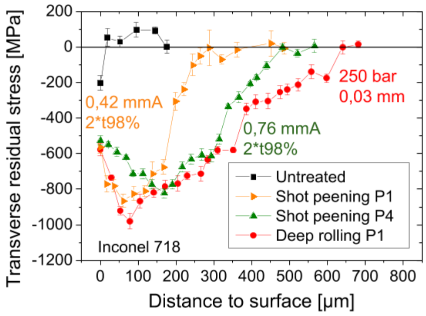

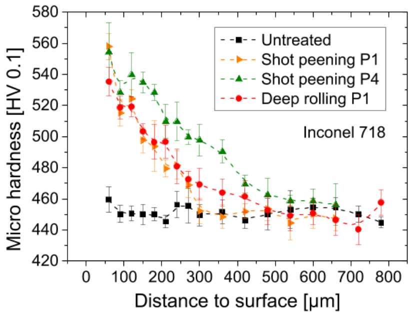

9 22.10.2019 Alexander Klumpp: Influence of mechanical surface treatments on propagation and opening behavior of physically short cracks in Inconel 718

IAM Institut für Angewandte Materialien

(Print version: All results of surface treatments)

- Shot peening

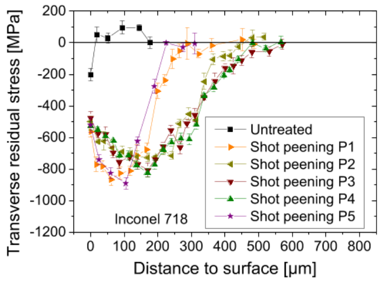

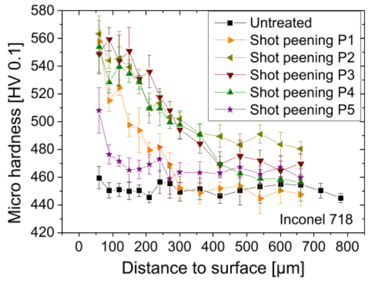

- Deep rolling / piezo peening

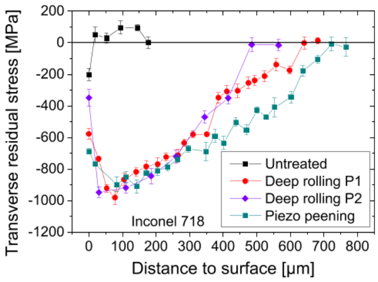

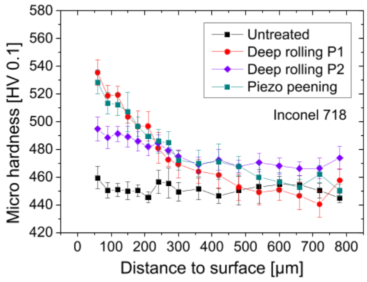

10 22.10.2019 Alexander Klumpp: Influence of mechanical surface treatments on propagation and opening behavior of physically short cracks in Inconel 718

IAM Institut für Angewandte Materialien

Experimental procedure

- Linear electro motor based test bench (Instron)
  → Fine vacuum to avoid oxidation
- Specimen geometry for 3P-bending

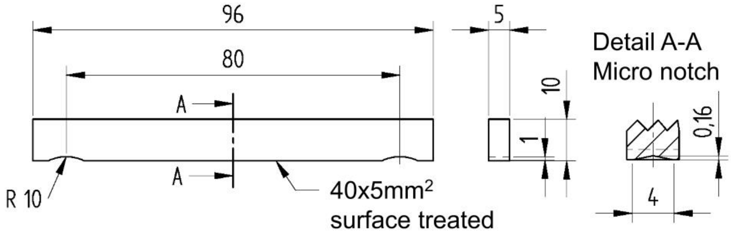

- Crack growth and opening tests
  - Load ratios: R_{nom} = 0,01 / 0,5 / 0,7
  - Test temperatures: 20 °C; 550 °C
  - Captured crack length: 0,25 mm ~ 1,60 mm
  - → Necessary: Measurements with very high resolution

11 22.10.2019 Alexander Klumpp: Influence of mechanical surface treatments on propagation and opening behavior of physically short cracks in Inconel 718

Determination of crack opening loads: Classic procedure: *Specimen compliance*

- Principle: Increasing stiffness due to crack closure

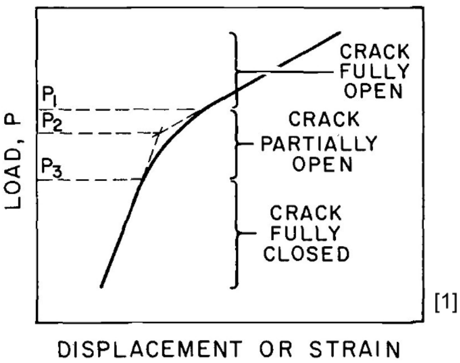

- Actual record for a long crack (1,56 mm)

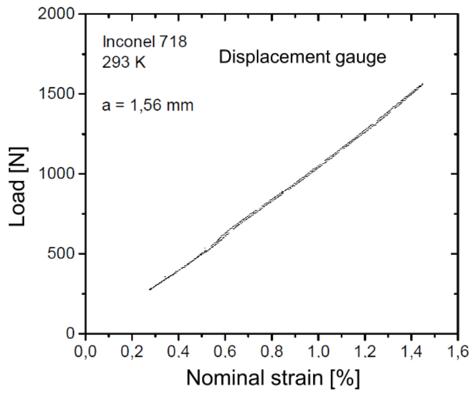

- Resolution is not sufficient for measurements on short cracks after mechanical surface treatments!

[1] Allison, J. E.; Ku, R. C.; Pompetzki, M. A.: A Comparison of Measurement Methods and Numerical Procedures for the Experimental Characterization of Fatigue Crack Closure. In: *Mechanics of Fatigue Crack Closure,* ASTM International, 1988

12 22.10.2019 Alexander Klumpp: Influence of mechanical surface treatments on propagation and opening behavior of physically short cracks in Inconel 718

Determination of crack opening loads: Classic procedure: *Potential drop method*

KIT Karlsruher Institut für Technologie

- Plateau formation of electrical voltage due to crack opening
- Suitable for long cracks; no proper resolution for short cracks

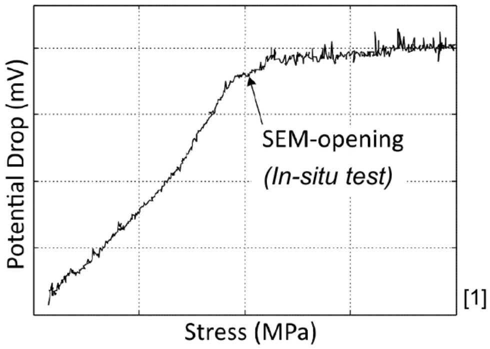

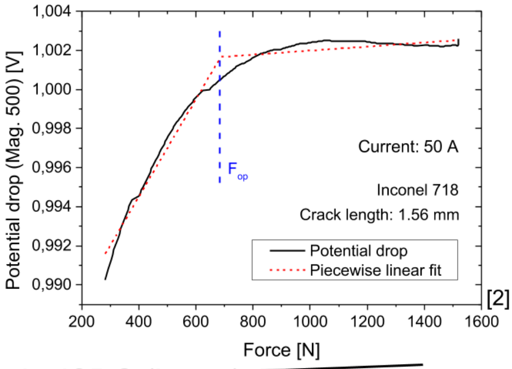

- ~~Other methods: DIC, Eddy, Ultrasonic, ISDG (Laser), Barkhausen~~

→ Get the maximum out of the potential drop method

[1] Andersson, M. et al.: Experimental and numerical investigation of crack closure measurements with electrical potential drop technique. *International Journal of Fatigue* 28 (2006), Nr. 9, S. 1059–1068
[2] Klumpp, A. et al.: Influence of work-hardening on fatigue crack growth, effective threshold and crack opening behavior in the nickel-based superalloy Inconel 718. In: *International Journal of Fatigue* 116 (2018), S. 257–267

13 22.10.2019 Alexander Klumpp: Influence of mechanical surface treatments on propagation and opening behavior of physically short cracks in Inconel 718

IAM Institut für Angewandte Materialien

The „elevated current potential drop method"

KIT Karlsruher Institut für Technologie

- Principle:
  - Extremely high currents (>300 A) → reduction of disturbance and noise
  - Setting of test temperature directly by Ohmic losses
  - Potential probes as near as possible to the crack → maximum sensitivity

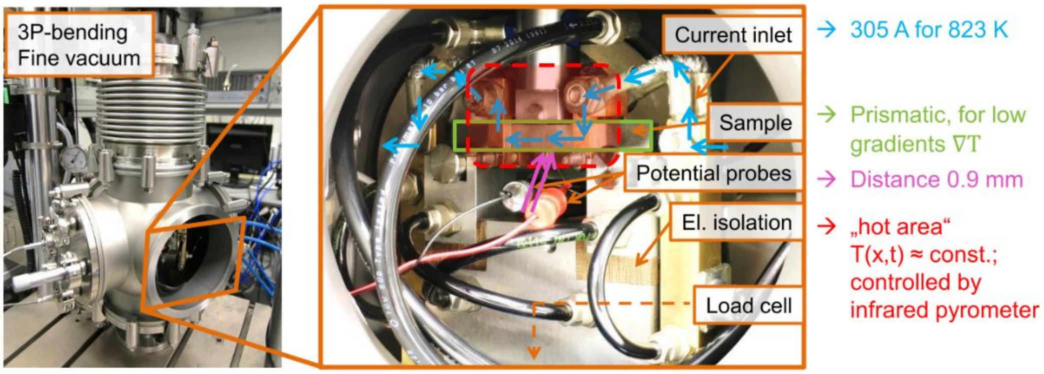

→ Necessary: Extensive preliminary studies

14 22.10.2019 Alexander Klumpp: Influence of mechanical surface treatments on propagation and opening behavior of physically short cracks in Inconel 718

IAM Institut für Angewandte Materialien

Reproducibility of test temperature

- Statistical deviations

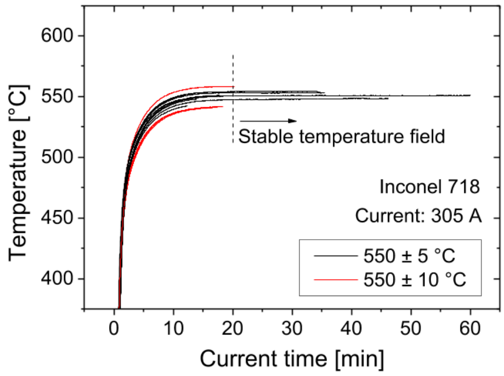

- Warming during tests

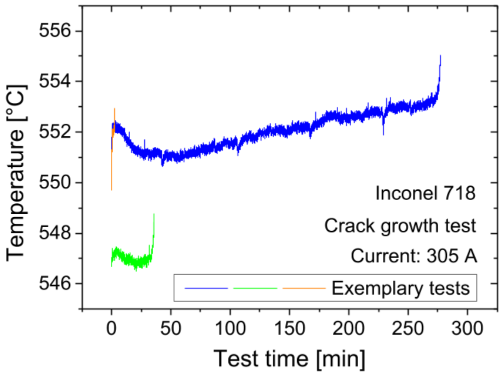

→ Reproducible and nearly constant test temperatures

→ Numerical error analyses regarding temperature, work hardening influence and probe positions: *Compromises are necessary*

→ *Measurement of crack opening loads becomes feasible*

15 22.10.2019 Alexander Klumpp: Influence of mechanical surface treatments on propagation and opening behavior of physically short cracks in Inconel 718

Determination of crack opening loads

- Untreated state

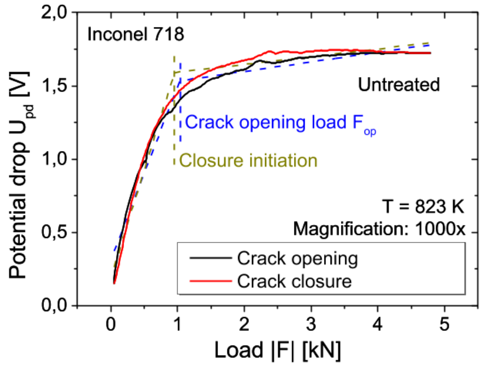

- Bilinear fit, equal to [1]

- Deep rolled state

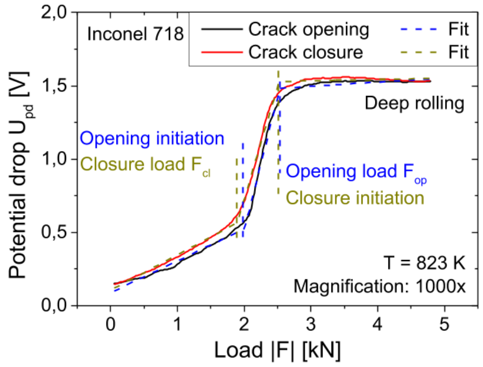

- Trilinear fit

- Significant effect of surface treatment: „complete" / „incomplete" crack closure may occur

[1] Andersson, M. et al.: Experimental and numerical investigation of crack closure measurements with electrical potential drop technique. *International Journal of Fatigue* 28 (2006), Nr. 9, S. 1059–1068

16 22.10.2019 Alexander Klumpp: Influence of mechanical surface treatments on propagation and opening behavior of physically short cracks in Inconel 718

Correlation opening - growth

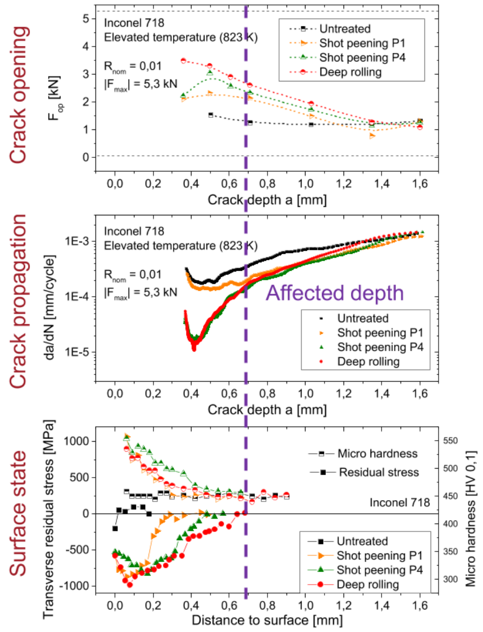

- Correlation between a, ΔK_{nom}, ΔK_{eff} (by means of FEM)

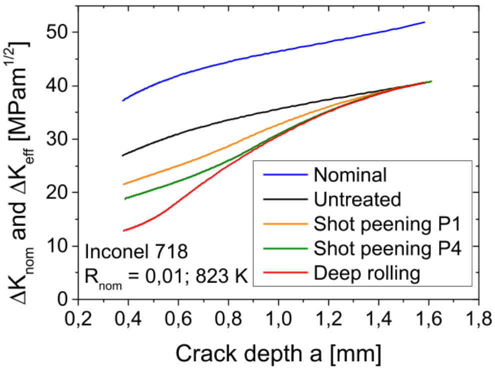

- Qualitative correlation exists:
  $F_{op}\uparrow \rightarrow \Delta K_{eff}\downarrow \rightarrow da/dN\downarrow$

17 22.10.2019 Alexander Klumpp: Influence of mechanical surface treatments on propagation and opening behavior of physically short cracks in Inconel 718

Discussion: Uncertainties during determination of crack driving forces

- Contribution of roughness-induced crack closure

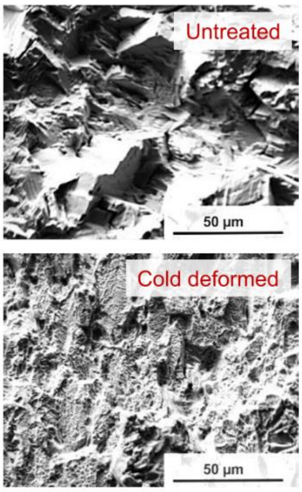

- Localization of deformation (shear bands)

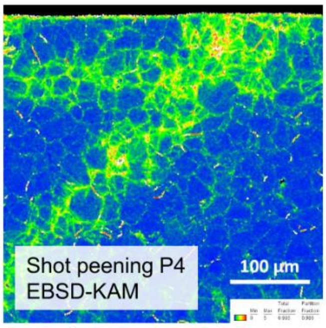

Credits: A. Kauffmann, IAM-WK

- Main challenge: Surface cracks after surface treatments

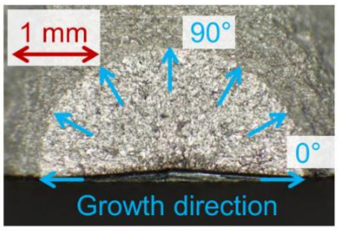

→ Further measures are necessary for clearer results

18 22.10.2019 Alexander Klumpp: Influence of mechanical surface treatments on propagation and opening behavior of physically short cracks in Inconel 718

Validation approach: FEM load analysis

- Quarter model; evaluation of K using „contour integral“ method
- Relaxed (cyclic-thermical) residual stresses as initial condition

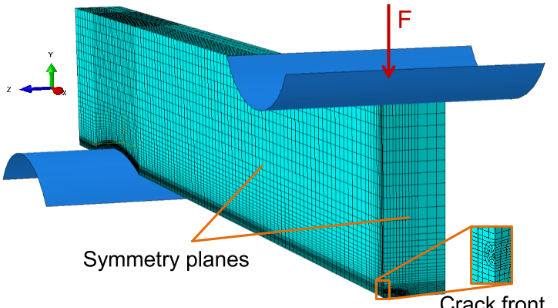

Approx. 100000x C3D20R
10 discrete models

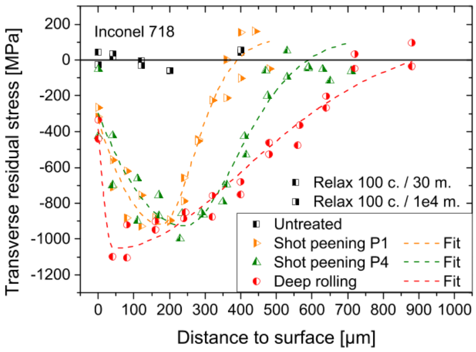

→ Determination of crack opening loads by using residual stress profiles approximately prevailing at crack initiation

19 22.10.2019 Alexander Klumpp: Influence of mechanical surface treatments on propagation and opening behavior of physically short cracks in Inconel 718

IAM Institut für Angewandte Materialien

Validation and discussion: Prediction of crack opening in the crack center

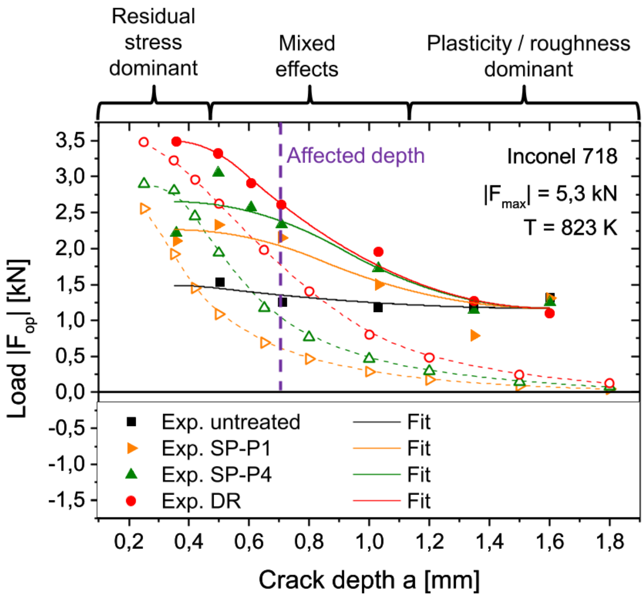

- Coincidence for very short cracks
- Increasing deviation with crack depth

→ Explanation: multicausal crack closure; no prediction possible by means of simple elastic FE analysis!

20 22.10.2019 Alexander Klumpp: Influence of mechanical surface treatments on propagation and opening behavior of physically short cracks in Inconel 718

IAM Institut für Angewandte Materialien

Absence of crack closure for R_{nom} > 0.5

- Untreated state

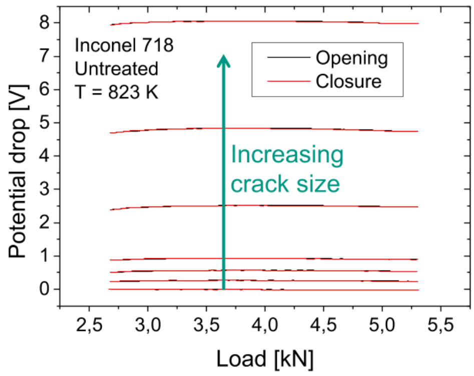

- Deep rolled state

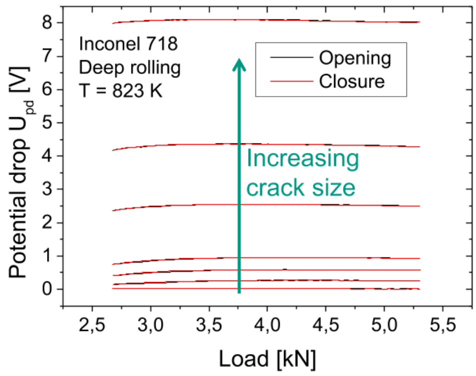

→ No closure regardless of surface treatment and crack size

21 22.10.2019 Alexander Klumpp: Influence of mechanical surface treatments on propagation and opening behavior of physically short cracks in Inconel 718

Absence of crack closure for R_{nom} > 0.5

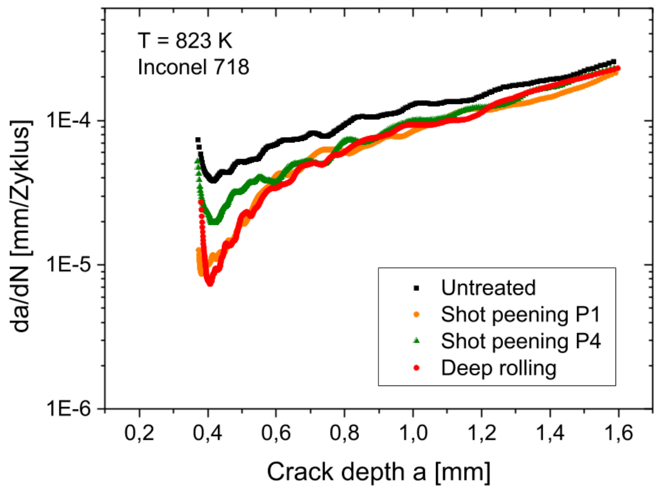

→ No closure regardless of surface treatment and crack size

→ But: Marked effect of mechanical surface treatments on crack growth

22 22.10.2019 Alexander Klumpp: Influence of mechanical surface treatments on propagation and opening behavior of physically short cracks in Inconel 718

Effective driving forces and crack growth rates

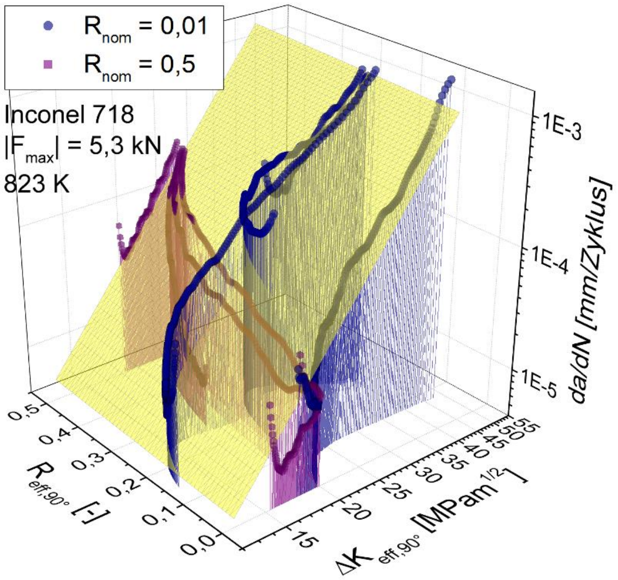

→ Partial correlation for various R_{nom}

→ Resulting lifetimes

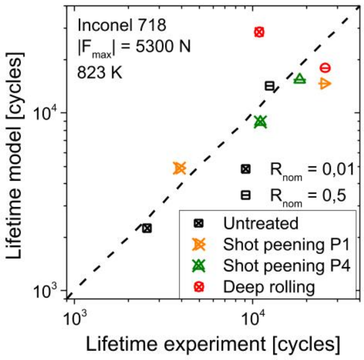

23 22.10.2019 Alexander Klumpp: Influence of mechanical surface treatments on propagation and opening behavior of physically short cracks in Inconel 718

Conclusion

- Crack propagation and opening behavior in untreated, shot peened and deep rolled Inconel 718 was investigated
- An experimental method for the measurement of crack opening loads was developed
  → Good means of characterization despite inherent uncertainties
- Closure-based crack growth description approach was presented
  - Strong effect of mechanical surface treatments even in the case of non-closure
  → Description of crack propagation in residual stress field requires at least two driving variables

24 22.10.2019 Alexander Klumpp: Influence of mechanical surface treatments on propagation and opening behavior of physically short cracks in Inconel 718

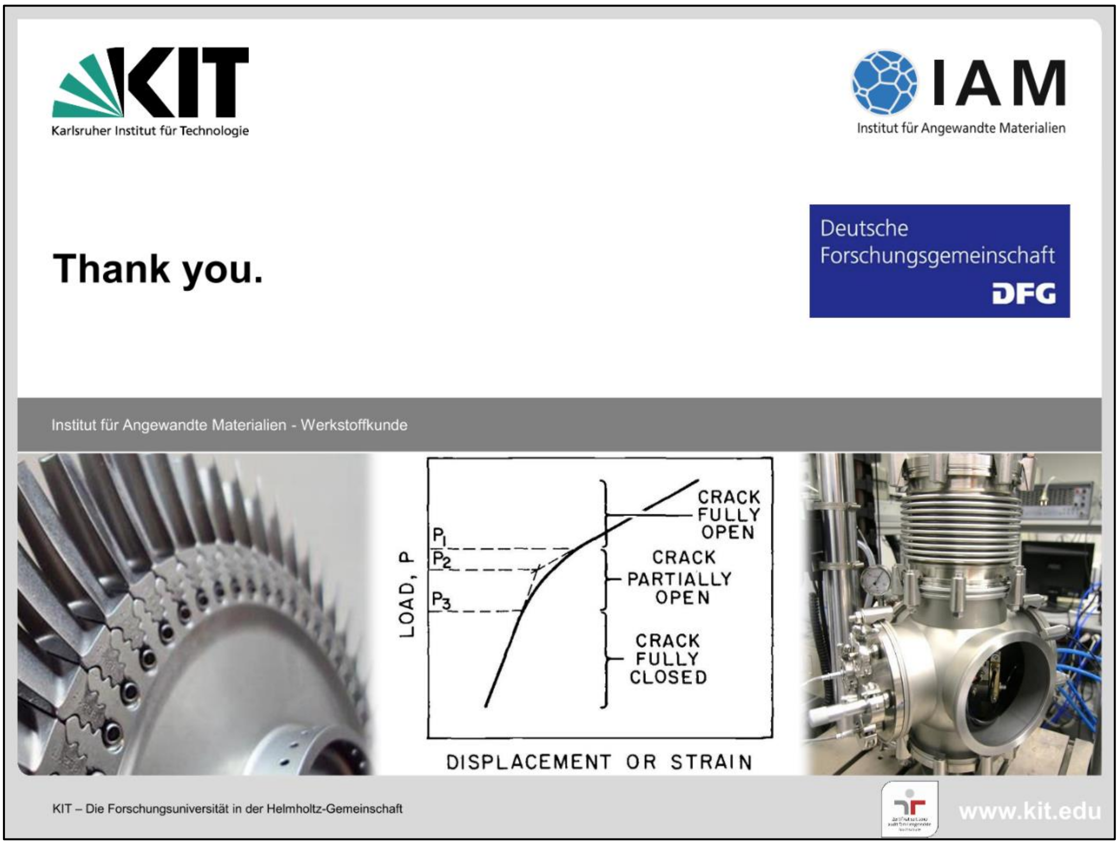
KIT
Karlsruher Institut für Technologie
IAM
Institut für Angewandte Materialien
Thank you.
Deutsche
Forschungsgemeinschaft
DFG
Institut für Angewandte Materialien - Werkstoffkunde
CRACK FULLY OPEN
CRACK PARTIALLY OPEN
CRACK FULLY CLOSED
P1
P2
P3
LOAD, P
DISPLACEMENT OR STRAIN
KIT – Die Forschungsuniversität in der Helmholtz-Gemeinschaft
www.kit.edu

Controlled Pneumatic Needle Peening – New Peening Technology for Aerospace Applications

Holger Polanetzki

MTU Aero Engines GmbH

Symposium – Mechanische Oberflächenbehandlung 2019
8th Workshop Machine Hammer Peening
Karlsruhe 22. und 23. Oktober

22.Oktober 2019 **Holger Polanetzki**

Pneumatic Needle Peening 1

Contents

Contents

- Objectives
- Technology Description
- Experimental Procedure
- Results
  - Surface Roughness
  - Residual Stress Distribution
  - Fatigue Testing
- Application
- Conclusion
- Acknowledgement

Pneumatic Needle Peening 2

Objective

- Develop new technique that could fulfill requirements:
  - Comparable or better results than conventional shot peening
    - Surface Finish
    - Residual Stress Distribution
    - Fatigue Life
  - Acceptable on Rotating Parts
    - Small head for better accessibility
    - No risk of Foreign Object Damage (FOD)
  - Very reproducible process
    - No operator influence

Pneumatic Needle Peening 3

SPIKER® Features

Different Heads and End Caps for different Geometries

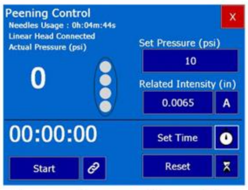

Each needle monitored in real time

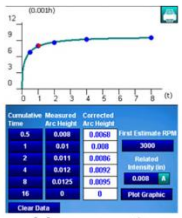

Interface guides operator, record process parameters and makes intensity calculations

Standoff distance maintained at all times

Portable unit for easy transportation

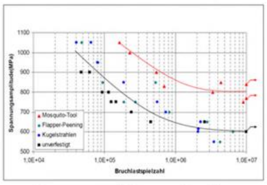

Comparable or better results than flapper or conventional peening

Save Data to USB key for quick reporting

Pneumatic Needle Peening 4

MTU Aero Engines

SPIKER® 4 Needle Linear Head with 3 End Caps

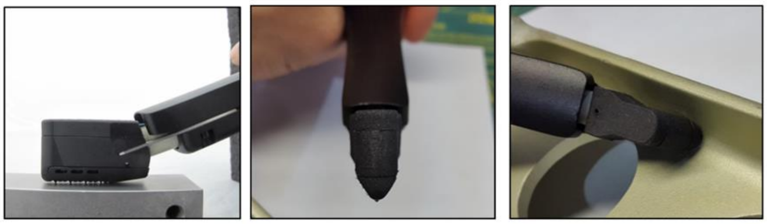

Needles	S230 tip (0.60mm), Tungsten Carbide, 4 needles
End Caps	3 included end caps: Flat surface, Corner radius down to 0.09" (2.3mm) and edge radius
Sensors	Individual tracking for each needle
Input	Proprietary air and electrical input
Maintenance	Replaceable needles and end caps
Intensity range	0.004A - 0.016A – Inch (0.10A - 0.40 mmA)
Pressure range	5 - 60 PSI (0.34 – 4.08 bar)

Pneumatic Needle Peening 5

MTU Aero Engines

SPIKER® - Radius 0.09 requirements interchangeable caps

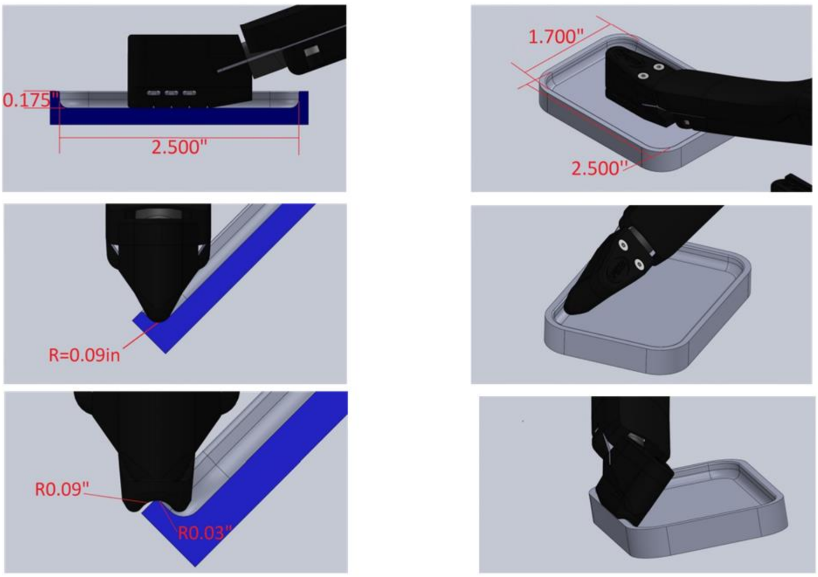

Pneumatic Needle Peening 6

SPIKER® 1 needle Corner Head

- Used on corner, pocket, radius
- Tool in contact with surface enables accurate intensity and repeatability
- Can meet radius of 0.09 inch
- Reach intensity between 4A to 16A

Pneumatic Needle Peening 7

SPIKER® Performance Testing

- Test program was performed at Technology University Clausthal in Germany under Prof. Dr. L. Wagner`s supervision
- Testing was done under the leadership of MTU Aero Engines AG
- Testing looked at surface roughness, residual stress distribution and fatigue life

Pneumatic Needle Peening 8

Experimental Procedure

- **Peening Equipment**

CNC Conventional Peening

Controlled Rotary Flapper Peening using the FlapSpeed® Controller

Controlled Needle Peening using the Spiker® tool

Pneumatic Needle Peening 9

Experimental Procedure

- **Controlled Rotary Flapper Peening**

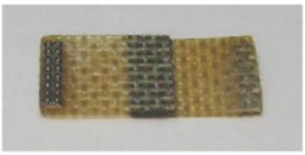

Flap

Mandrel

Magnetic Block

Almen Intensity vs. RPM Curve

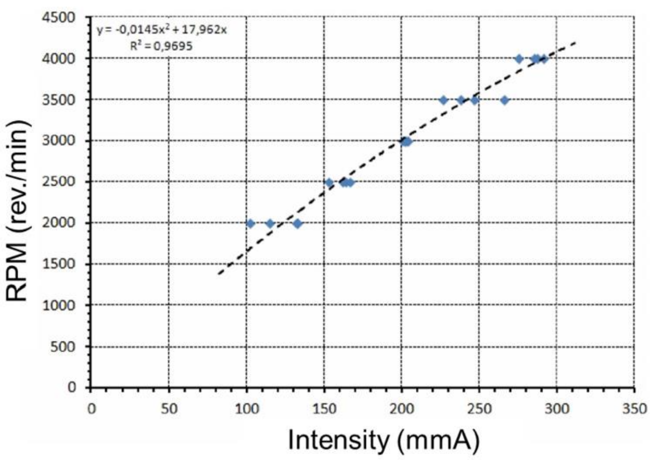

Pneumatic Needle Peening 10

Experimental Procedure

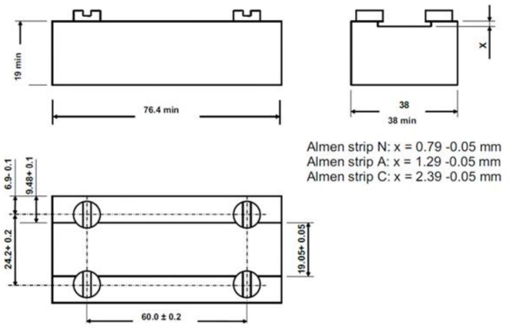

Almen strip holder for
Controlled Pneumatic Needle Peening and Forming
(all dimensions are in millimeter)

Almen Intensity vs. Pressure Curve

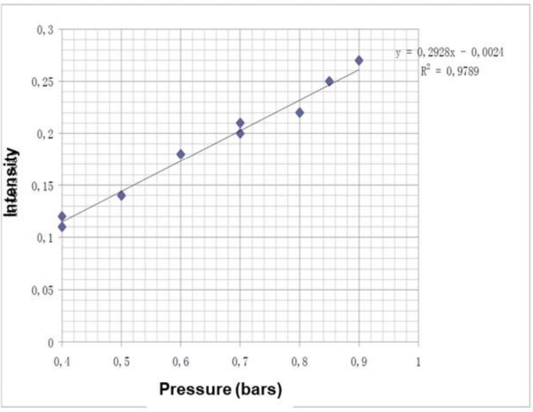

Pneumatic Needle Peening 11

Experimental Procedure

- **Material**

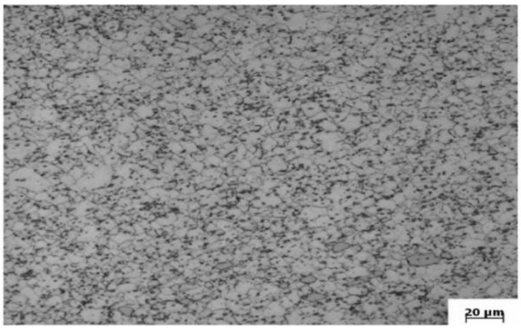

Ti-6Al-2Sn-4Zr-6Mo
- Near-β-Alloy
  Lamellar Microstructure

DA718
Nickelbase-Superalloy

Pneumatic Needle Peening 12

Experimental Procedure

- **Coupon Design**

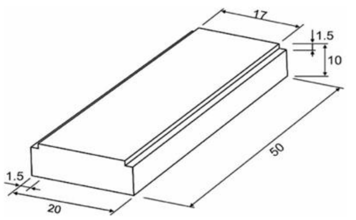

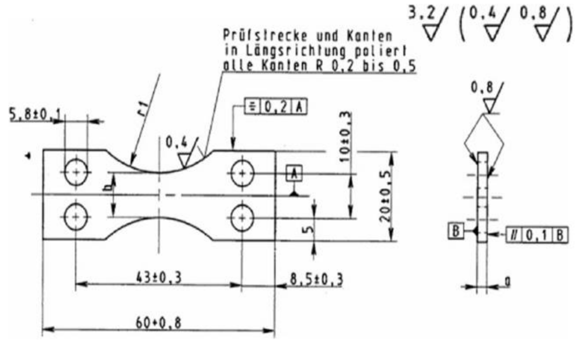

Flat Specimen for:
- Roughness measurement
  Residual stress measurement
- Metallographic Examination

Flat-Bar Bending Test Specimen for Cyclic Bending Test

Pneumatic Needle Peening 13

Experimental Procedure

- **Specimen Holder**

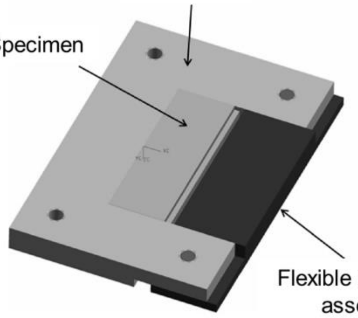

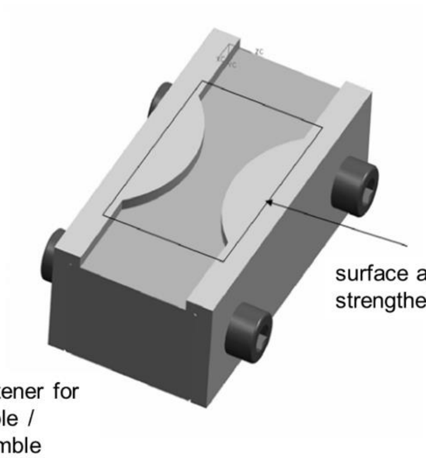

Pneumatic Needle Peening 14

MTU Aero Engines

Results

•Surface Finish: A strip, 0.006-0.008A Intensity

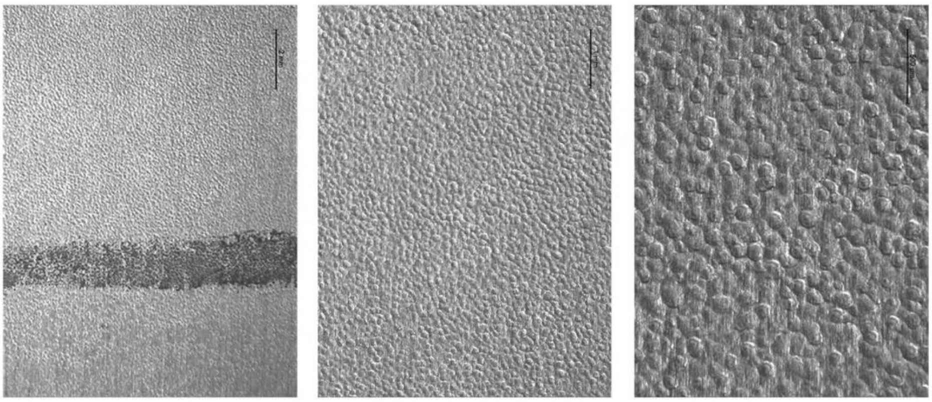

10x 20x 50x

Pneumatic Needle Peening 15

MTU Aero Engines

Results

- **Surface Roughness Ti-6246**

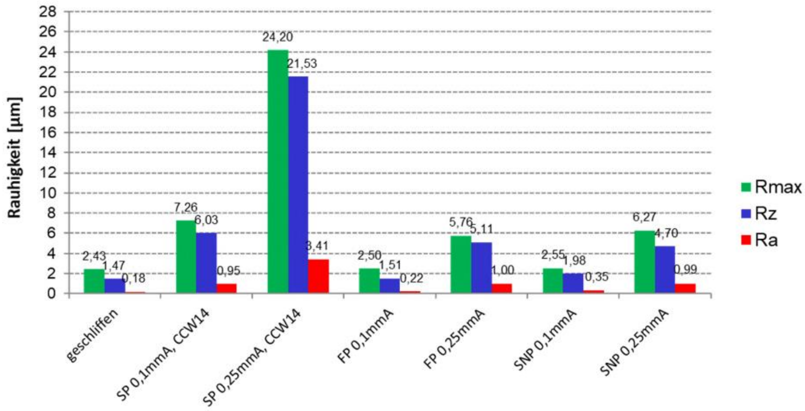

•Roughness rises with Intensity.

•Roughness achieved by the Flapper Peening is an order of magnitude lower than Shot Peening.

•Pneumatic needle peening tool gives roughness in the same scale as Flapper Peening.

Pneumatic Needle Peening 16

MTU Aero Engines

Results

•Surface Roughness DA718

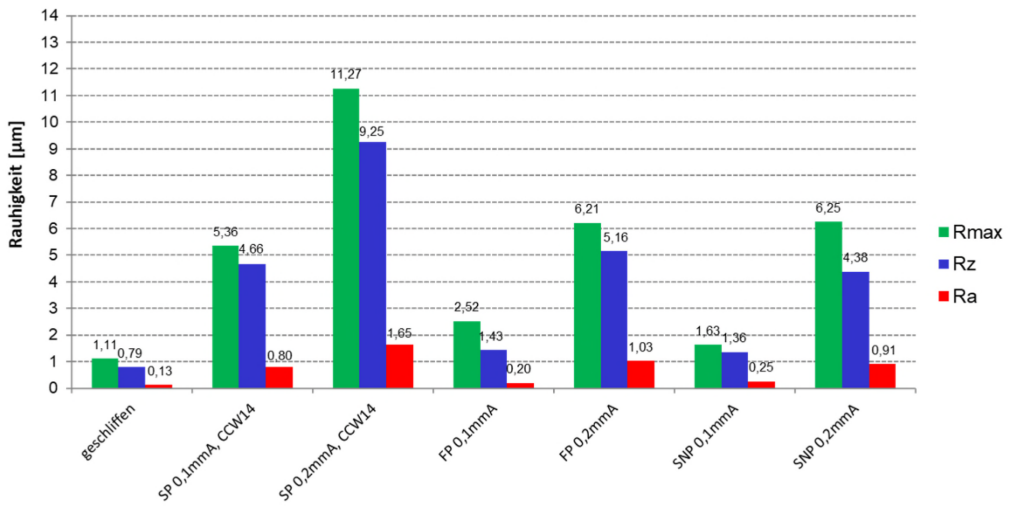

Pneumatic Needle Peening 17

MTU Aero Engines

Results

- **Residual Stress Distribution Ti6246, Intensity = 0.004A**

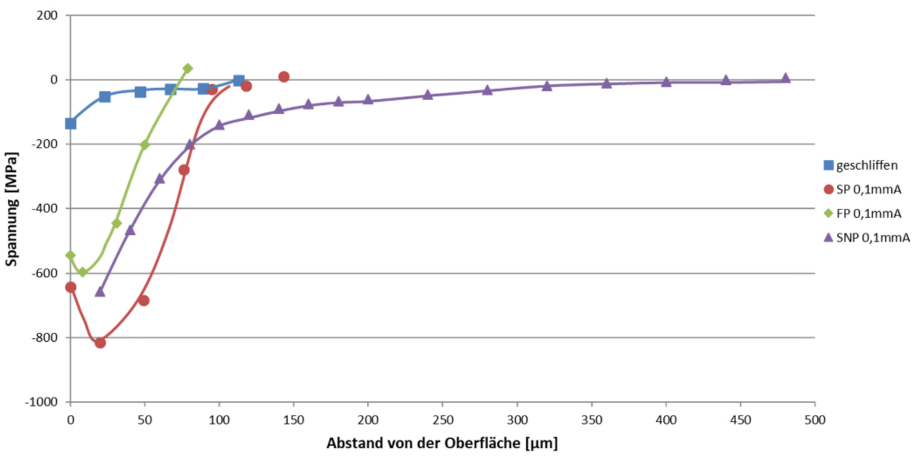

•Graph shows no significant difference between the different techniques.

Pneumatic Needle Peening 18

Results

- **Residual Stress Distribution Ti6246, Intensity = 10A**

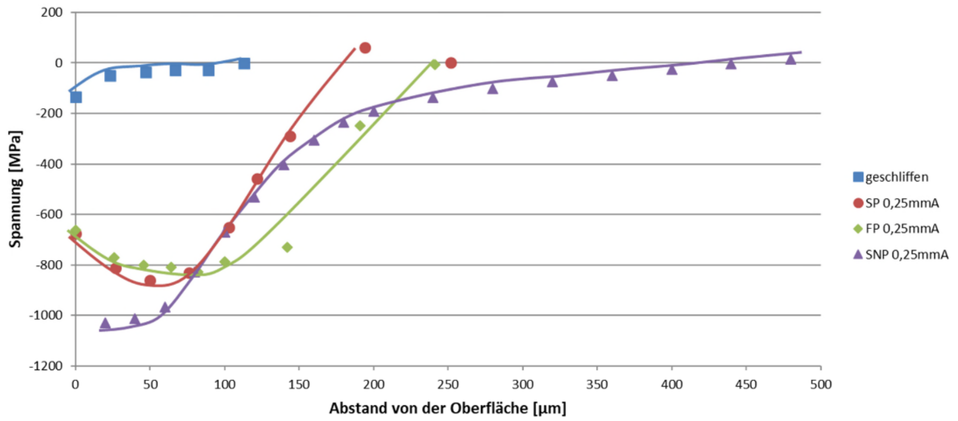

- Conventional Peening produced the greatest depth of compressive layer.
- The Spiker® produced the most negative stress level on the surface.

Pneumatic Needle Peening 19

Results

- **Residual Stress Distribution DA718, Intensity = 0.004A**

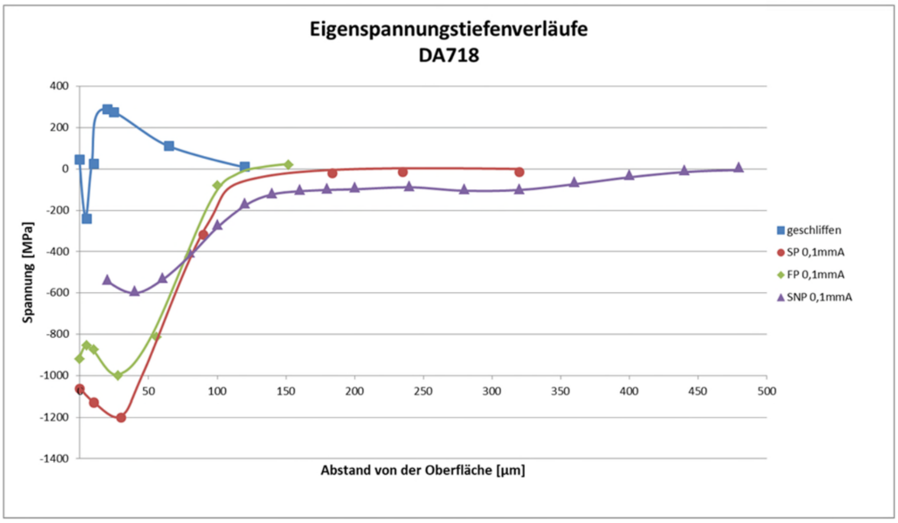

Pneumatic Needle Peening 20

MTU Aero Engines

Results

- **Residual Stress Distribution DA718, Intensity = 0.008A**

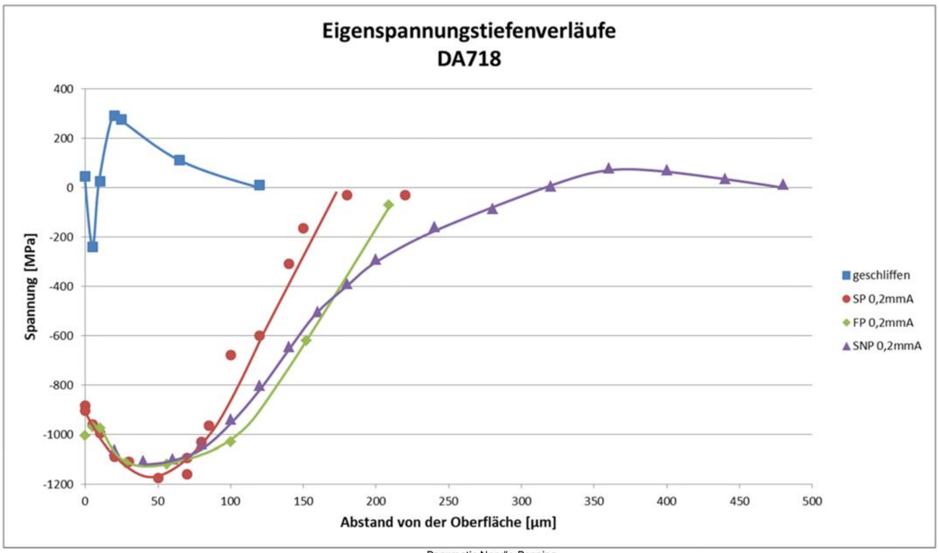

MTU Aero Engines

Results

- **Fatigue Results Ti6246, Intensity = 0.004A**

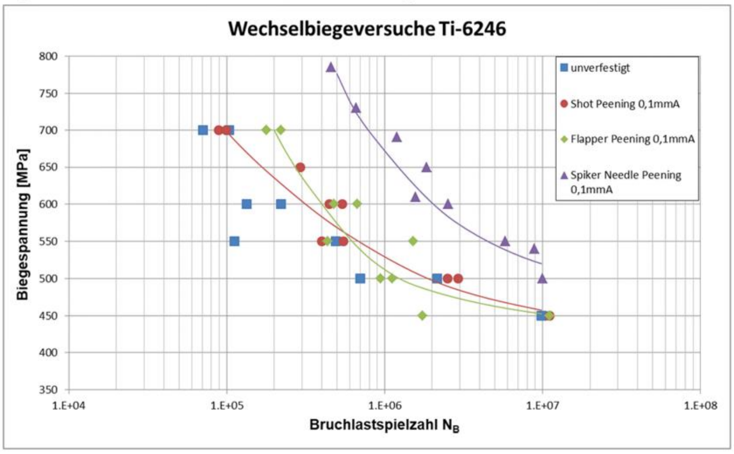

- Conventional Peening and Flapper Peening produced similar results
- The Spiker® provided the most significant fatigue life improvement

MTU Aero Engines

Results

- **Fatigue Results Ti6246, Intensity = 0.010A**

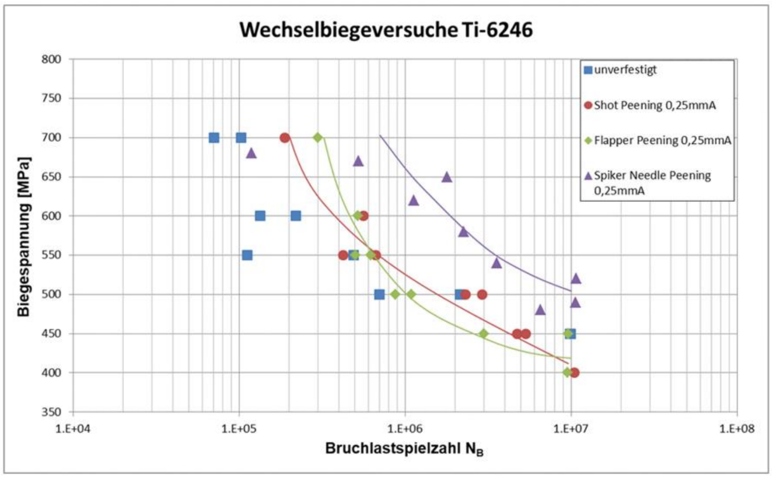

- Higher intensity peening confirms the trend shown in the previous slides.

Pneumatic Needle Peening 23

MTU Aero Engines

Results

- **Fatigue Results DA718, Intensity = 0.004A**

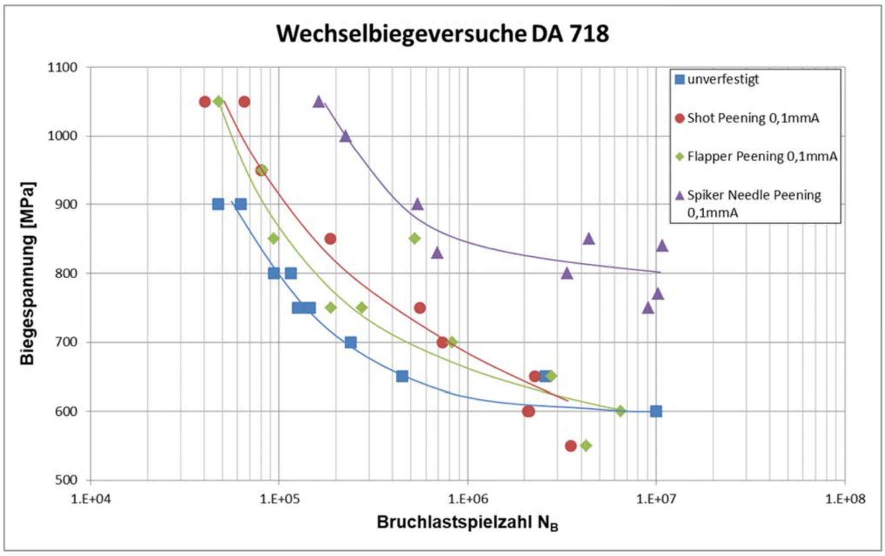

Pneumatic Needle Peening 24

Results

- **Fatigue Results DA718, Intensity = 0.008A**

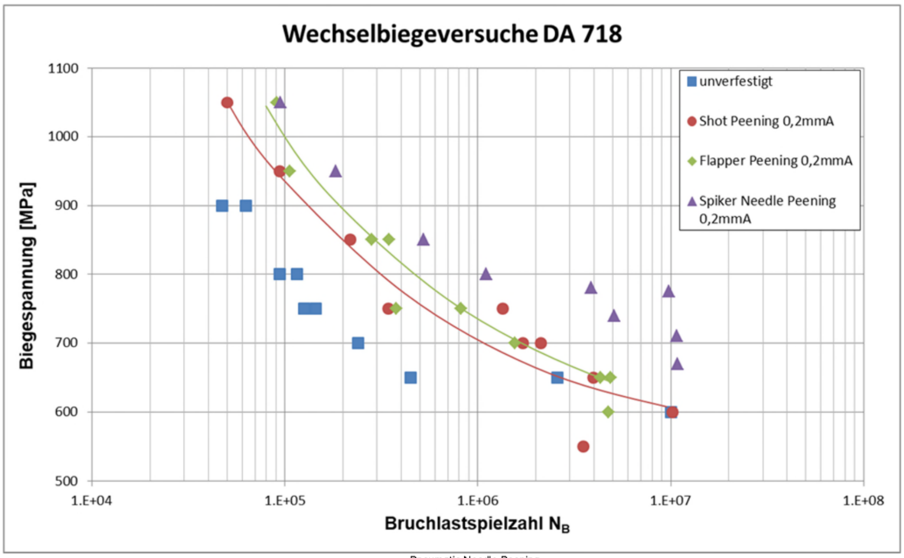

Pneumatic Needle Peening 25

Spiker® Applications

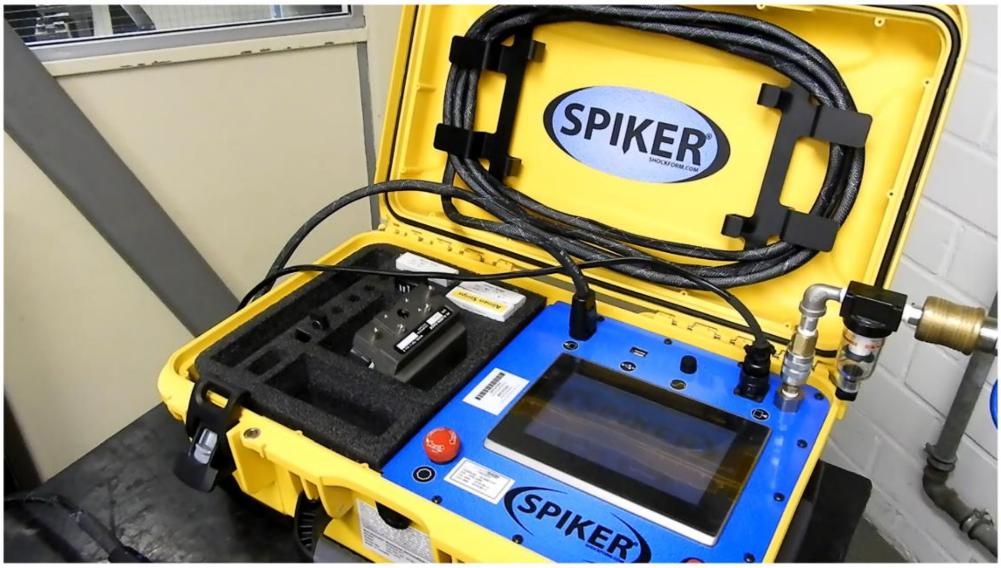

Pneumatic Needle Peening 26

MTU Aero Engines

Spiker® Applications

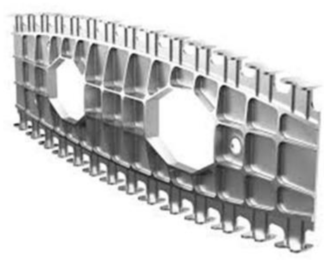

V2500 Turbine Exhaust Case
Save of 40 man hours

CF6-80 HPT Blades
Tip-Repair

Bulhead Pockets and
difficult to reach geometries

Pneumatic Needle Peening 27

MTU Aero Engines

Specification

AMS 2545 Controlled Pneumatic Needle Peening, Straightening and Forming

Issued 2017 – 11

Nadcap Checklist AC7117/6 for Needle Peening

Ballot for Approval 2019 - 07

Pneumatic Needle Peening 28

Conclusion

- **In this study, the new Spiker® Needle Peening Tool has shown:**
    - A Surface Finish that is equivalent to flapper peening and usually better than conventional peening
    - Residual Stress Distribution that can be deeper on the surface that conventional or flapper peening
    - Fatigue Life that are equivalent and often much better than conventional or flapper peening
    - Easy application on aero-engine components with significant cost saving potential

Acknowledgement

- Prof. Dr. L. Wagner and his employees at the institute of material technology at the University of Technology Clausthal for their support and realization of the scientific investigations.
- Mr. Norbert Huber and Götz Lebküchner for their support and helpful consultation during the development of the head for the Spiker™ tool

Experimental analysis of the surface integrity of stainless steel modified by robot based machine hammer peening

Lars Uhlmann

Laboratory for Machine Tools and Production Engineering WZL

RWTH Aachen University

Experimental analysis of the surface integrity of stainless steel modified by robot based machine hammer peening

Thomas Bergs, Lars Uhlmann*, Robby Mannens, Daniel Trauth

Laboratory for Machine Tools and Production Engineering (WZL) of RWTH Aachen

Symposium Mechanical Surface Treatment 2019,
Karlsruhe, 22.10.2019

Fraunhofer IPT | WZL | RWTH AACHEN UNIVERSITY

Motivation
Usage of stainless steel X5CrNi18-10 (1.4301)

X5CrNi18-10 is used in chemically active environments, e.g. for shafts of seawater pumps.

- The surface layer is exposed to
  - high tribological loads and
  - dynamic loads leading to the formation of microcracks.
- This results in the following surface requirements:
  - hard and wear-resistant surface layer and
  - soft and ductile inner material.

Fraunhofer IPT | WZL | RWTH AACHEN UNIVERSITY

Slide 2

Introduction
Machine hammer peening (MHP)

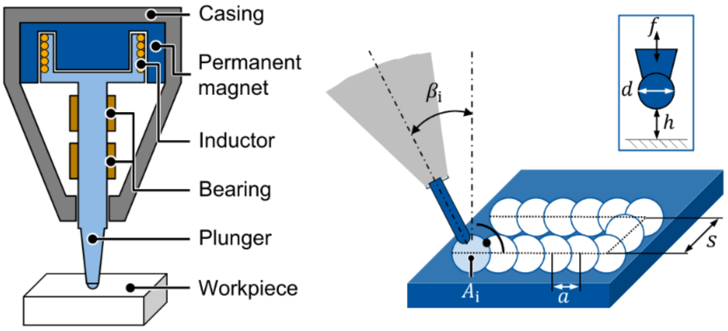

Process parameter	Symbol
Impact angle	β_i
Stepover distance	s
(Hammer) head diameter	d
Hammering frequency	f
Stroke	h
Projected area of indentation	A_i
Distance of indentations	a

(acc. to VDI 3416)

- Work hardening and compressive residual stresses are induced into the surface layer.
- Surface of the specimen may be structured or smoothed.

Source: [VDI18]

Fraunhofer IPT | WZL | RWTH AACHEN UNIVERSITY

Agenda

1 **Introduction**

2 **Experimental set-up**

3 **Surface integrity of peened surfaces**

4 **Description model for the Vickers hardness**

5 **Summary and outlook**

Fraunhofer IPT | WZL | RWTH AACHEN UNIVERSITY

Experimental set-up
Processing of X5CrNi18-10 with a robot based MHP system

Experimental design

Full factorial experimental design with variation of the factors:

Head diameter d [mm]	6	12
Stroke h [mm]	0.3	1.2
Distance of indentation a [mm]	0.05	0.4
Impact angle β_i [°]	0	30

In addition:

Experiment with multiple processing (n = 5):
$d = 6$ mm; $h = 1.2$ mm; $a = 0.05$ mm; $\beta_i = 0°$

Center point experiment:
$d = 8$ mm; $h = 0.75$ mm; $a = 0.225$ mm; $\beta_i = 15°$

n: number of processing

MHP system adapted to an industrial robot

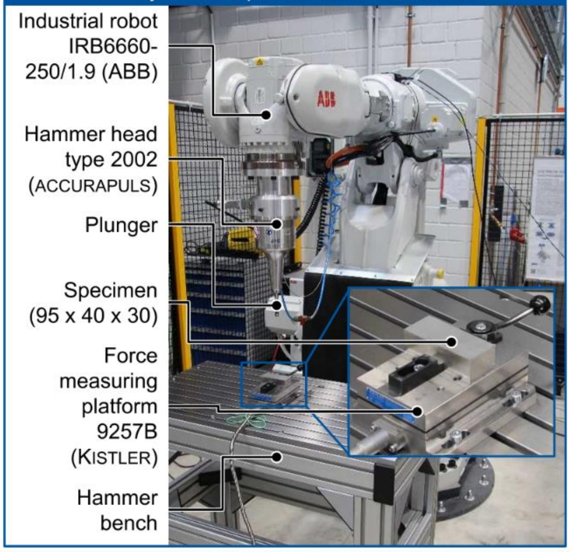

Fraunhofer IPT | WZL | RWTH AACHEN UNIVERSITY
Slide 5

Experimental set-up
Robot based machine hammer peening

Velocity profile of a linear robot movement

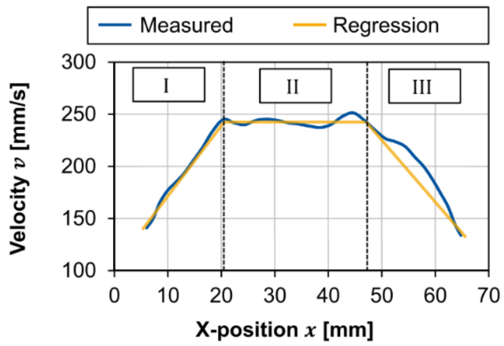

- The velocity profile consists of three characteristic areas.
- The highest set speed was reached sufficiently fast.

Path accuracy

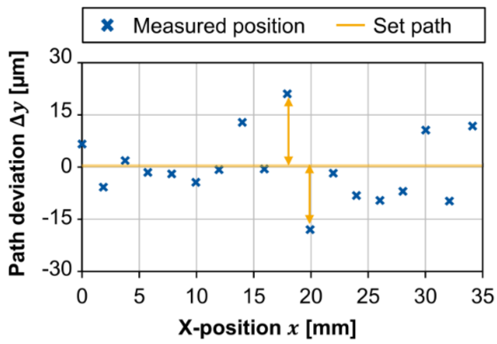

- The maximum path deviation was $\Delta y = 21$ µm.
- Overshoot in opposite direction after maximum deviation was observed.

Consideration of the robot acceleration is necessary. The high path accuracy is reached due to a high robot stiffness.

Fraunhofer IPT | WZL | RWTH AACHEN UNIVERSITY
Slide 6

Experimental set-up
Peening force

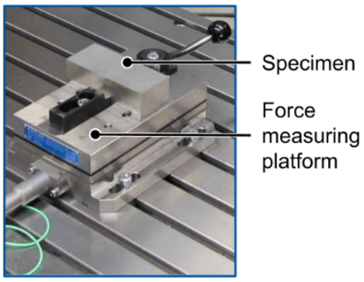

- The specimen was fixed by clamping.
- MHP at the center of the specimen to ensure a direct force application.
- Specimen (42CrMo4) was treated by MHP in advance to the tests.

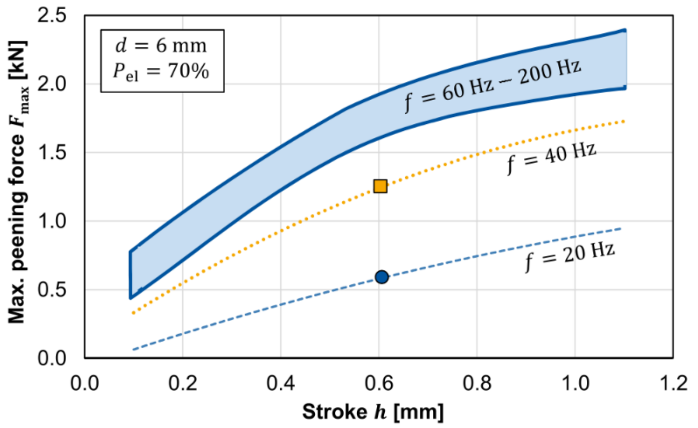

f: hammer frequency, d: head diameter, P_{el}: percentage of electrical power

Up to a frequency of 60 Hz the maximum force rises with frequency. Between 60 Hz and 200 Hz the maximum force does not vary much. Results qualitatively in accordance with TRAUTH [TRAU16].

Fraunhofer IPT WZL RWTH AACHEN UNIVERSITY

Slide 7

Experimental set-up
Limitation of the adjustable stroke by the frequency (Video)

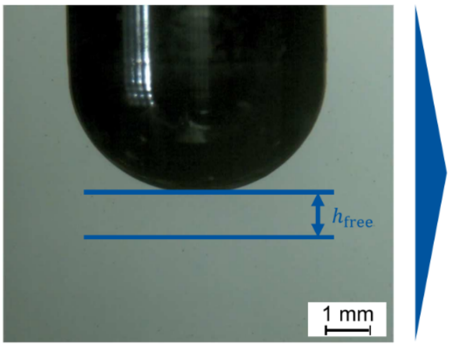

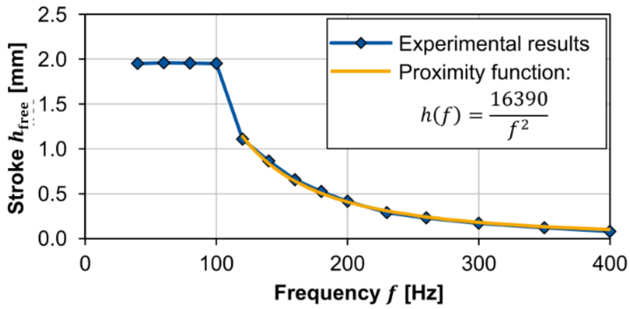

- Free stroke decreases with increasing frequency.
- The stroke may not be greater than the free stroke.
- Restriction of the combination of the stroke and the frequency exists.
- For frequencies smaller or equal $f = 100$ Hz the stroke may be $h < 1.955$ mm. For $f = 200$ Hz the stroke may only be $h < 0.416$ mm.

Fraunhofer IPT WZL RWTH AACHEN UNIVERSITY

Slide 8

Agenda

1 Introduction

2 Experimental set-up

3 Surface integrity of peened surfaces

4 Description model for the Vickers hardness

5 Summary and outlook

Fraunhofer IPT | WZL | RWTH AACHEN UNIVERSITY

Slide 9

Surface integrity of peened surfaces
Evaluation of the residual stresses

ESPI hole drilling method (PRISM System of STRESSTECH)

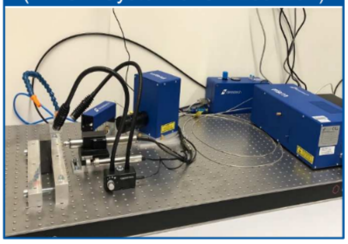

- Removing material results in a new stress equilibrium achieved by deformation.
- Deformation is measured by using optical interferometry.
- Removed stress is calculated from measured displacement.

Source: www.stresstech.com

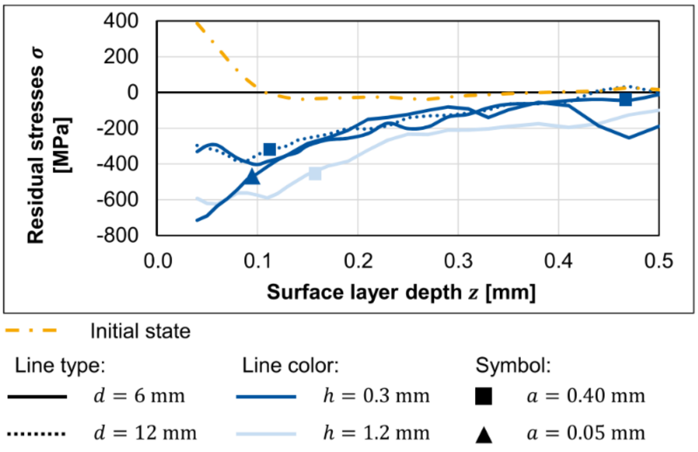

- Raising the stroke results in inducing compressive residual stresses into a deeper surface layer depth.
- Decreasing the distance of indentation a results in higher compressive residual stresses until a depth of $z \approx 0.11$ mm.

Fraunhofer IPT | WZL | RWTH AACHEN UNIVERSITY

Slide 10

Surface integrity of peened surfaces
EBSD analysis

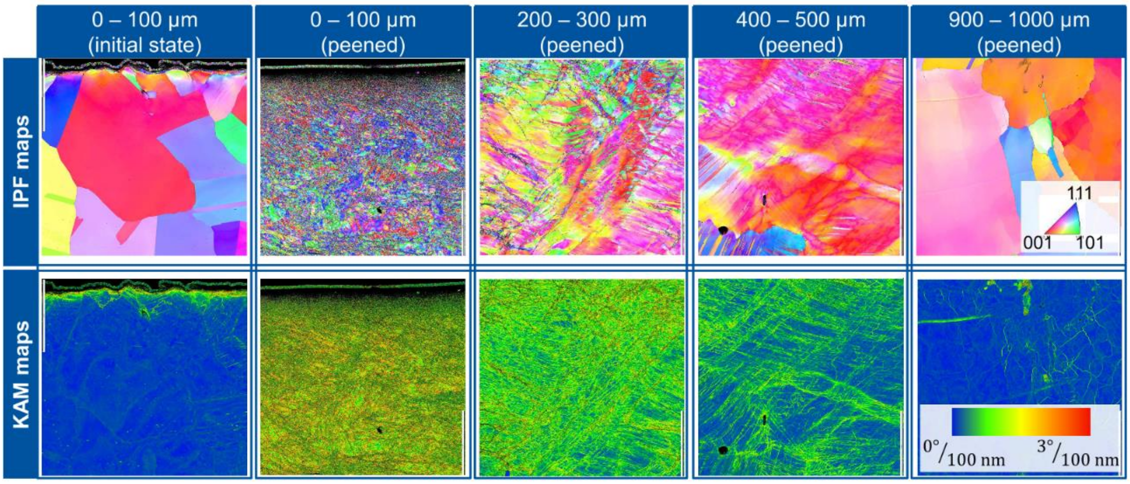

KAM: Kernel average misorientation, IPF: Inverse pole figure

Subgrain refinement in the surface layer until a depth of $z = 900$ µm observed. Misorientation maps suggest an increase in dislocation density.

Slide 11

Surface integrity of peened surfaces
Evaluation of the surface roughness

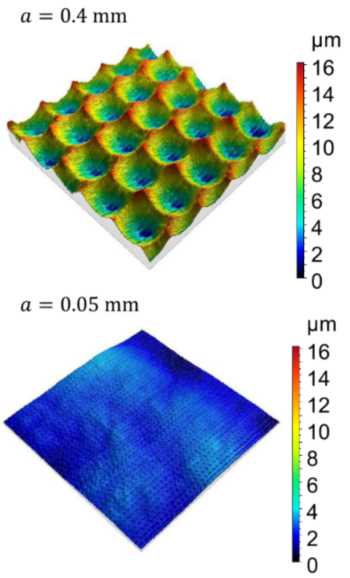

The surface is **smoothened** by adjusting the parameter settings as followed:

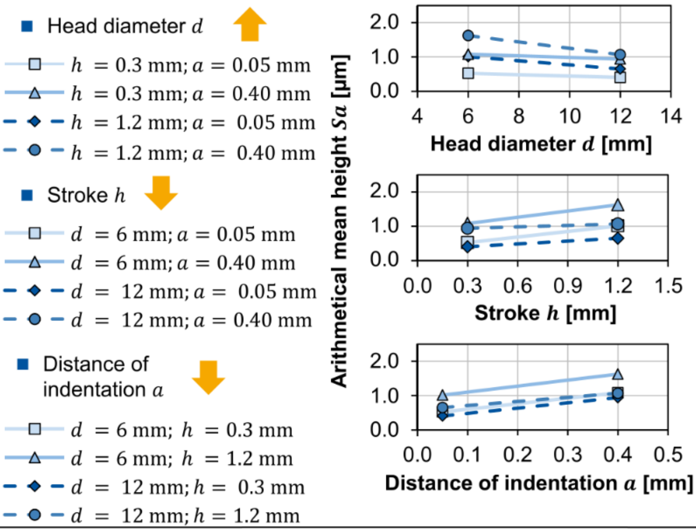

Slide 12

Surface integrity of peened surfaces
Evaluation of the surface hardness

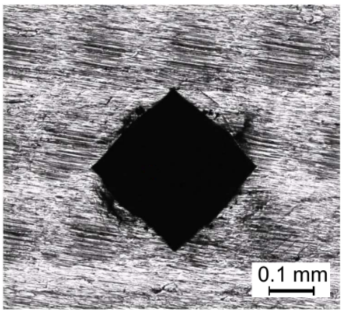

Work hardening is influenced by the investigated process parameters as followed:

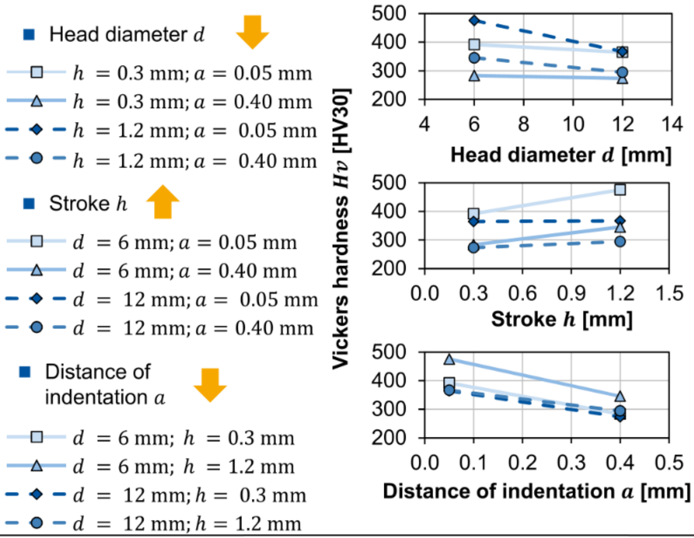

Fraunhofer IPT | WZL | RWTH AACHEN UNIVERSITY

Slide 13

Agenda

1 **Introduction**

2 **Experimental set-up**

3 **Surface integrity of peened surfaces**

4 **Description model for the Vickers hardness**

5 **Summary and outlook**

Fraunhofer IPT | WZL | RWTH AACHEN UNIVERSITY

Slide 14

Description model for the Vickers hardness
Developing the description model

Equation of a description model acc. to KLOCKE

$$\hat{y}(x,t,u,\dots) = c_0 \cdot x^{c_1} \cdot t^{c_2} \cdot u^{c_3} \dots ()^0$$

$\hat{y}$	: Quality feature
x, t, u	: Input variables
c_0, c_1, c_2, c_3	: Coefficients of the regression model

$$\widehat{HV}(d,h,a,\beta_i) = c_0 \cdot d^{c_1} \cdot h^{c_2} \cdot a^{c_3} \cdot \beta_i^{c_4}$$

$\widehat{HV}$	: Vickers hardness as quality feature
d	: Hammer diameter
h	: Stroke
a	: Distance of Indentation
β_i	: Impact angle
c_0, c_1, c_2, c_3	: Coefficients of the regression model

- The regression model was developed from the friction model of FILZEK and LUDWIG.
- KLOCKE extendet the existing model to be suitable for general use. Therefore the model is suitable to be used to describe the behavior of the Vickers hardness after MHP.
- The experimental parameters and results served as data to determine the coefficients of the regression model c_0, c_1, c_2 and c_3.
- The parameters and results of the center point experiment was not used to determine the coefficients of the regression model. Instead they were used for the validation.

Source: [KLOC15], [FILZ13]

Fraunhofer IPT | WZL | RWTH AACHEN UNIVERSITY

Slide 15

Description model for the Vickers hardness
Accuracy of the description model

$$\widehat{HV}(d,h,a,\beta_i) = 2.19 \cdot d^{-0.393} \cdot h^{0.227} \cdot a^{-0.285} \cdot \beta_i^{1.057}$$

$\widehat{HV}$	: Vickers hardness as quality feature	a	: Distance of Indentation
d	: Hammer diameter	β_i	: Impact angle
h	: Stroke		

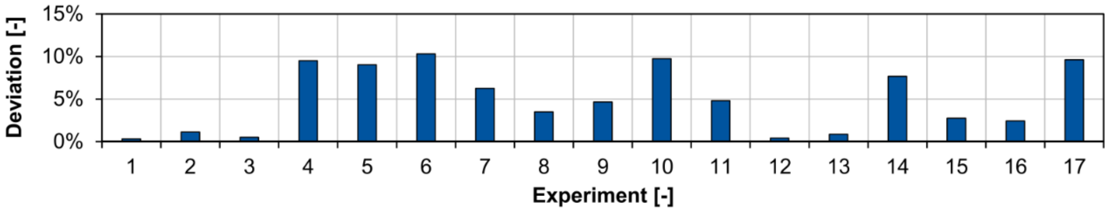

The Vickers hardness of the center point experimental measurement and the model prediction deviates by 9.6 %. The highest deviation of the model and the measured value is 10.3 %.

Fraunhofer IPT | WZL | RWTH AACHEN UNIVERSITY

Slide 16

Agenda

1 Introduction

2 Experimental set-up

3 Surface integrity of peened surfaces

4 Description model for the Vickers hardness

5 Summary and outlook

Slide 17

Summary and outlook
Conclusions from the investigations

Summary

- The positioning accuracy of the industrial robot is high during MHP.
- Grain refinement due to MHP was observed up to a depth of $z \approx 900\ \mu m$.
- Compressive residual stresses of maximal $\sigma = -820$ Mpa were induced.
- The linear description model has a high prediction accuracy with a maximum deviation of 7.6 % within the considered process room.

Outlook

- Investigation of the cause-effect relations between process parameters, grain refinement and dislocation density.
- Developing an accurate description model for the roughness by extending the linear description model to a quadratic model.
- Improving a finite element model to support the experimental results by predicting the dislocation density and grain size.

Slide 18

Your contact persons

Chair of Manufacturing Technology
Laboratory for Machine Tools and Production Engineering WZL of RWTH Aachen
Campus-Boulevard 30
D-52074 Aachen

Lars Uhlmann, M.Sc. M.Sc.

Research Associate
0 241/ 80 27428
l.uhlmann@wzl.rwth-aachen.de

Robby Mannens, M.Sc. RWTH

Research Associate
0 241/ 80 28244
r.mannens@wzl.rwth-aachen.de

Fraunhofer IPT

Slide 19

Bibliography

[FILZ13] Filzek, J.; Ludwig, M.: Berücksichtigung der Reibung in der FEM-Simulation. In: Umformen, Schneiden, Verbinden im Leichtbau. Machbarkeit - Produktivität - Qualität ; Tagungsband des 33. EFB-Kolloquiums Blechverarbeitung 2013 am 16. und 17. April 2013 in Fellbach. (Reihe: Tagungsband / Europäische Forschungsgesellschaft für Blechverarbeitung e.V. T 36). Aufl. Hannover: EFB, 2013

[KLOC15] Klocke, F.; Trauth, D.; Shirobokov, A.; Mattfeld, P.: FE-analysis and in situ visualization of pressure-, slip-rate-, and temperature-dependent coefficients of friction for advanced sheet metal forming. Development of a novel coupled user subroutine for shell and continuum discretization. In: The International Journal of Advanced Manufacturing Technology, 81. Jg., 2015, Nr. 1-4, S. 397–410

[VDI18] VDI 3416 (2018): Maschinelles Oberflächenhämmern

Fraunhofer IPT

Slide 20

Analyses of technical and true overlap in hammer peening operations

Eric Segebade

wbk Institute of Production Science

Karlsruhe Institute of Technology


Karlsruhe Institute of Technology
wbk
Institute of Production Science
ANALYSES OF TECHNICAL AND TRUE OVERLAP IN HAMMER PEENING OPERATIONS
E. Segebade, A. Hilligardt, V. Schulze
KIT – The Research University in the Helmholtz Association
www.wbk.kit.edu

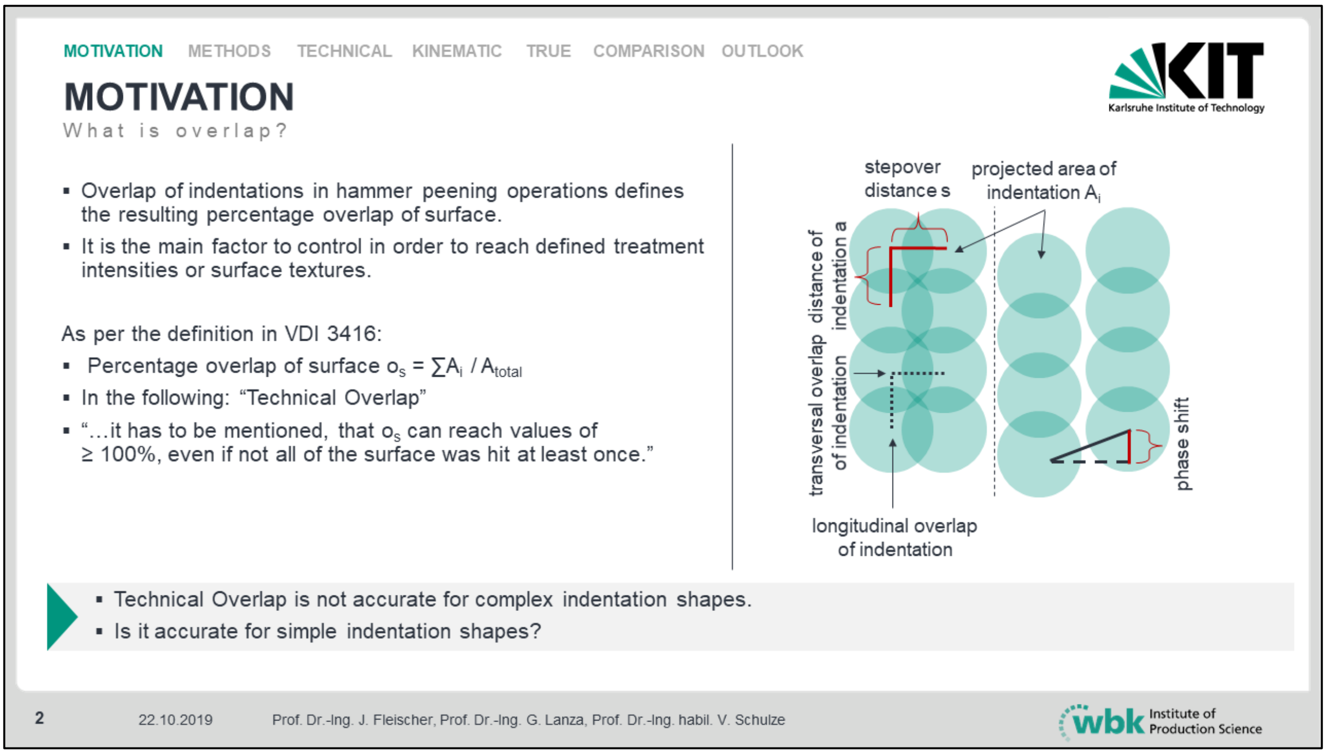
MOTIVATION METHODS TECHNICAL KINEMATIC TRUE COMPARISON OUTLOOK
MOTIVATION
What is overlap?
Karlsruhe Institute of Technology
▪ Overlap of indentations in hammer peening operations defines the resulting percentage overlap of surface.
▪ It is the main factor to control in order to reach defined treatment intensities or surface textures.
As per the definition in VDI 3416:
▪ Percentage overlap of surface $o_s = \sum A_i / A_{total}$
▪ In the following: "Technical Overlap"
▪ "…it has to be mentioned, that o_s can reach values of ≥ 100%, even if not all of the surface was hit at least once."
stepover distance s
projected area of indentation A_i
transversal overlap of indentation
distance of indentation a
longitudinal overlap of indentation
phase shift
▪ Technical Overlap is not accurate for complex indentation shapes.
▪ Is it accurate for simple indentation shapes?
2
22.10.2019
Prof. Dr.-Ing. J. Fleischer, Prof. Dr.-Ing. G. Lanza, Prof. Dr.-Ing. habil. V. Schulze
wbk Institute of Production Science

MOTIVATION METHODS TECHNICAL KINEMATIC TRUE COMPARISON OUTLOOK

METHODS

Technical overlap vs. kinematic overlap vs. true overlap

Technical overlap

Simple calculation of area of indentation:

- Calculate secant
  - $s = \sqrt{i_{depth} * (d - i_{depth})}$
- Calculate area of indentation
  - $A_i = (s/2)^2 * \pi$
- Calculate o_s
  - $o_s = n * A_i / A_{total}$

Kinematic overlap

Numerical calculation in Matlab:

- Load .stl geometry
- Create master-indentation (dexel)
- Create translation matrix
- Calculate new surface with (w) and without (w/o) consideration of former indentations

True overlap

Full thermo-mechanical FEM:

Material model

- Voce-Kocks-Vöhringer (AISI 4140)

Body boundary conditions

- 5 x 5 x 5 mm elastic body
- 0.5 x 0.5 x 0.1 mm elastic-plastic body
- Rigid tool, constant Temperature: RT

Surface element edge length

- 0.005 mm, no remeshing

Tool movement

- Position & velocity based

- Kinematic overlap w/o consideration of former indentations and technical overlap should be the same.
- Elasto-plastic FE-simulation result should be closest to the truth and higher than kinematic overlap (w).

3 22.10.2019 Prof. Dr.-Ing. J. Fleischer, Prof. Dr.-Ing. G. Lanza, Prof. Dr.-Ing. habil. V. Schulze

MOTIVATION METHODS TECHNICAL KINEMATIC TRUE COMPARISON OUTLOOK

TECHNICAL OVERLAP

Exemplary calculation

Technical overlap

Simple calculation of area of indentation:

- Calculate secant
  - $s = \sqrt{i_{depth} * (d - i_{depth})}$
- Calculate area of indentation
  - $A_i = (s/2)^2 * \pi$
- Calculate o_s
  - $o_s = n * A_i / A_{total}$

Example:

- Ball diameter d = 2 mm,
- A_{total} = 0.5 x 0.5 mm = 0.25 mm²
- n = 25 (5 * 5 indentations)
- a = s = 0.05 mm

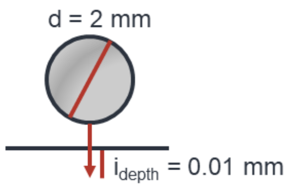

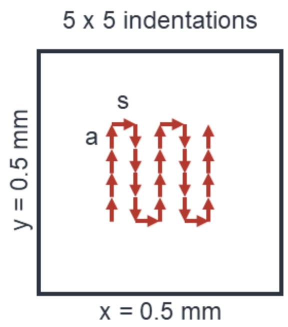

- A_i = 0.029 mm², o_s = 5 x 5 x A_i / A_{total} = 6.252
- Technical overlap in our example totals 625.2% as per VDI 3416.

4 22.10.2019 Prof. Dr.-Ing. J. Fleischer, Prof. Dr.-Ing. G. Lanza, Prof. Dr.-Ing. habil. V. Schulze

MOTIVATION METHODS TECHNICAL **KINEMATIC** TRUE COMPARISON OUTLOOK

KIT Karlsruhe Institute of Technology

KINEMATIC OVERLAP

Exemplary calculation

Kinematic overlap

Numerical calculation in Matlab:

- Load .stl geometry
- Create master-indentation (dexel)
- Create translation matrix
- Calculate overlap with and without consideration of former indentations

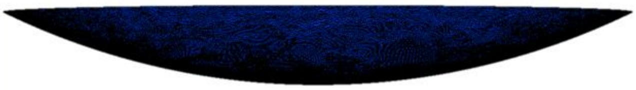

.stl – ball segment

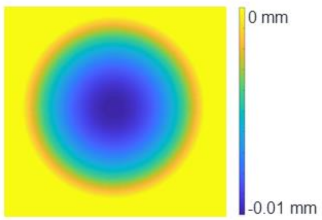

3D master-indentation

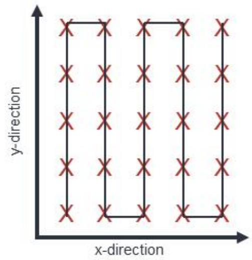

tool translation-matrix

5 22.10.2019 Prof. Dr.-Ing. J. Fleischer, Prof. Dr.-Ing. G. Lanza, Prof. Dr.-Ing. habil. V. Schulze

wbk Institute of Production Science

MOTIVATION METHODS TECHNICAL **KINEMATIC** TRUE COMPARISON OUTLOOK

KIT Karlsruhe Institute of Technology

KINEMATIC OVERLAP

Exemplary calculation

Kinematic overlap

Numerical calculation in Matlab:

- Load .stl geometry
- Create master-indentation (dexel)
- Create translation matrix
- Calculate overlap with and without consideration of former indentations

Main sources of errors

- .stl element edge length (eel)
- x-y surface resolution (res)

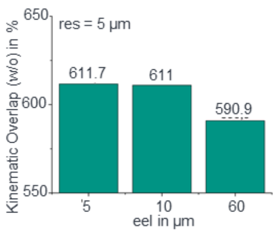

stl element edge length convergency

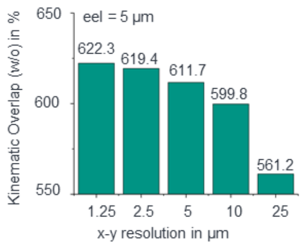

resolution convergency

6 22.10.2019 Prof. Dr.-Ing. J. Fleischer, Prof. Dr.-Ing. G. Lanza, Prof. Dr.-Ing. habil. V. Schulze

wbk Institute of Production Science

KINEMATIC OVERLAP

Exemplary calculation

Kinematic overlap

Numerical calculation in Matlab:

- Load .stl geometry
- Create master-indentation (dexel)
- Create translation matrix
- Calculate overlap with and without consideration of former indentations
  - eel = 5 µm
  - res = 1.25 µm

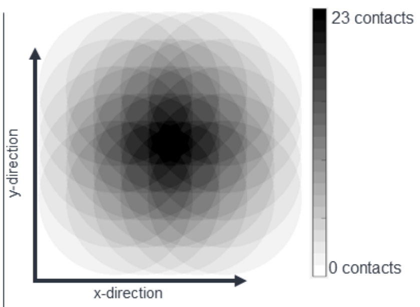

Kinematic Overlap (w/o)
without consideration of former indentations
→ o_s = 622.3%

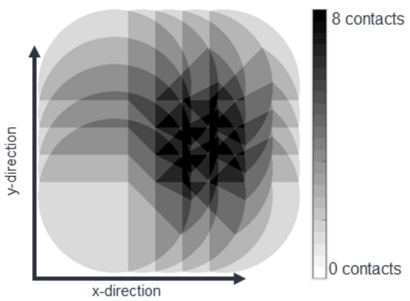

Kinematic Overlap (w)
with consideration of former indentations
→ o_s = 252.7%

- Kinematic overlap w/o consideration of former indentations ~ technical overlap (622.3% vs. 625.2%)
- Kinematic overlap considering former indentations is significantly lower: 252.7%
- Maximum number of tool contacts is also very different (23 w/o vs. 8 w)

TRUE OVERLAP

Exemplary calculation

True overlap

Full thermo-mechanical FEM:

Material model

- Voce-Kocks-Vöhringer (AISI 4140)

Body boundary conditions

- 5 x 5 x 5 mm elastic body
- 0.5 x 0.5 x 0.1 mm elastic-plastic body
- Rigid tool, constant Temperature: RT

Surface element edge length

- 0.005 mm, no remeshing

Tool movement

- Position & velocity based

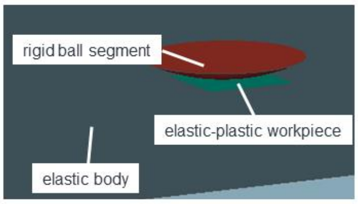

Model setup:
Workpiece comprised of "glued" elastic and elasto-plastic bodies.

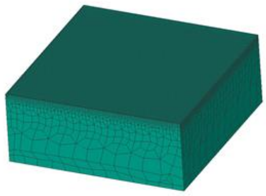

Elasto-plastic body:
Persistent hexmesh comprised of 26k elements with 10.2k nodes on relevant surface.

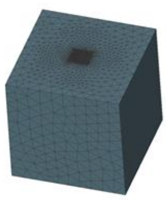

Elastic body:
Persistent tetmesh comprised of 38k elements.

Rigid body:
Persistent surface mesh comprised of 65k tri-facets.

MOTIVATION METHODS TECHNICAL KINEMATIC TRUE COMPARISON OUTLOOK

TRUE OVERLAP

Exemplary calculation

True overlap

Full thermo-mechanical FEM:

Material model

- Voce-Kocks-Vöhringer (AISI 4140)

Body boundary conditions

- 5 x 5 x 5 mm elastic body
- 0.5 x 0.5 x 0.1 mm elastic-plastic body
- Rigid tool, constant Temperature: RT

Surface element edge length

- 5 µm, no remeshing

Tool movement

- Position & velocity based

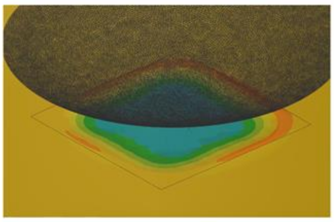

Animation: tool movement

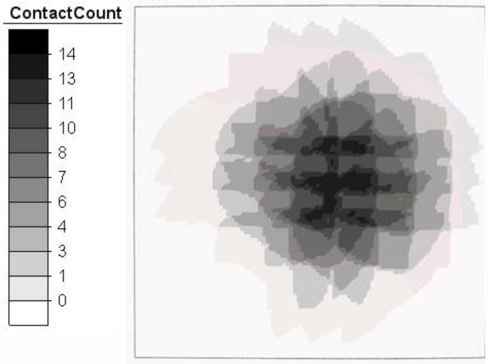

True Overlap
→ o_s = 378.5%

- Full thermo-mechanical FEM enables calculation of true overlap considering material displacement
- True overlap is significantly lower than technical overlap (378.5% vs. 625.2%)
- True overlap is significantly higher than kinematic overlap considering former indentations (378.5% vs. 252.7%)

9 22.10.2019 Prof. Dr.-Ing. J. Fleischer, Prof. Dr.-Ing. G. Lanza, Prof. Dr.-Ing. habil. V. Schulze

MOTIVATION METHODS TECHNICAL KINEMATIC TRUE COMPARISON OUTLOOK

COMPARISON

Is technical overlap accurate enough for simple indentation shapes?

Technical overlap

Simple calculation of area of indentation:

- 625.5%

Kinematic overlap

- 622.3% w/o consideration of former indentations
- 252.7% w consideration of former indentations

True overlap

- 378.5% full thermo-mechanical FE-simulation

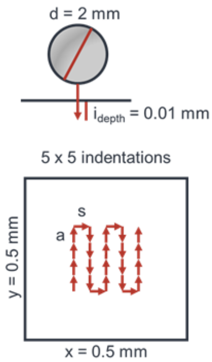

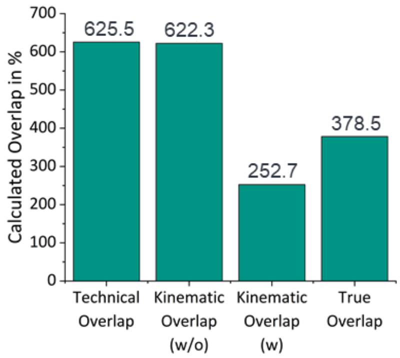

Overlap: differences by calculation method

- Technical overlap severely overestimates the contact area!
- True overlap is closer to kinematic overlap (w) than technical overlap.
  →Kinematic overlap (w) features the best time invested vs. accuracy ratio.

10 22.10.2019 Prof. Dr.-Ing. J. Fleischer, Prof. Dr.-Ing. G. Lanza, Prof. Dr.-Ing. habil. V. Schulze

MOTIVATION METHODS TECHNICAL KINEMATIC TRUE **COMPARISON** OUTLOOK

COMPARISON

Is kinematic overlap accurate enough for complex indentation shapes?

Technical overlap

- Supposing an area comprised of two half-ovals

Kinematic overlap

- w/o consideration of former indentations
- w consideration of former indentations

True overlap

- Thermo-mechanical FE-Simulation

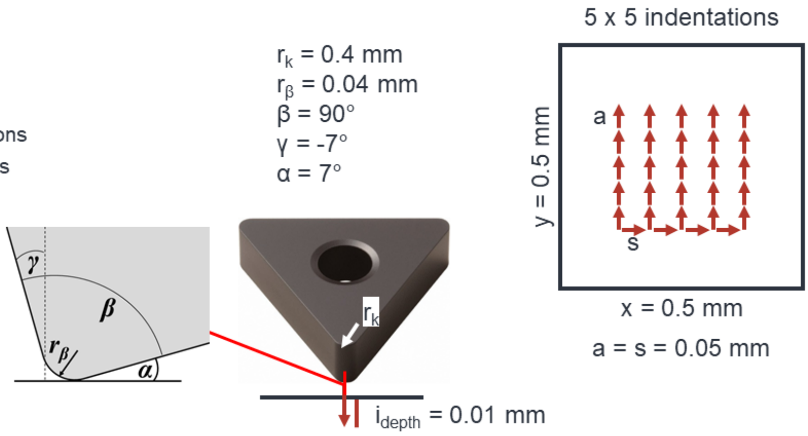

11 22.10.2019 Prof. Dr.-Ing. J. Fleischer, Prof. Dr.-Ing. G. Lanza, Prof. Dr.-Ing. habil. V. Schulze

MOTIVATION METHODS TECHNICAL KINEMATIC TRUE **COMPARISON** OUTLOOK

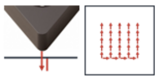

COMPARISON

Exemplary calculation

Technical overlap

Simple calculation of area of indentation:

- Calculate half-ovals area:
  - $A_i = (a_1 * b_1 + a_2 * b_2) * \pi/2$
- Calculate Overlap
  - $o_s = n * A_i / A_{total}$
- Technical Overlap = 144.5%

Kinematic overlap

Numerical calculation in Matlab:

- Load .stl geometry
- Create master-indentation (dexel)
- Create translation matrix
- Calculate new surface with and without consideration of former indentations

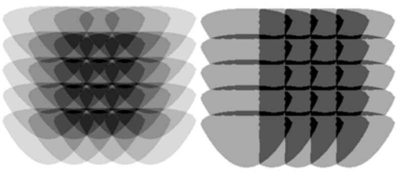

True overlap

Full thermo-mechanical FEM:

Material model

- Voce-Kocks-Vöhringer (AISI 4140)

Body boundary conditions

- 5 x 5 x 5 mm elastic body
- 0.5 x 0.5 x 0.1 mm elastic-plastic body
- Rigid tool, constant Temperature: RT

Surface element edge length

- 0.005 mm, no remeshing

Tool movement

- Position & velocity based

- Kinematic overlap (w/o) and technical overlap should be the same.
- Elasto-plastic FE-simulation result should be closest to the truth and higher than kinematic overlap (w).

12 22.10.2019 Prof. Dr.-Ing. J. Fleischer, Prof. Dr.-Ing. G. Lanza, Prof. Dr.-Ing. habil. V. Schulze

MOTIVATION METHODS TECHNICAL KINEMATIC TRUE **COMPARISON** OUTLOOK

COMPARISON

Is kinematic overlap accurate enough for complex indentation shapes?

Technical overlap

Simple calculation of area of indentation:

- 144.5%

Kinematic overlap

- 139.5% w/o consideration of former indentations
- 72.8% w consideration of former indentations

True overlap

- 117.5% full thermo-mechanical FE-simulation

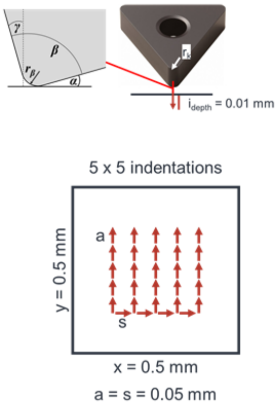

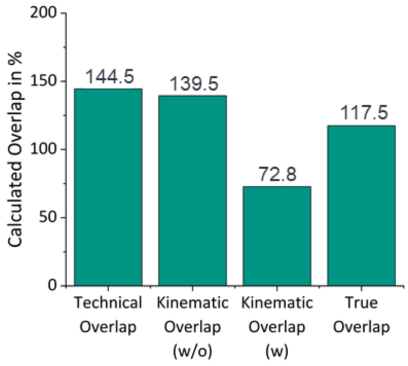

Overlap: differences by calculation method

- Technical overlap is harder to calculate for complex indentation shapes.
- Analogous to simple indentation shapes, kinematic overlap (w/o) is closest to technical overlap.
  →Kinematic overlap (w) is less accurate for the indentation shape we analyzed!

13 22.10.2019 Prof. Dr.-Ing. J. Fleischer, Prof. Dr.-Ing. G. Lanza, Prof. Dr.-Ing. habil. V. Schulze

MOTIVATION METHODS TECHNICAL KINEMATIC TRUE **COMPARISON** OUTLOOK

VDI 3416 EXTENSION?

Considering deterministic surface topographies produced by hammer peening

Deterministic, recurring surface topographies

- Depend on all process parameters (distance of indentation, stepover distance, indenter shape etc.)
- Result in calculable technical and kinematic percentage overlap of surface

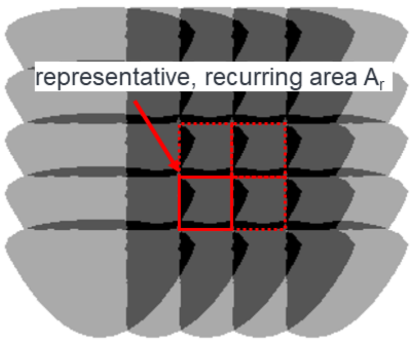

Representative percentage of overlap o_r

- Calculated as per VDI within A_r
- Allows comparison of processes or process parameters without defining arbitrary areas or including peripheral phenomenon in the calculation

14 22.10.2019 Prof. Dr.-Ing. J. Fleischer, Prof. Dr.-Ing. G. Lanza, Prof. Dr.-Ing. habil. V. Schulze

MOTIVATION METHODS TECHNICAL KINEMATIC TRUE COMPARISON **OUTLOOK**

OUTLOOK

Karlsruhe Institute of Technology

We did

- Calculate overlap of indentations in different ways considering arbitrary indentation shapes

We found

- Technical overlap is neither accurate, nor comparable regardless of indentation shape
- All overlap values calculated so far require knowledge of the surface area considered

We propose

- Extension of VDI 3416 considering deterministic surfaces: *representative percentage of overlap* o_r

What comes next

- Compare calculated overlap and surface topography with experimental results using different indentation shapes
- Refine tool movement in FE-simulation and in kinematic calculations (e.g. acceleration & energy based)

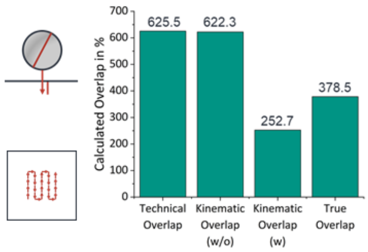

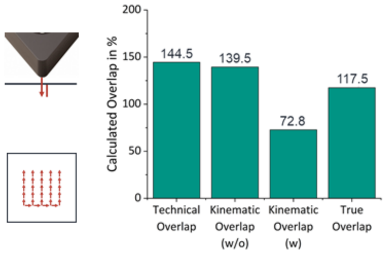

15 22.10.2019 Prof. Dr.-Ing. J. Fleischer, Prof. Dr.-Ing. G. Lanza, Prof. Dr.-Ing. habil. V. Schulze

wbk Institute of Production Science

Karlsruhe Institute of Technology

wbk Institute of Production Science

Thank you for your kind attention!

Eric Segebade M.Sc.
Research Associate
Tel.: +49 1523 9502615
E-Mail: eric.segebade@kit.edu

wbk **Institut of Produktionstechnik**
Kaiserstraße 12
76131 Karlsruhe
https://www.wbk.kit.edu/

16 22.10.2019 Prof. Dr.-Ing. J. Fleischer, Prof. Dr.-Ing. G. Lanza, Prof. Dr.-Ing. habil. V. Schulze

wbk Institute of Production Science

Influence of the process parameters on the penetration behaviour of ceramic particles in Composite Peening

Michael Seitz

IAM-WK – Institute for Applied Materials

Karlsruhe Institute of Technology

Karlsruhe Institute of Technology

IAM Institute for Applied Materials

Influence of the process parameters on the penetration behaviour of ceramic particles in Composite Peening

Symposium Mechanische Oberflächenbehandlung 2019, Karlsruhe
Michael Seitz
Hybrid and Lightweight Materials

Institute for Applied Materials (IAM-WK)

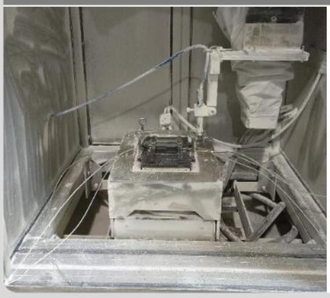

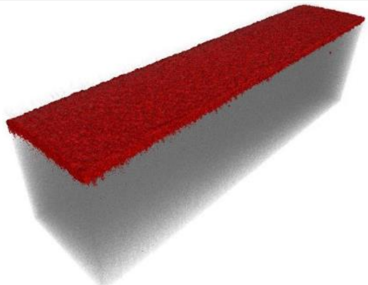

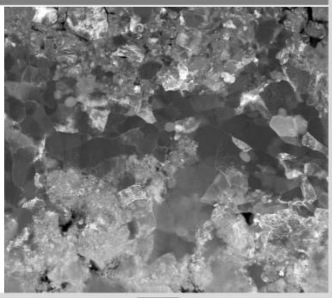

KIT – Die Forschungsuniversität in der Helmholtz-Gemeinschaft   www.kit.edu

Motivation
Composite Peening

Metal Matrix Composites (MMC)
- Improvement of specific properties, for instance by particle reinforcement
- Strengthening of the surface layer
- Functionally graded materials (FGM)

Micro Shot Peening
- Surface strengthening process
- Increase in fatigue strength
- Lower roughness compared to shot peening
- Ceramic blasting particles < 100 µm
- Embedment of blasting particles [2]

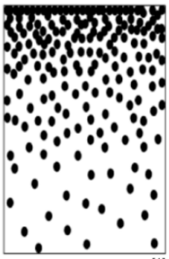

[1]

Composite Peening
- Manufacturing of a metal matrix composite by peening process
- Introduction of particles without liquid phase

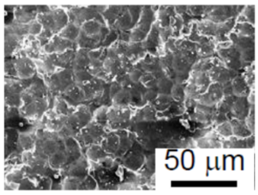

[2]

SiO_2

[1] Gupta, 2012
[2] Ando et al., 2008

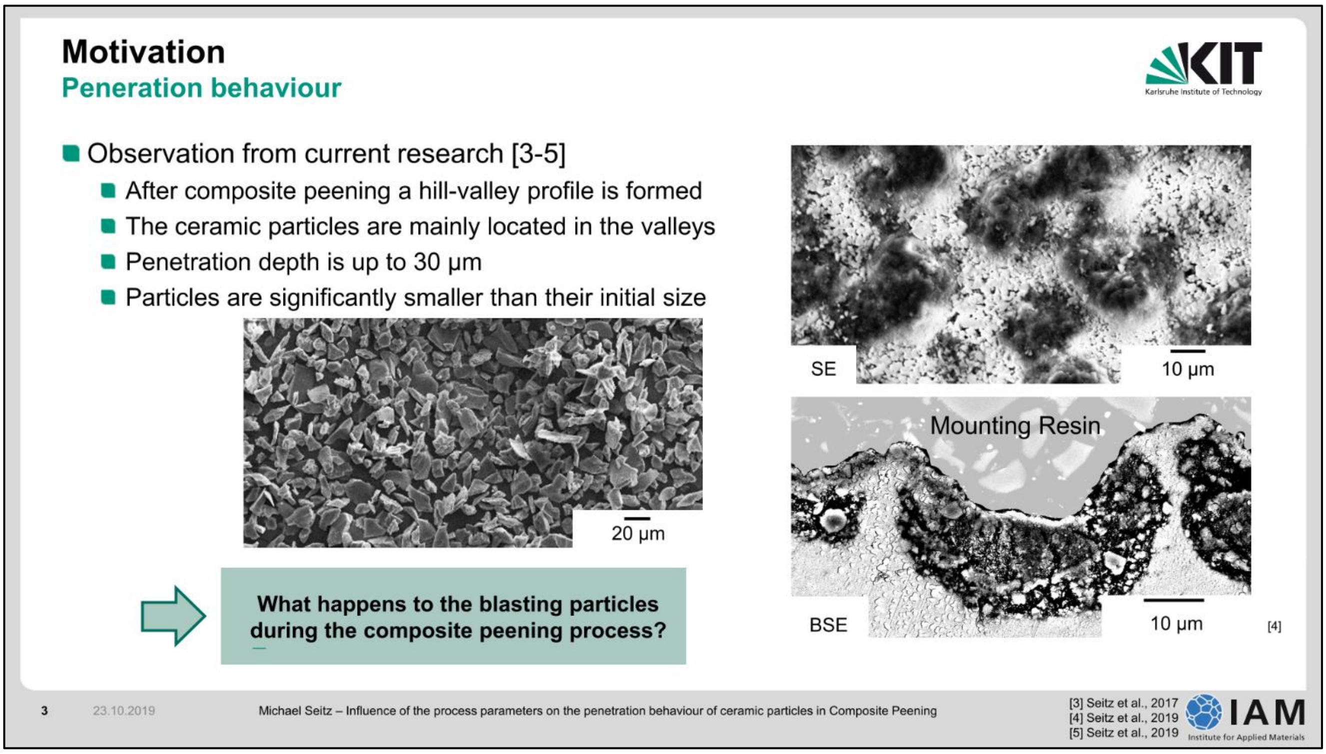
Motivation
Peneration behaviour
Karlsruhe Institute of Technology
Observation from current research [3-5]
After composite peening a hill-valley profile is formed
The ceramic particles are mainly located in the valleys
Penetration depth is up to 30 µm
Particles are significantly smaller than their initial size
20 µm
What happens to the blasting particles during the composite peening process?
SE
10 µm
Mounting Resin
BSE
10 µm
[4]
3
23.10.2019
Michael Seitz – Influence of the process parameters on the penetration behaviour of ceramic particles in Composite Peening
[3] Seitz et al., 2017
[4] Seitz et al., 2019
[5] Seitz et al., 2019
IAM
Institute for Applied Materials

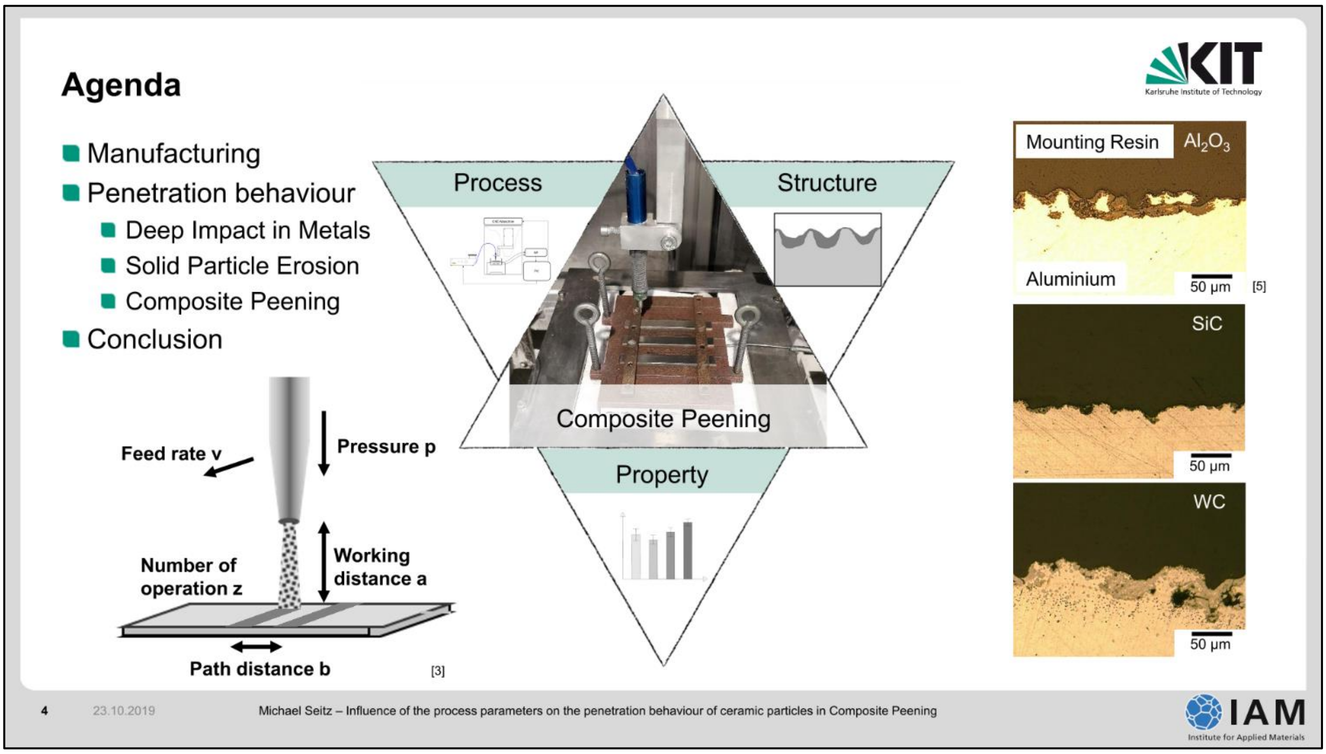
Agenda
Karlsruhe Institute of Technology
Manufacturing
Penetration behaviour
Deep Impact in Metals
Solid Particle Erosion
Composite Peening
Conclusion
Process
Structure
Composite Peening
Property
Feed rate v
Pressure p
Number of operation z
Working distance a
Path distance b
[3]
Mounting Resin
Al2O3
Aluminium
50 µm
[5]
SiC
50 µm
WC
50 µm
4
23.10.2019
Michael Seitz – Influence of the process parameters on the penetration behaviour of ceramic particles in Composite Peening
IAM
Institute for Applied Materials

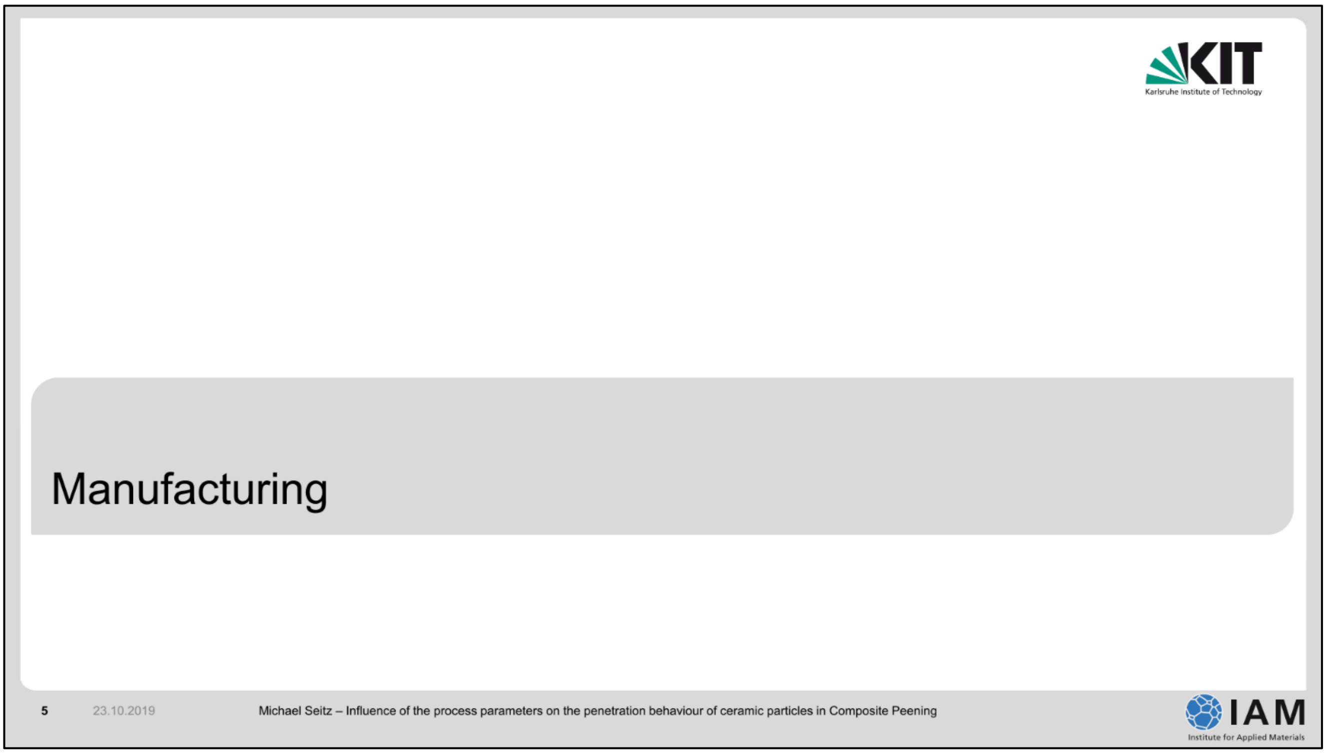
Karlsruhe Institute of Technology
Manufacturing
5
23.10.2019
Michael Seitz – Influence of the process parameters on the penetration behaviour of ceramic particles in Composite Peening
IAM
Institute for Applied Materials

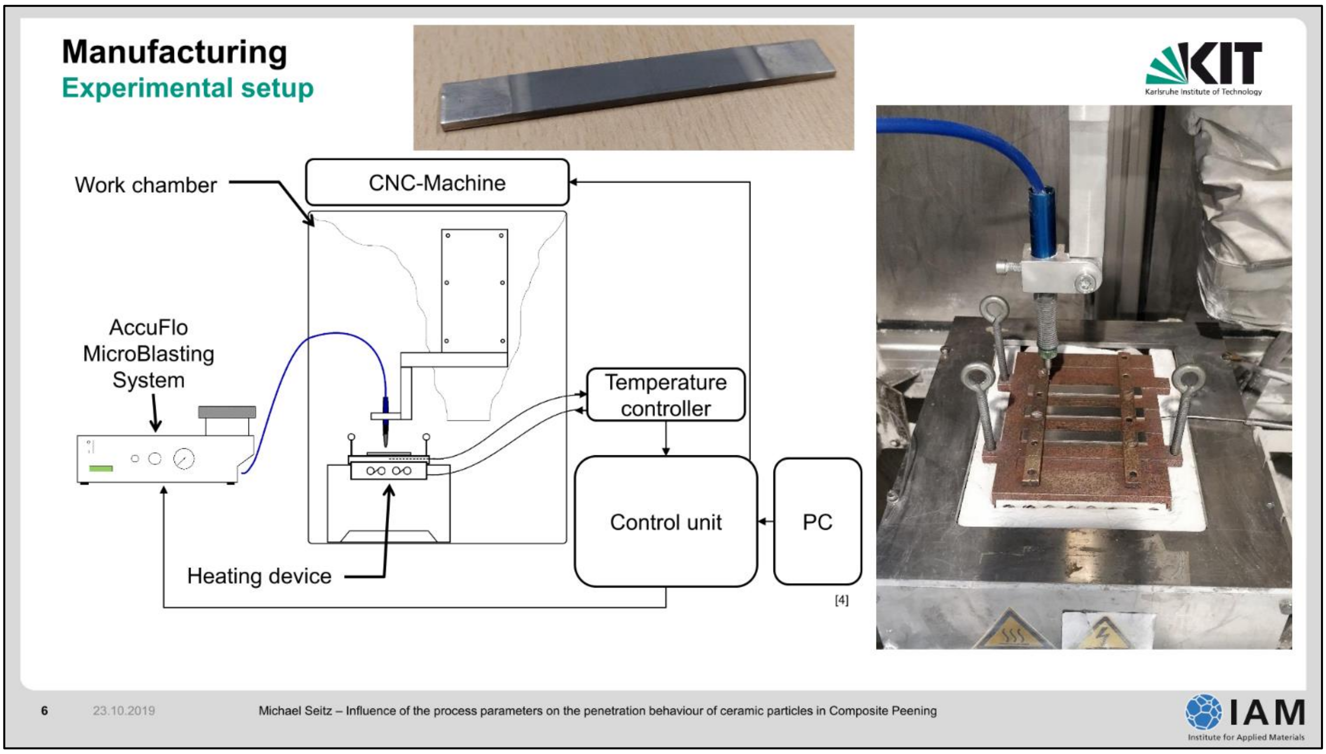
Manufacturing
Experimental setup
Karlsruhe Institute of Technology
Work chamber
CNC-Machine
AccuFlo
MicroBlasting
System
Temperature
controller
Control unit
PC
Heating device
[4]
6
23.10.2019
Michael Seitz – Influence of the process parameters on the penetration behaviour of ceramic particles in Composite Peening
IAM
Institute for Applied Materials

Manufacturing
Temperature profile

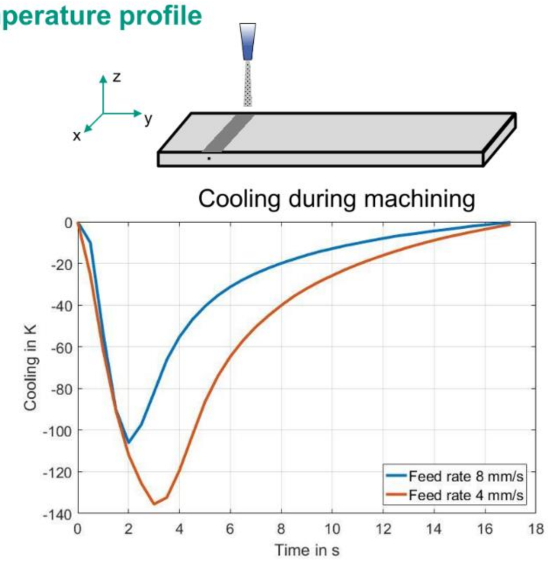

→ **Higher velocity**

→ **Dwell time between machining operations**

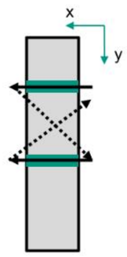

→ **Symmetrical machining**

7 23.10.2019 Michael Seitz – Influence of the process parameters on the penetration behaviour of ceramic particles in Composite Peening

Manufacturing
Process parameters for Composite Peening

[6] Esska GmbH
[7] Gerhardi AluTechnik GmbH
[8] Bierther Submikron GmbH
[9] Haussen GmbH
[10] H.C. Starck GmbH

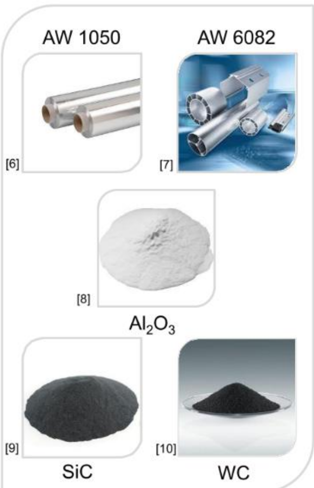

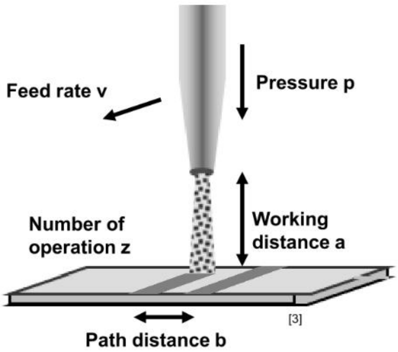

Working distance	Path distance	Feed rate	Angle
(mm)	(mm)	(mm/s)	(°)
10	1	8	90

Pressure	Number of operation	Temperature
(bar)	(-)	(T/T_s)
4; 7	2; 4; (10)	0,8; 0,9; 0,95

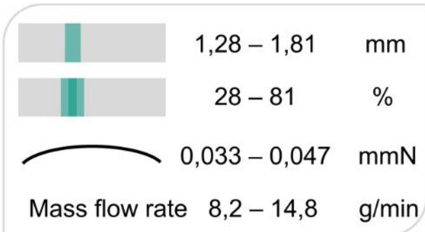

→ **100.000.000 Particles/mm²**

8 23.10.2019 Michael Seitz – Influence of the process parameters on the penetration behaviour of ceramic particles in Composite Peening

Deep Impact in Metals

9 23.10.2019 Michael Seitz – Influence of the process parameters on the penetration behaviour of ceramic particles in Composite Peening

Deep Impact in Metals

Determination of the penetration depth

- „Deep penetration of a non-deformable projectile with different geometrical characteristics“ [11]
  - Single particle impact
  - Penetration depth depends on momentum conservation, geometry of the projectile and dynamic-cavity expansion.

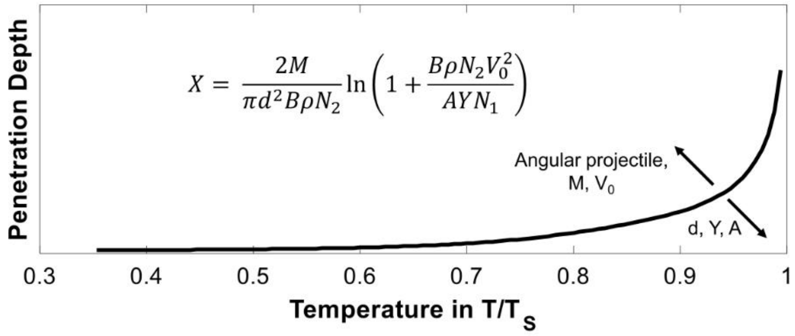

$$X = \frac{2M}{\pi d^2 B \rho N_2} \ln\left(1 + \frac{B \rho N_2 V_0^2}{A Y N_1}\right)$$

Particle properties

M	Mass of the projectile
d	Diameter of the projectile
N_1, N_2	Projectile Shape

Target properties

A, B	Material constants
ρ	Density
Y	Yield strength

Process properties

V_0	Velocity of the projectile
X	Penetration depth

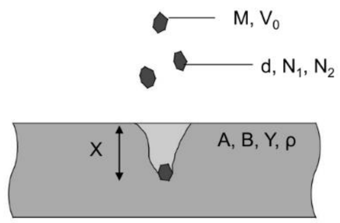

[11] Chen et al., 2002

10 23.10.2019 Michael Seitz – Influence of the process parameters on the penetration behaviour of ceramic particles in Composite Peening

Deep Impact in Metals
Particle properties

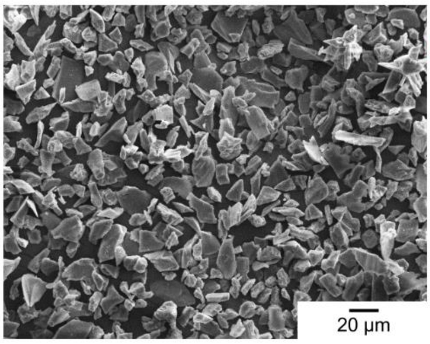

$$X = \frac{2M}{\pi d^2 B \rho N_2} \ln\left(1 + \frac{B\rho N_2 V_0^2}{AYN_1}\right)$$

[8]

Al_2O_3

- Shape and Size
  - Fracturing of the particles during processing?
  - Average Diameter and size distribution
    - Before Peening: 12.8 +/- 0.2 µm
    - After Peening: 12.2 +/- 0.1 µm

10 %	90 %
5.38 µm	20.47 µm

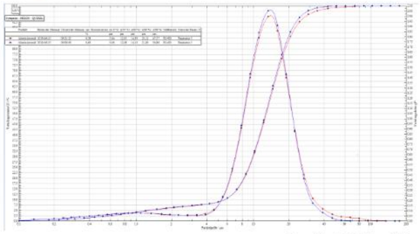

Credits: E. Seiler, ICT

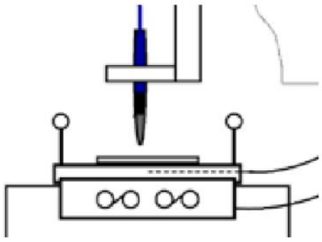

No significant reduction in grain size

11 23.10.2019 Michael Seitz – Influence of the process parameters on the penetration behaviour of ceramic particles in Composite Peening

KIT Karlsruhe Institute of Technology · IAM Institute for Applied Materials

Deep Impact in Metals
Particle properties

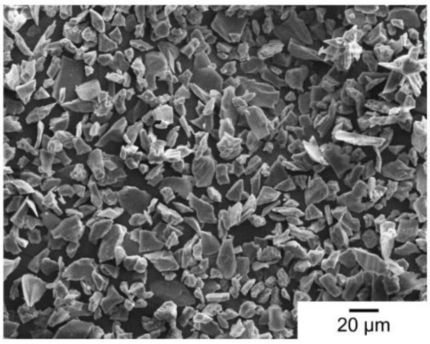

$$X = \frac{2M}{\pi d^2 B \rho N_2} \ln\left(1 + \frac{B\rho N_2 V_0^2}{AYN_1}\right)$$

[8]

Al_2O_3

- Shape and Size
  - Angular Shape
  - Conical nose geometry
    - N1 = 1.30
    - N2 = 0.13

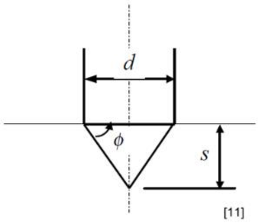

[11]

- Calculated weigth of a particle
  - M = 1.9 ng (double cone)

10 %	90 %
0.2 ng	8.9 ng

- Velocity of the particles
  - V_{7bar} = 195 m/s

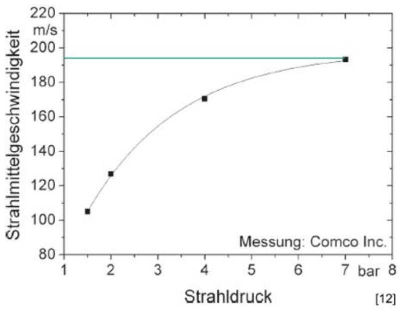

[12]

[12] Weingärtner et al., 2015

12 23.10.2019 Michael Seitz – Influence of the process parameters on the penetration behaviour of ceramic particles in Composite Peening

KIT Karlsruhe Institute of Technology · IAM Institute for Applied Materials

Deep Impact in Metals
Target properties

- Certain material properties depend on the process temperature during composite peening
  - Yield Strength
  - Young´s modulus

→ **High temperature tensile test**

- B = 1.041 for Aluminium [13]
- ρ_{Al} = 2.7 g/cm³

$$X = \frac{2M}{\pi d^2 B \rho N_2} \ln\left(1 + \frac{B \rho N_2 V_0^2}{A Y N_1}\right)$$

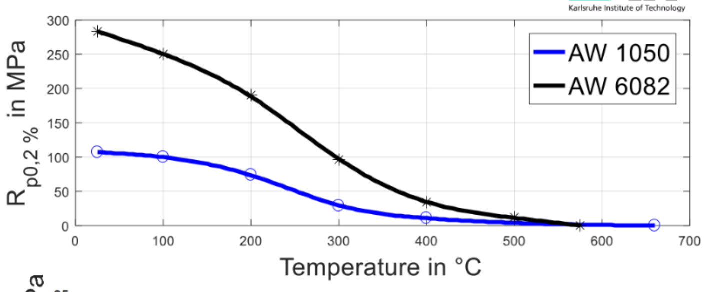

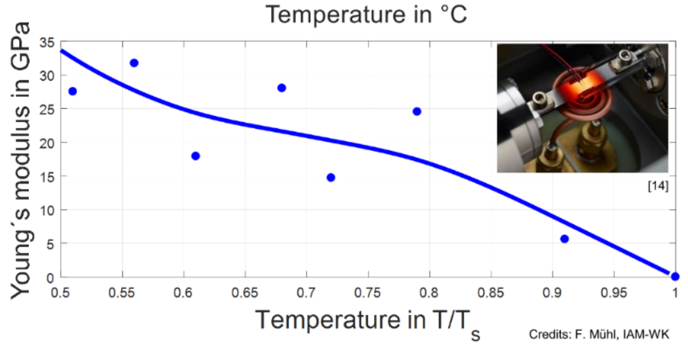

Credits: F. Mühl, IAM-WK

13 23.10.2019 Michael Seitz – Influence of the process parameters on the penetration behaviour of ceramic particles in Composite Peening

[13] Forrestal et al., 1988
[14] TA Instruments, Inc

IAM Institute for Applied Materials

Deep Impact in Metals
Penetration depth

Influence of the target material

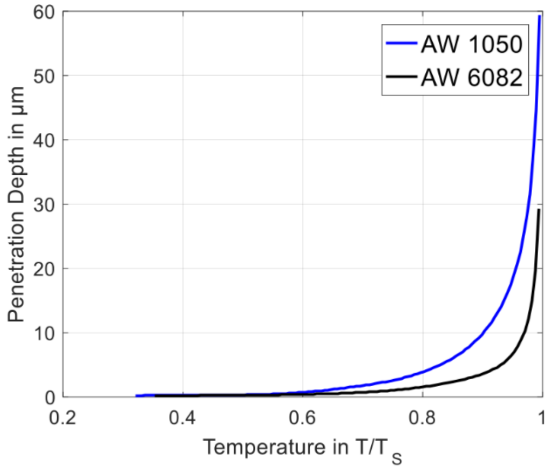

Influence of the projectile size

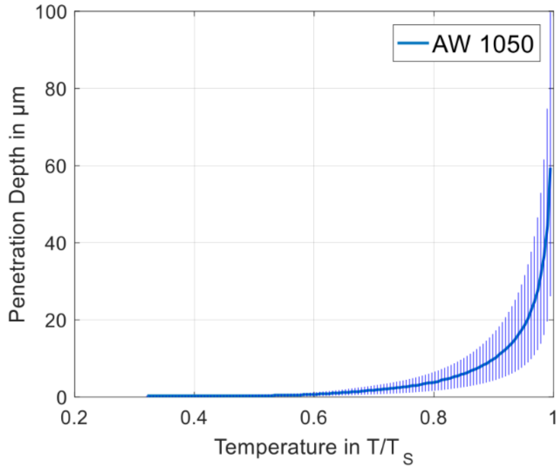

14 23.10.2019 Michael Seitz – Influence of the process parameters on the penetration behaviour of ceramic particles in Composite Peening

IAM Institute for Applied Materials

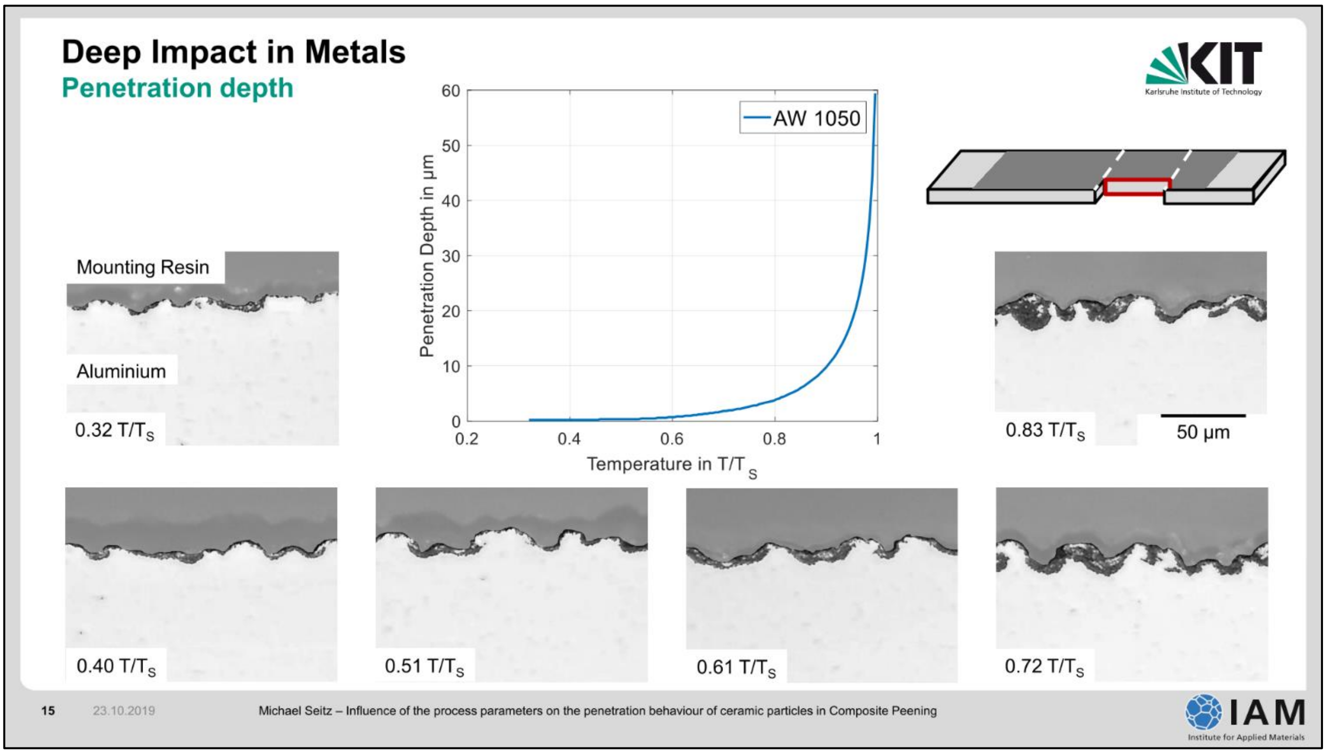
Deep Impact in Metals
Penetration depth
Karlsruhe Institute of Technology
Mounting Resin
Aluminium
0.32 T/T_S
AW 1050
Penetration Depth in µm
Temperature in T/T_S
0.83 T/T_S
50 µm
0.40 T/T_S
0.51 T/T_S
0.61 T/T_S
0.72 T/T_S
15
23.10.2019
Michael Seitz – Influence of the process parameters on the penetration behaviour of ceramic particles in Composite Peening
IAM
Institute for Applied Materials

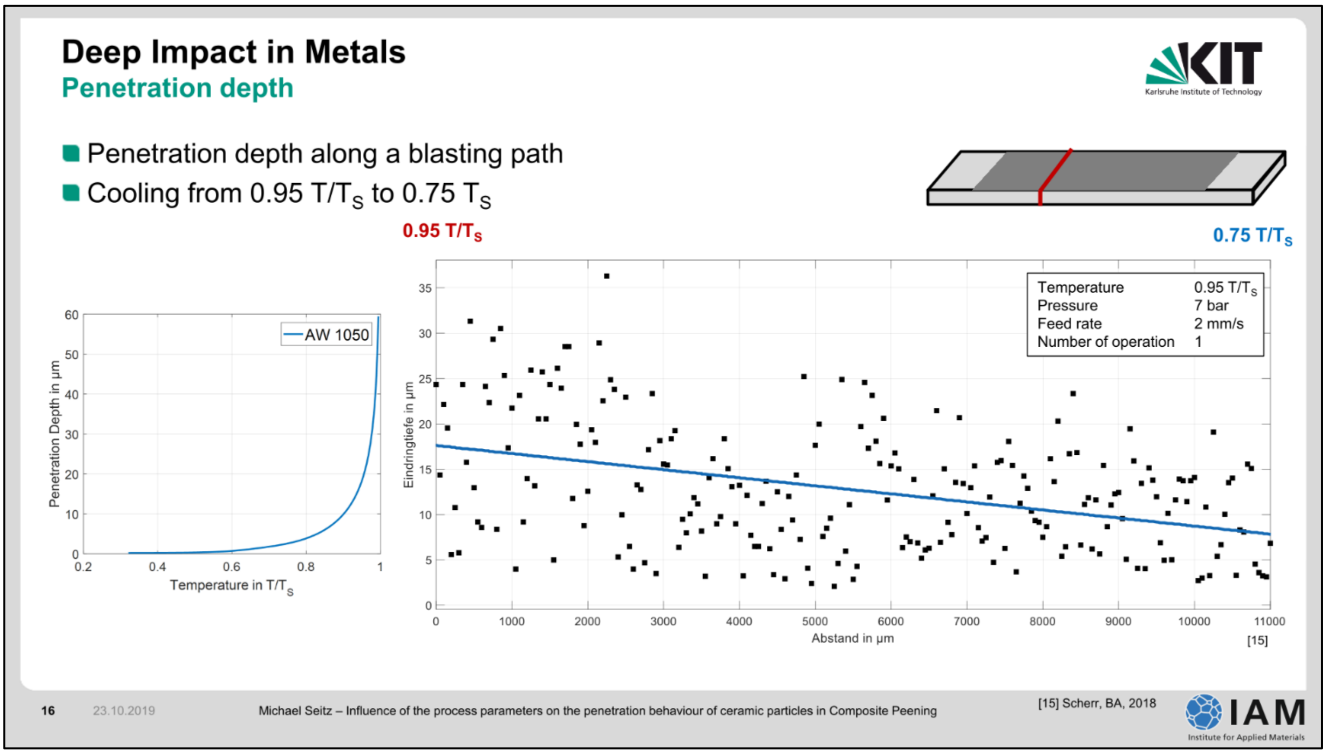
Deep Impact in Metals
Penetration depth
Karlsruhe Institute of Technology
Penetration depth along a blasting path
Cooling from 0.95 T/T_S to 0.75 T_S
0.95 T/T_S
0.75 T/T_S
AW 1050
Penetration Depth in µm
Temperature in T/T_S
Temperature 0.95 T/T_S
Pressure 7 bar
Feed rate 2 mm/s
Number of operation 1
Eindringtiefe in µm
Abstand in µm
[15]
16
23.10.2019
Michael Seitz – Influence of the process parameters on the penetration behaviour of ceramic particles in Composite Peening
[15] Scherr, BA, 2018
IAM
Institute for Applied Materials

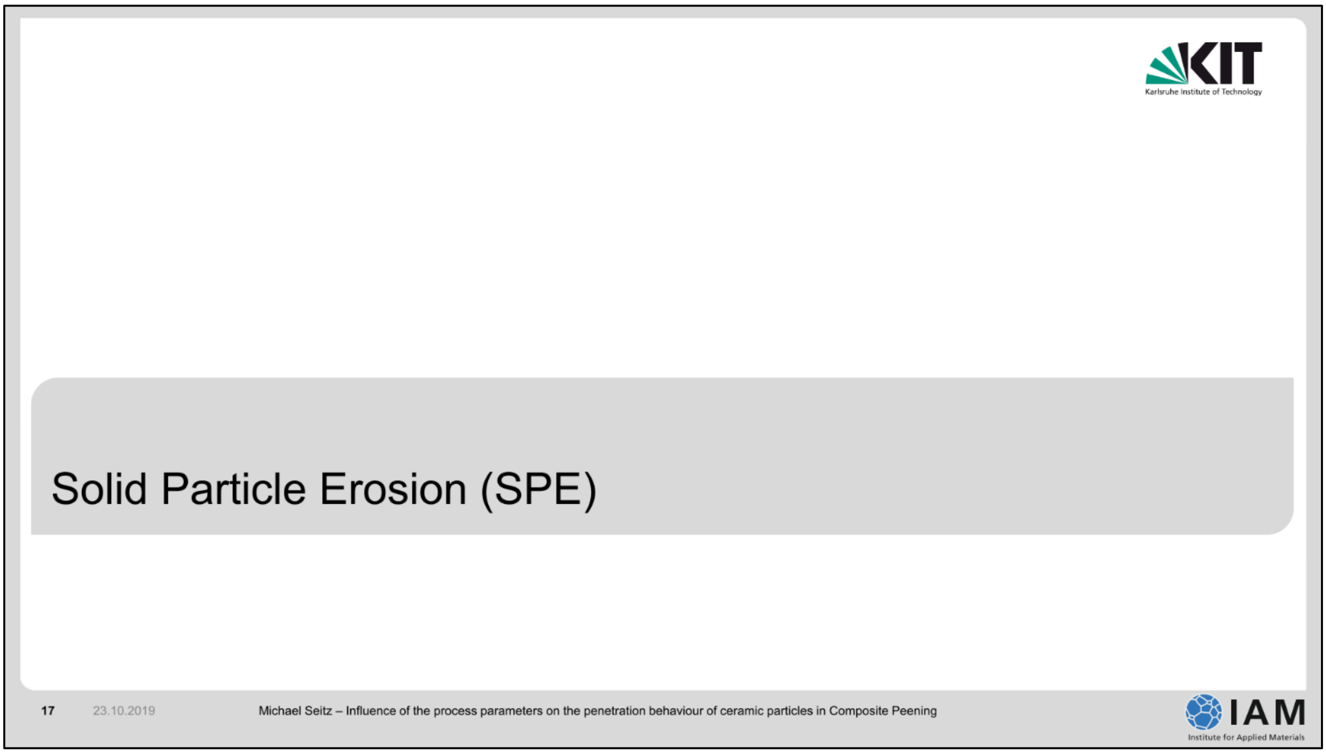
Karlsruhe Institute of Technology
Solid Particle Erosion (SPE)
17
23.10.2019
Michael Seitz – Influence of the process parameters on the penetration behaviour of ceramic particles in Composite Peening
IAM
Institute for Applied Materials

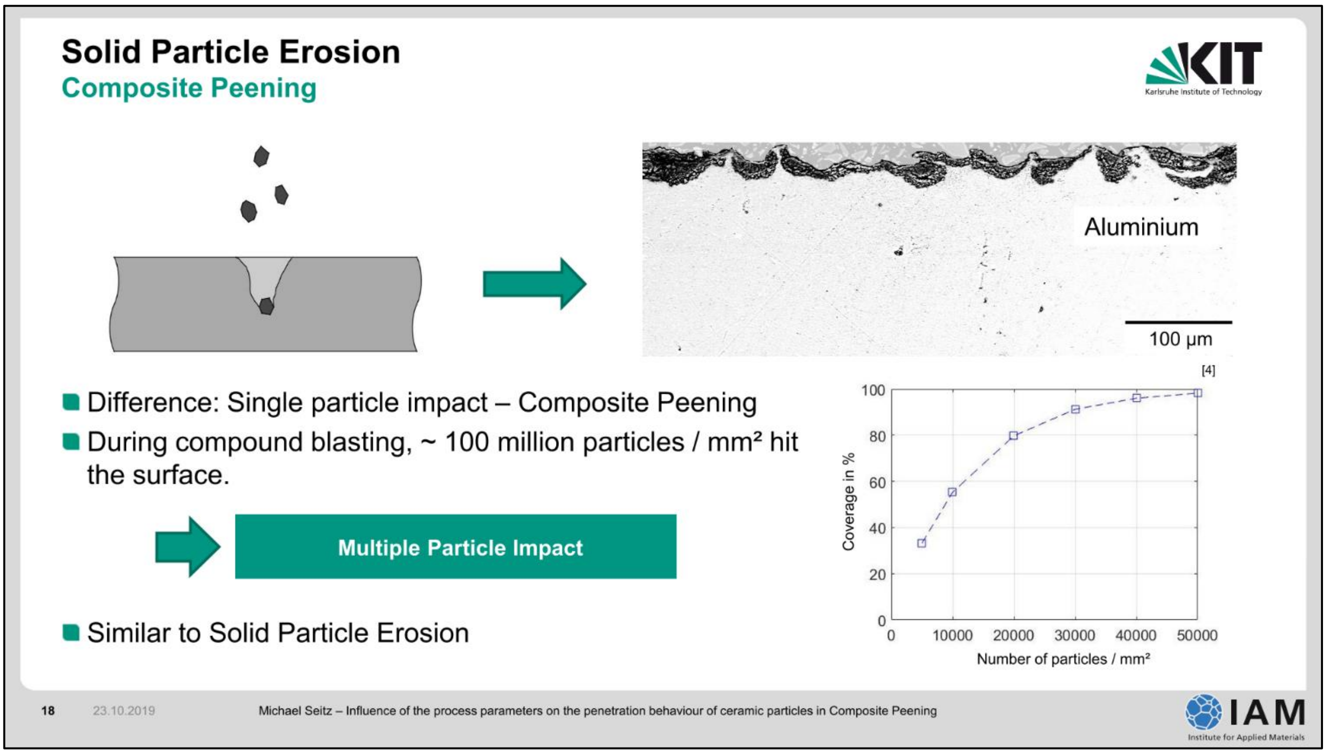
Solid Particle Erosion
Composite Peening
Karlsruhe Institute of Technology
Aluminium
100 µm
[4]
Difference: Single particle impact – Composite Peening
During compound blasting, ~ 100 million particles / mm² hit the surface.
Multiple Particle Impact
Similar to Solid Particle Erosion
Coverage in %
100
80
60
40
20
0
0
10000
20000
30000
40000
50000
Number of particles / mm²
18
23.10.2019
Michael Seitz – Influence of the process parameters on the penetration behaviour of ceramic particles in Composite Peening
IAM
Institute for Applied Materials

Solid Particle Erosion
Overview

- Field of research since WW II [16]
  - Power plant vessel
  - Pneumatic transportation systems
  - Helicopter rotor blades
- Occurs when granular particles hit a material surface
- Impact angle is an important factor in SPE
  - Maximum erosion of brittle materials at 90°
  - Maximum erosion of ductile materials at 15° - 45°
- Kinetic energy is mainly converted into elastic-plastic deformation and fracture energy
- Luminescence can also be observed [17]

Composite Peening, Al_2O_3 & AW 1050

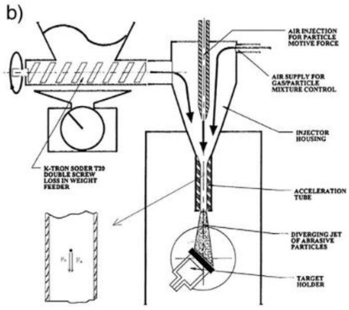

[18]

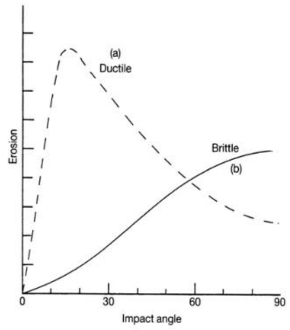

[19]

19 23.10.2019 Michael Seitz – Influence of the process parameters on the penetration behaviour of ceramic particles in Composite Peening

[16] Kleis et al., 2008 [19] Hutchings, 1992
[17] Thiessen, 1967
[18] Deng et al., 2008

Solid Particle Erosion
Aluminium

- With aluminium, no erosion rate can be observed at an impact angle of 90° because blasting particles are embedded [16]
- SPE at AW 1100 showed a hill-valley profile and embedded particles [20]

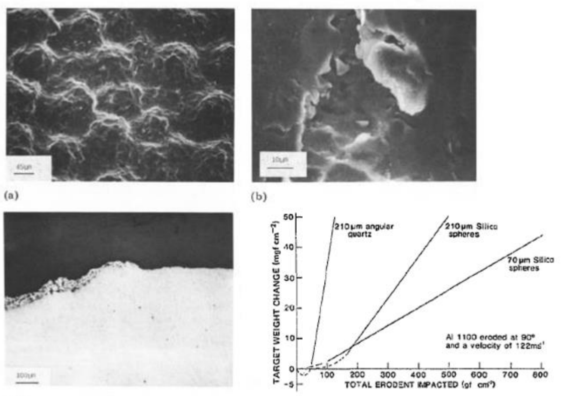

[20]

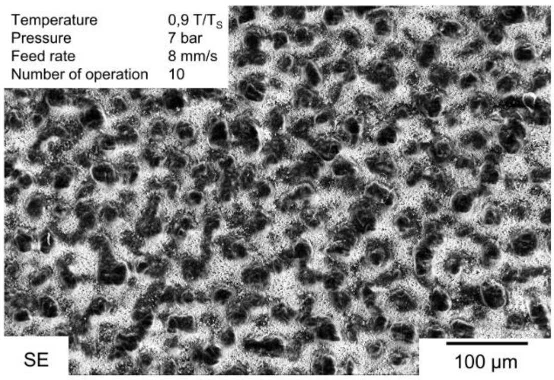

20 23.10.2019 Michael Seitz – Influence of the process parameters on the penetration behaviour of ceramic particles in Composite Peening

[20] Brown et al., 1983

Solid Particle Erosion
Particle Fracturing

- Several authors have proven that particles fracture on impact (according to Bousser [21])
  - Wada presents the thesis that particles fragment upon impact when the hardness of the particles ≤ hardness target material [23]
  - Particle toughness is also important

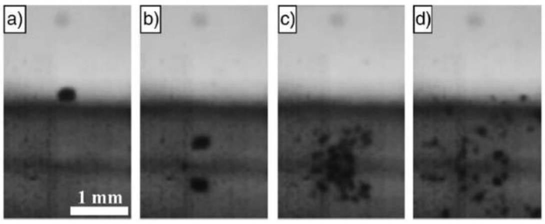

Sand particle on tungsten carbide surface [22]

- After Composite Peening, nanoscale aluminium oxide particles can be found in the surface layer

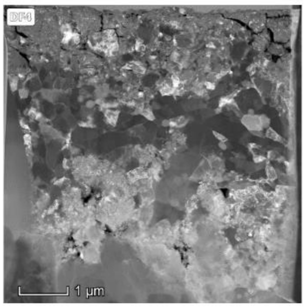

➡ **Multiple impacts cause the particles to fracture**

21 23.10.2019 Michael Seitz – Influence of the process parameters on the penetration behaviour of ceramic particles in Composite Peening

[21] Bousser et al., 2014
[22] Celotta et al., 2007
[23] Wada, 1992

Composite Peening

22 23.10.2019 Michael Seitz – Influence of the process parameters on the penetration behaviour of ceramic particles in Composite Peening

Composite Peening
Determination of penetration depth

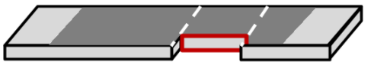

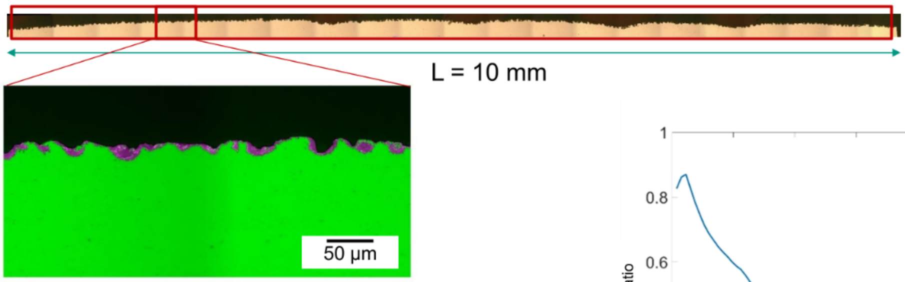

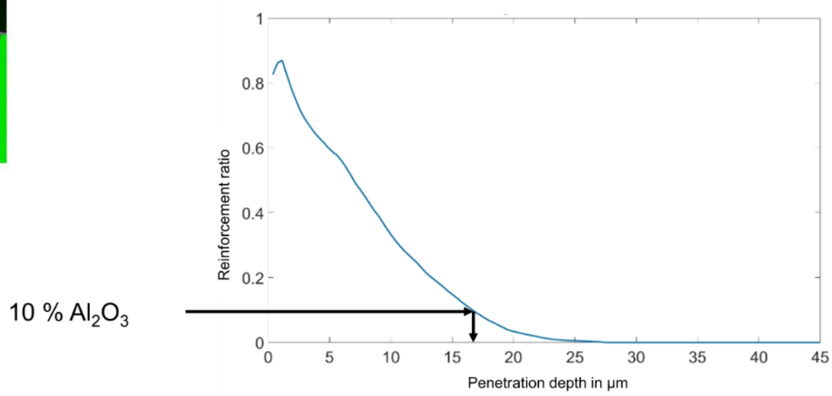

23 23.10.2019 Michael Seitz – Influence of the process parameters on the penetration behaviour of ceramic particles in Composite Peening

Composite Peening
Penetration depth

- The penetration depth of Composite Peening is slightly above the penetration depth of the single particle impact
- The model of Chen [11] can be used to estimate the influence of the process parameters during Composite Peening
- Penetration depth of up to 30 µm is achieved
- The penetration depth can be increased by multiple processing

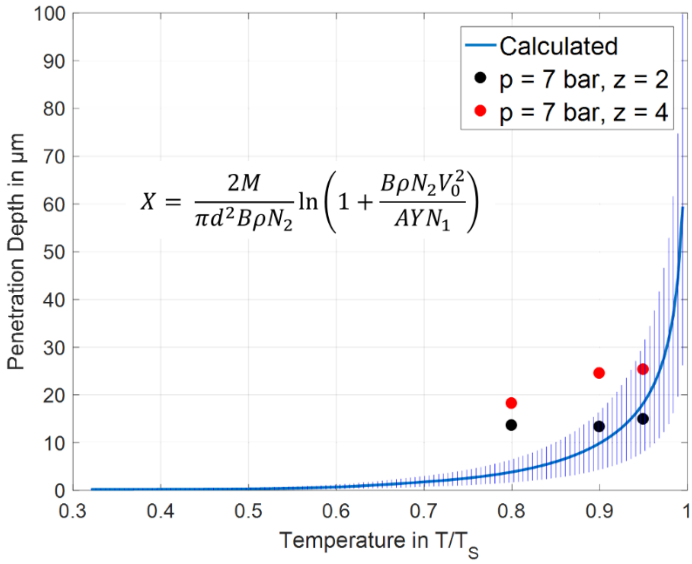

24 23.10.2019 Michael Seitz – Influence of the process parameters on the penetration behaviour of ceramic particles in Composite Peening

Conclusion & Outlook

- Estimation of penetration depth during compound peening based on a ballistic model
- Influence of individual process parameters on the penetration depth
- Correlation between Composite Peening and Solid Particle Erosion

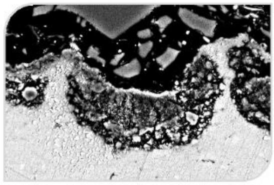

- Adaptation of the model to other material combinations
  - WC and SiC as blasting particles

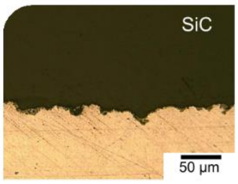

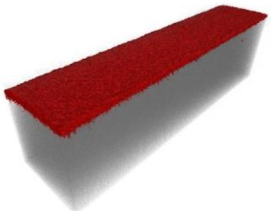

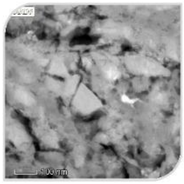

25 23.10.2019 Michael Seitz – Influence of the process parameters on the penetration behaviour of ceramic particles in Composite Peening

Thank you for your attention!

Michael Seitz

Karlsruhe Institute of Technology

Institute for Applied Materials
IAM-WK

Hybrid and Lightweight Materials

Kaiserstr. 12
Building. 10.96, office 113
76131 Karlsruhe, Germany
+49 721 608-47450

Michael.Seitz@kit.edu

The authors would like to thank the German Research Foundation (DFG) for the financial support.

DFG

WE4273/15-1

26 23.10.2019 Michael Seitz – Influence of the process parameters on the penetration behaviour of ceramic particles in Composite Peening

References

- [1] K. M. Gupta, Materials Science, Metallurgy and Engineering Materials, Umesh Publications, New Delhi, (2012).
- [2] Ando, M., Kitano, H., Usami, H., Endo, T. Applicability of fine particle peening on surface modification of aluminum alloy. In: The 10th International Conference On Shot Peening procedure, pp. 223-227 (2008).
- [3] Seitz, M., Reeb, A., Klumpp, A., Weidenmann, K. A. Composite Peening - A Novel Processing Technology for Graded Reinforced Aluminium Matrix Composites. Key Engineering Materials, 742, 137-144 (2017).
- [4] Seitz, M., Weidenmann, K. A. Influence of the Process Parameters on the Penetration Depth of the Reinforcing Phase During Composite Peening for the Production of Functionally Graded Metal Matrix Composites. Key Engineering Materials, 809, 73-78 (2019).
- [5] Seitz, M., Weidenmann, K. A. Investigations on Composite Peened Aluminium. In: International Conference on Advanced Surface Enhancement, pp. 10-18 (2019).
- [11] Chen, X. W., Li, Q. M. Deep penetration of a non-deformable projectile with different geometrical characteristics. International Journal of Impact Engineering, 27.6, pp. 619-637 (2002).
- [12] Weingärtner, R., Hoffmeister, J., Schule, V. Mechanische Oberflächenbearbeitung durch das Mikrostrahlen. Journal of Heat Treatment and Materials, 70.2, pp. 59-65 (2015).
- [13] Forrestal, M. J., Okajima, K., Luk, V. K. Penetration of 6061-T651 aluminum targets with rigid long rods. Trans ASME J Appl Mech, 55, pp. 755–760 (1988).
- [15] Scherr, T. Einfluss der Verbundstrahlparameter auf die Prozesstemperatur und Eindringtiefe. IAM-WK, Bachelorarbeit, (2018).
- [16] Kleis, I., Kulu, P. Solid particle erosion: occurrence, prediction and control. Springer Science & Business Media, 2007.
- [17] Thiessen, P. A. Phyikalisch-chemische Untersuchungen tribomechanischer Vorgänge. Grundlagen der Tribochemie. Akademie-Verlag, pp. 7-23 (1967).
- [18] Deng, T., Bingley, M. S., Bradley, M. S. A., De Silva, S. R. A comparison of the gas-blast and centrifugal-accelerator erosion testers: The influence of particle dynamics. Wear, 265, pp. 945-955 (2008).
- [19] Hutchings, I. M. Transitions, threshold effects and erosion maps. Key Engineering Materials. Trans Tech Publications, 71, pp. 75-92 (1999).
- [20] Brown, R., Kosco, S., Jun, E. J. The effect of particle shape and size on erosion of aluminum alloy 1100 at 90 impact angles. Wear, 88.2, pp.181-193 (1983).
- [21] Bousser, E., Martinu, L., Klemberg-Sapieha, J. E. Solid particle erosion mechanisms of protective coatings for aerospace applications. Surface and Coatings Technology, 257, pp. 165-181 (2014).
- [22] Celotta, D. W., Qureshi, U. A., Stepanov, E. V., Goulet, D. P., Hunter, J., Buckberry, C. H., Hill, R., Sherikar, S. V., Moshrefi-Torbati, M., Wood, R. J. K. Sand erosion testing of novel compositions of hard ceramics. Wear, 263, pp. 278-283 (2007).
- [23] Wada, S. WADA, S. Effects of hardness and fracture toughness of target materials and impact particles on erosion of ceramic materials. Key Engineering Materials. Trans Tech Publications, 71, pp. 51-74 (1992).

27 23.10.2019 Michael Seitz – Influence of the process parameters on the penetration behaviour of ceramic particles in Composite Peening

Residual stress relaxation in HFMI-treated fillet welds after single overload peaks

Jan Schubnell

Institute for Mechanics of Materials IWM

Fraunhofer

RESIDUAL STRESS RELAXATION IN HFMI-TREATED FILLET WELDS AFTER SINGLE OVERLOAD PEAKS

Symposium Mechanische Oberflächenbehandlung
KIT Karlsruhe, 22.-23.10.2019

Jan Schubnell, Eva Carl, Majid Farajian (IWM)
Stefanos Gkatzogiannis, Peter Knödel, Thomas Ummenhofer (KIT)
Robert Wimpory (HZB)
Hamdollah Eslami (IFS)

1

AGENDA

Residual stress relaxation at HFMI-treated fillet welds after single overload peaks

IIW – Document XIII-2829-19

- Motivation
- Experimental set-up
  - Material and weld detail
- Residual stress analysis
  - Experimental study
  - Numerical study
- Conclusion

X-ray-diffr.

Neutron-diffr.

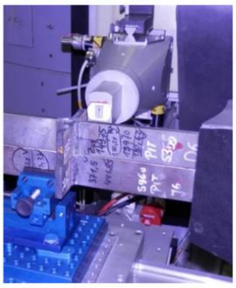

FEA

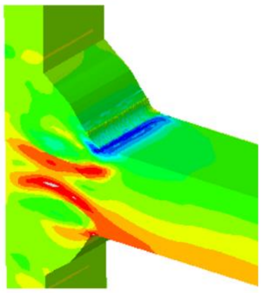

2

Motivation

- Significant fatigue life improvement of HFMI-treated welded joints is statistically proved (*Marquis and Barsoum 2016*) based on numerous studies under constant amplitude (CA) loading
- Studies have shown that the fatigue life benefit decreases at variable amplitude (VA) loading (*Marquis 2010, Leitner et al. 2018)*.
- It is assumed that this decrease is strongly related to the compressive residual stress relaxation under high peak stresses

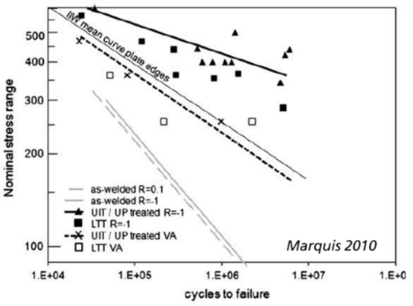

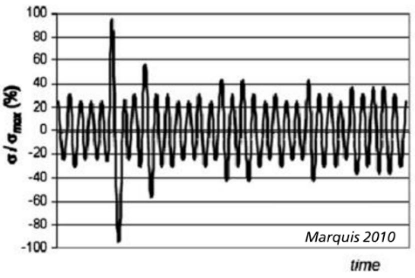

3
© Fraunhofer IWM

Motivation

- Multiple recommendations exist to limit the RS-relaxation:

$S_{max}/S_{min} = +/-0.45 f_y$ *Marquis et al. (2013)** (R < -0.125)

$S_{max}/S_{min} = +/-0.6 f_y$ *Mikkola et al. (2017)* (R = -1)

$S_{max}/S_{min} = +/-0.8 f_y$ *Haagensen and Maddox (2013)***

$S_{min} = -0.8 f_y$ / $S_{max} = f_y$ *Kuhlmann et al. (2018)****

Aim: Quantify the compressive residual stress relaxation

Improvement factor = $\Delta\sigma_{HFMI,k=free}/\Delta\sigma_{AW,k=3}$

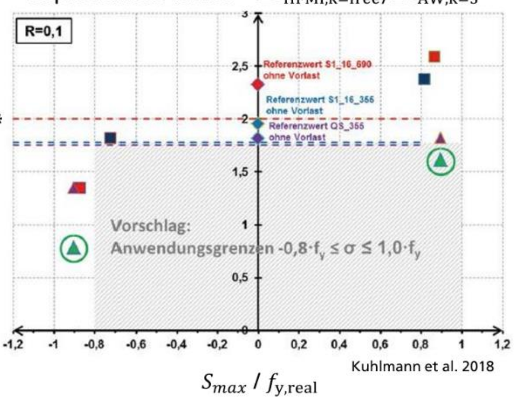

S_{max} = Maximum nominal stress, f_y = nominal yield of the base material

R = Stress ratio

*Current IIW-Recommendation (HFMI) / ** Hammer & Needle Penning / *** German DASt guideline (not realesed yet)

4
© Fraunhofer IWM

Material and specimen details

- Steel: S355J2+N / S960QL
- Weld detail: Transverse stiffener
- Weld type: Single layer fillet weld*
- Weld process: GMAW (135)*
- HFMI: Pneumatical Impact treatment (PIT)

Materials	Yield strength [MPa]	Ultimate Strength [MPa]	Elongation [%]	Hardness [HV10]
S355J2+N	420	538	25*	169
S960QL	1011	1060	14*	316

*data sheet

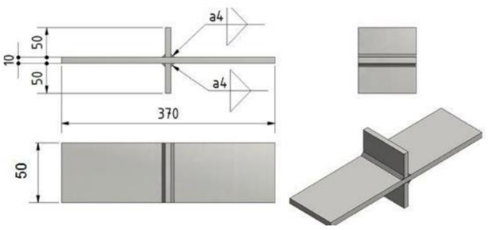

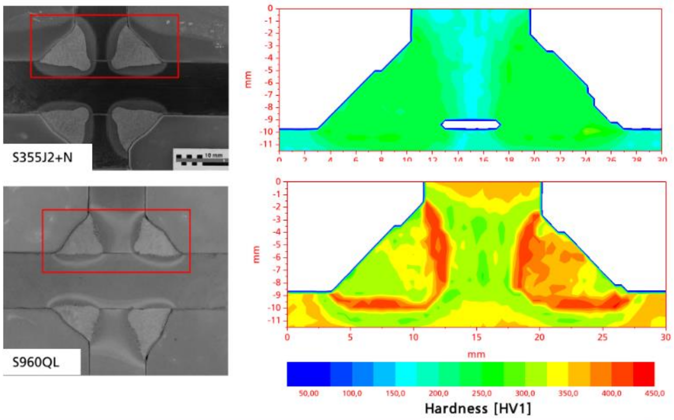

*J. Schubnell, D. Discher, and M. Farajian, "Static, dynamic and cyclic properties of the heat affected zone for different steel grades," *Mater. Test.*, vol. 61, no. 7, 2019

5
© Fraunhofer IWM

ifs HZB Helmholtz Zentrum Berlin KIT Karlsruher Institut für Technologie Fraunhofer IWM

Experimental test set-up / residual stress analysis

„Stress peaks" from VA loading were approximated by single static loads (majority of residual stress relaxation occurs at N=1 (Farajian et al. 2010, Leitner et al. 2018)

Load set-up (IFS)

PLm 630N

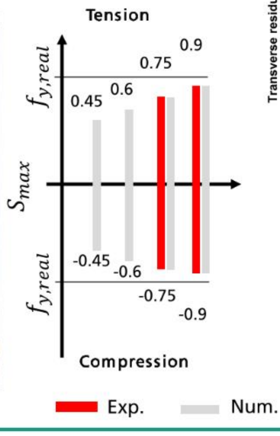

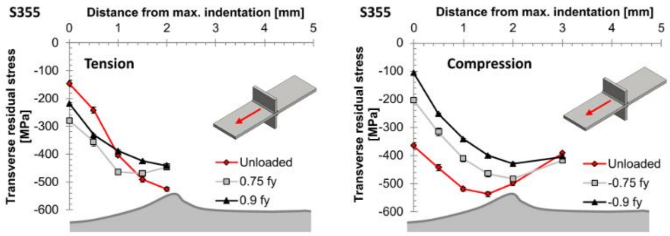

6
© Fraunhofer IWM

ifs HZB Helmholtz Zentrum Berlin KIT Karlsruher Institut für Technologie Fraunhofer IWM

Experimental test set-up / residual stress analysis

„Stress peaks" from VA loading were approximated by single static loads (majority of residual stress relaxation occurs at N=1 (Farajian et al. 2010, Leitner et al. 2018)

Load set-up (IFS)

PLm 630N

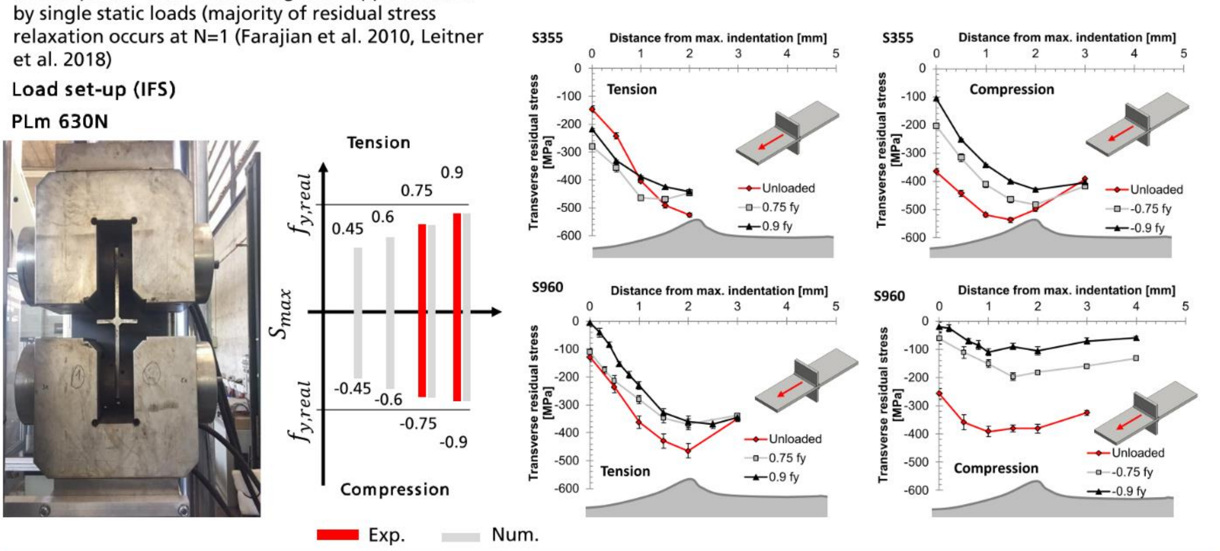

7

Material modelling: Heat affected zone*

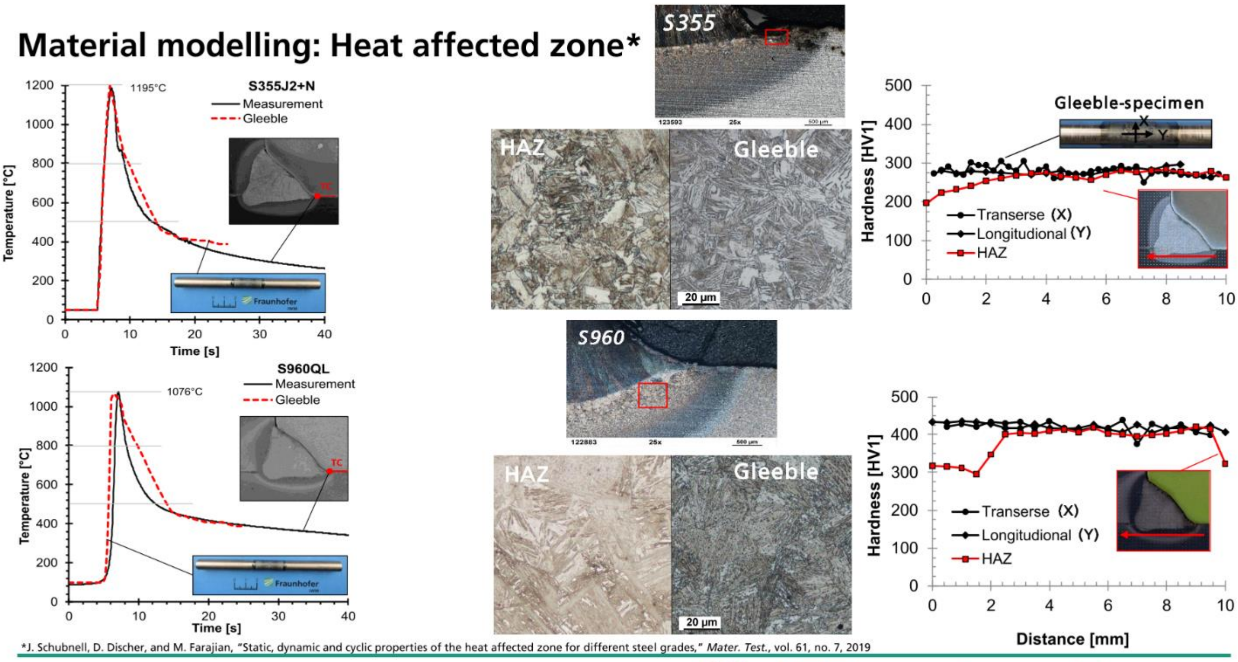

*J. Schubnell, D. Discher, and M. Farajian, "Static, dynamic and cyclic properties of the heat affected zone for different steel grades," *Mater. Test.*, vol. 61, no. 7, 2019

8

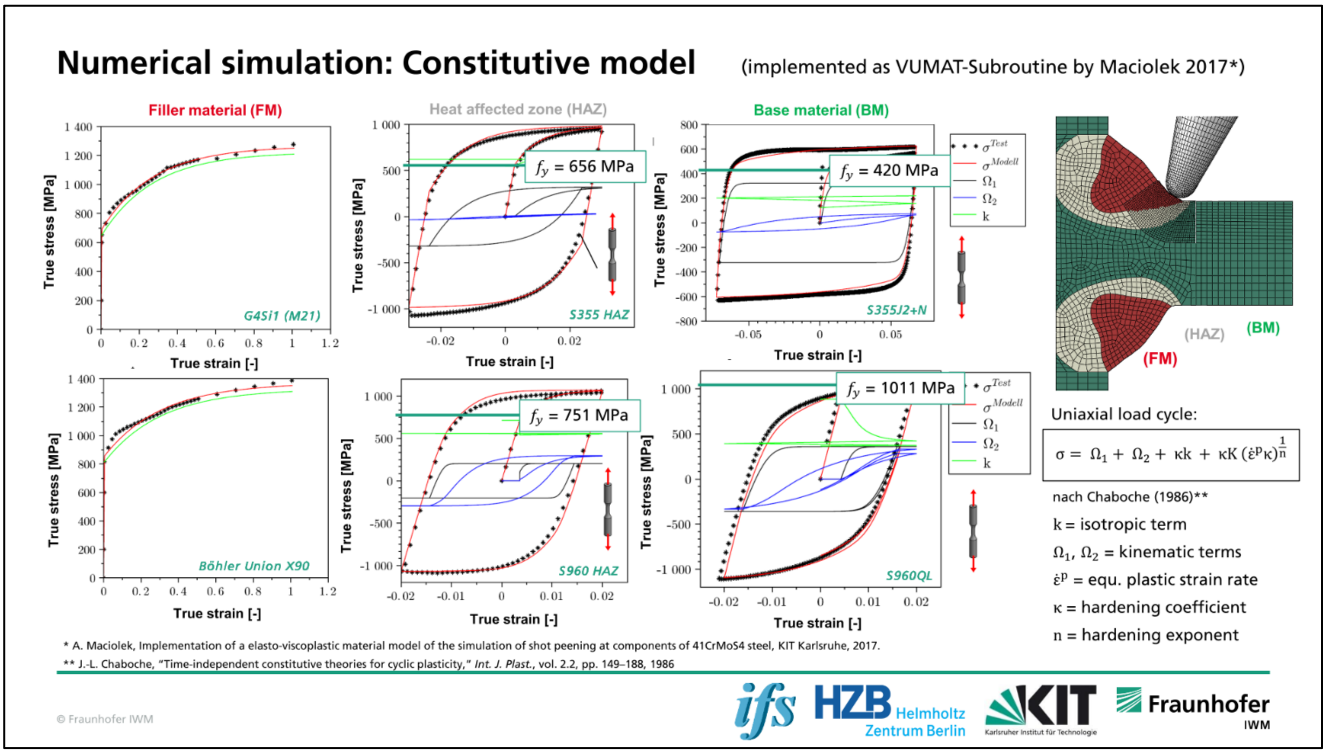
Numerical simulation: Constitutive model
(implemented as VUMAT-Subroutine by Maciolek 2017*)
Filler material (FM)
Heat affected zone (HAZ)
Base material (BM)
True stress [MPa]
True strain [-]
G4Si1 (M21)
S355 HAZ
S355J2+N
Böhler Union X90
S960 HAZ
S960QL
f_y = 656 MPa
f_y = 420 MPa
f_y = 751 MPa
f_y = 1011 MPa
σ^{Test}
σ^{Modell}
Ω_1
Ω_2
k
(HAZ)
(BM)
(FM)
Uniaxial load cycle:
$\sigma = \Omega_1 + \Omega_2 + \kappa k + \kappa K (\dot{\varepsilon}^p \kappa)^{\frac{1}{n}}$
nach Chaboche (1986)**
k = isotropic term
Ω_1, Ω_2 = kinematic terms
$\dot{\varepsilon}^p$ = equ. plastic strain rate
κ = hardening coefficient
n = hardening exponent
* A. Maciolek, Implementation of a elasto-viscoplastic material model of the simulation of shot peening at components of 41CrMoS4 steel, KIT Karlsruhe, 2017.
** J.-L. Chaboche, "Time-independent constitutive theories for cyclic plasticity," Int. J. Plast., vol. 2.2, pp. 149–188, 1986
© Fraunhofer IWM
HZB Helmholtz Zentrum Berlin
Fraunhofer IWM

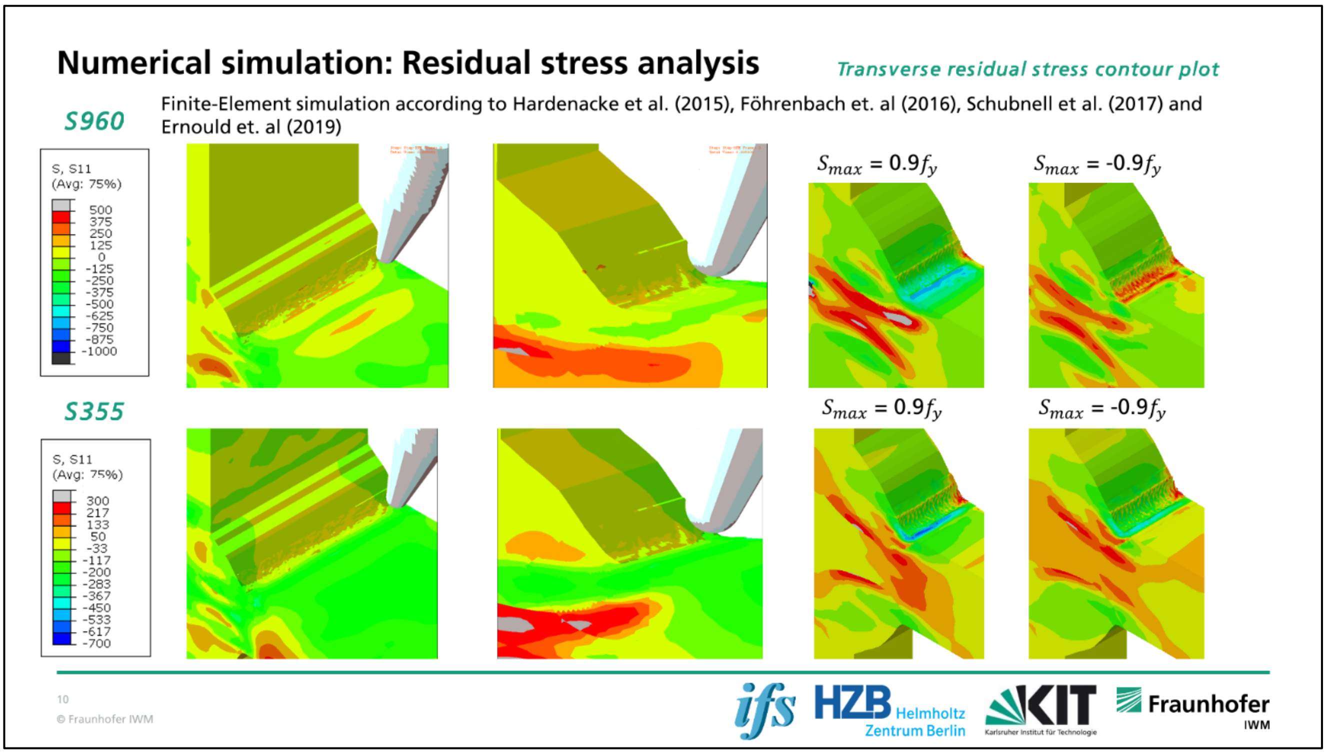
Numerical simulation: Residual stress analysis
Transverse residual stress contour plot
S960
Finite-Element simulation according to Hardenacke et al. (2015), Föhrenbach et. al (2016), Schubnell et al. (2017) and Ernould et. al (2019)
S, S11
(Avg: 75%)
500
375
250
125
0
-125
-250
-375
-500
-625
-750
-875
-1000
S_{max} = 0.9f_y
S_{max} = -0.9f_y
S355
S, S11
(Avg: 75%)
300
217
133
50
-33
-117
-200
-283
-367
-450
-533
-617
-700
S_{max} = 0.9f_y
S_{max} = -0.9f_y
10
© Fraunhofer IWM
HZB Helmholtz Zentrum Berlin
Fraunhofer IWM

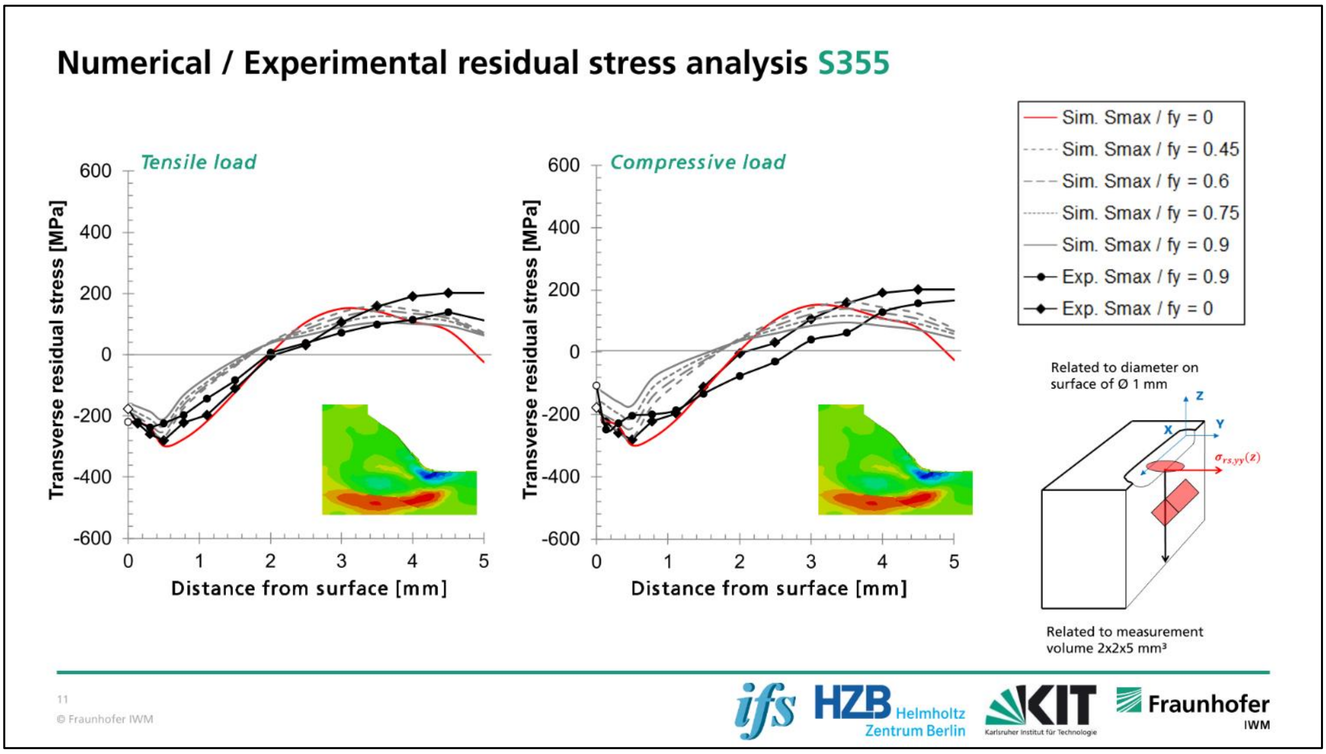
Numerical / Experimental residual stress analysis S355
Tensile load
Compressive load
Transverse residual stress [MPa]
Distance from surface [mm]
Sim. Smax / fy = 0
Sim. Smax / fy = 0.45
Sim. Smax / fy = 0.6
Sim. Smax / fy = 0.75
Sim. Smax / fy = 0.9
Exp. Smax / fy = 0.9
Exp. Smax / fy = 0
Related to diameter on surface of Ø 1 mm
Related to measurement volume 2x2x5 mm³
11
© Fraunhofer IWM
ifs
HZB Helmholtz Zentrum Berlin
KIT Karlsruher Institut für Technologie
Fraunhofer IWM

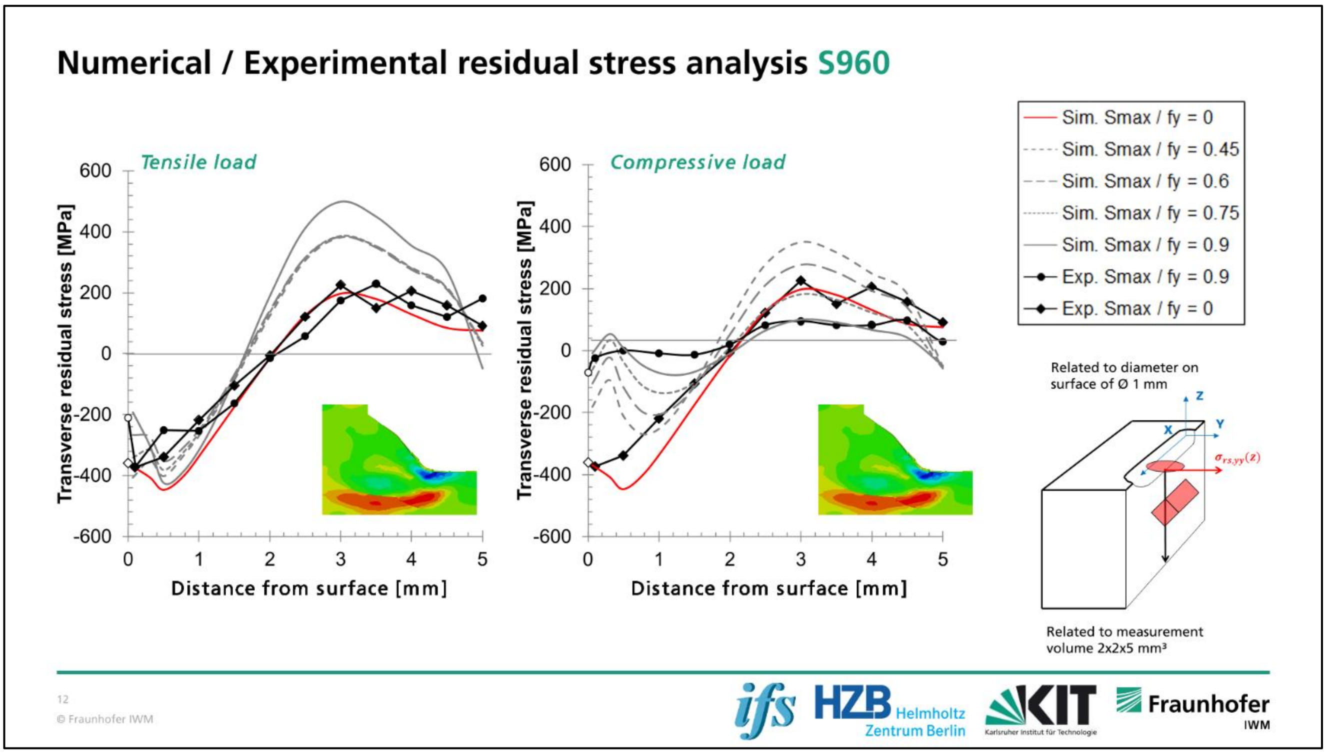
Numerical / Experimental residual stress analysis S960
Tensile load
Compressive load
Transverse residual stress [MPa]
Distance from surface [mm]
Sim. Smax / fy = 0
Sim. Smax / fy = 0.45
Sim. Smax / fy = 0.6
Sim. Smax / fy = 0.75
Sim. Smax / fy = 0.9
Exp. Smax / fy = 0.9
Exp. Smax / fy = 0
Related to diameter on surface of Ø 1 mm
Related to measurement volume 2x2x5 mm³
12
© Fraunhofer IWM
ifs
HZB Helmholtz Zentrum Berlin
KIT Karlsruher Institut für Technologie
Fraunhofer IWM

Residual stress analysis: $S_{max} \sim \Delta\sigma_{RES}$

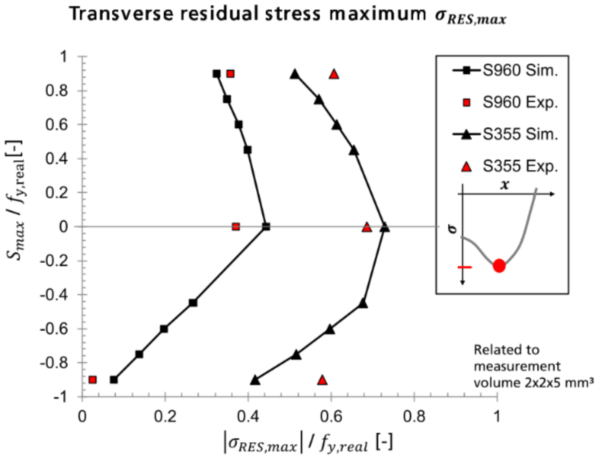

S_{max}= Maximum nominal stress, f_y = yield strength of the base material

13
© Fraunhofer IWM

Residual stress analysis: $S_{max} \sim \Delta\sigma_{RES}$

S_{max}/S_{min} =+/−0.45f_y S_{max}/S_{min} =+/−0.6f_y $S_{min} = -0.8f_y$ / $S_{max} = f_y$

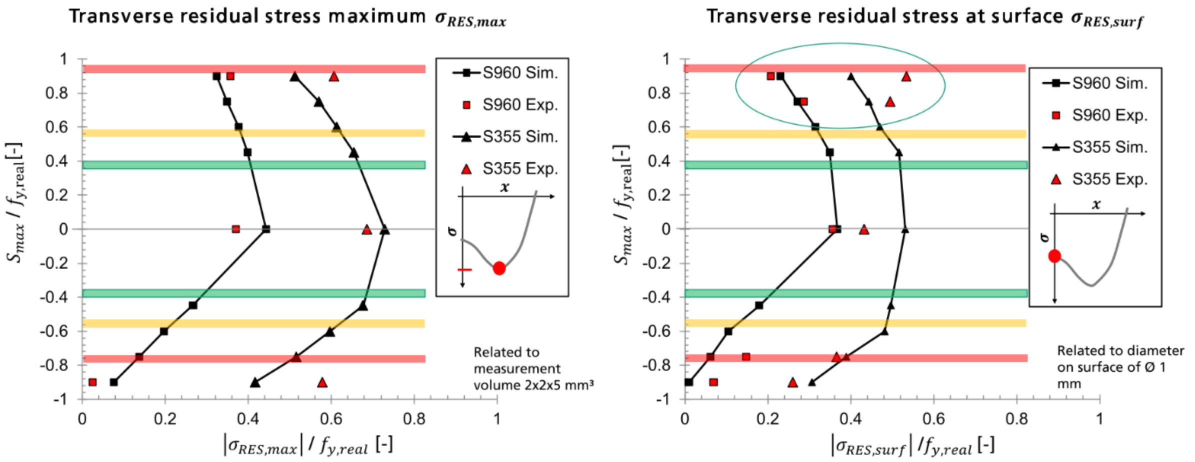

S_{max}= Maximum nominal stress, $f_{y,real}$ = real yield strength of the base material

14
© Fraunhofer IWM

Conclusion

- Compressive overloads close to the base materials yield strength (-0.9f_y) lead to nearly full residual stress relaxation for S960 and around half residual stress relaxation for S355.
- For tensile overloads close to the base materials (0.9f_y) yield strength only minor residual stress (-10% to -35%) relaxation was observed for both steel grades.
- Significantly less residual stress relaxation was determined for S355 than for S960 at the same normalized nominal stress S_{max}/f_y.
- IIW-recommendation of S_{max}/f_y shows a clear over-conservatism.

15

Literature

Marquis et al. (2013) — G. B. Marquis, E. Mikkola, H. C. Yildirim, and Z. Barsoum, “Fatigue strength improvement of steel structures by high-frequency mechanical impact: proposed fatigue assessment guidelines,” *Weld. World*, vol. 57, no. 6, pp. 803–822, Nov. 2013

Haagensen & Maddox (2013) — P. J. Haagensen and S. J. Maddox, *IIW recommendations on post weld improvement of steel and aluminium structures*, no. 79. Cambridge: Woodhead Publishing Ltd, 2013.

Mikkola et al. (2013) — E. Mikkola and H. Remes, “Allowable stresses in high-frequency mechanical impact (HFMI)-treated joints subjected to variable amplitude loading,” *Weld. World*, vol. 61, no. 1, 2017.

Kuhlmann et al. (2018) — U. Kuhlman, S. Breunig, T. Ummenhofer, and P. Weidner, “Entwicklung einer DASt-Richtlinie für höherfrequente Hämmerverfahren - Zusammenfassung der durchgeführten Untersuchungen und Vorschlag eines DASt-Richtlinien-Entwurfs (in German),” *Stahlbau*, vol. 10, no. 87, 2018

16

Interne Verfestigungsdomänen durch mechanische Oberflächenbehandlung während der additiven Fertigung

Dr.-Ing. Daniel Meyer

IWT Manufacturing Technologies

University of Bremen

IWT

Interne Verfestigungsdomänen durch mechanische Oberflächenbehandlung während der additiven Fertigung

Symposium Mechanische Oberflächenbehandlung am 22. und 23. Oktober 2019

Dr.-Ing. D. Meyer
M.Sc. N. Wielki

Leibniz Gemeinschaft

IWT

Scope of this presentation

Additive Manufacturing

EOS.info

Parts with limited surface quality and complex microstructures

Leibniz-IWT

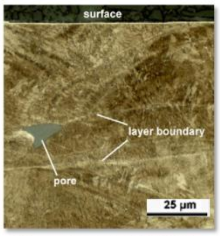

Brinksmeier et al., CIRP 2010

Post-Processing influencing the Surface Integrity

Dmgmori.com

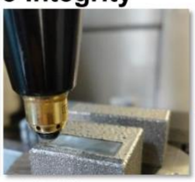

Leibniz-IWT

2

Potential of milling and deep rolling

in post-processing of AM parts

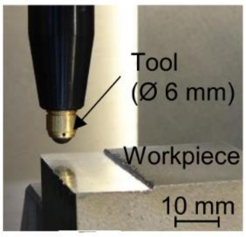

Experimental setup

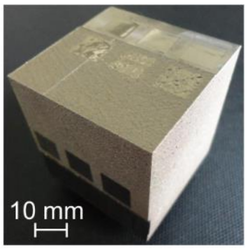

Cube after processing

Printing parameters	
•Layer thickness l	50 µm
•Laser power P_L	235 W
•Scan velocity v_s	700 mm/s
•Hatch distance h_d	150 µm, 120 µm
Milling parameters	
• Cutting speed v_c	80 mm/min
• Feed speed v_f	100 mm/min
• Depth of cut a_e	0.3 mm
Deep rolling parameters	
• Ball diameter d_b	6 mm
• Deep rolling pressure p_r	100, 200, 400 bar
• Rolling speed v_r	100 mm/min
• Stepover s_f	0.1 mm

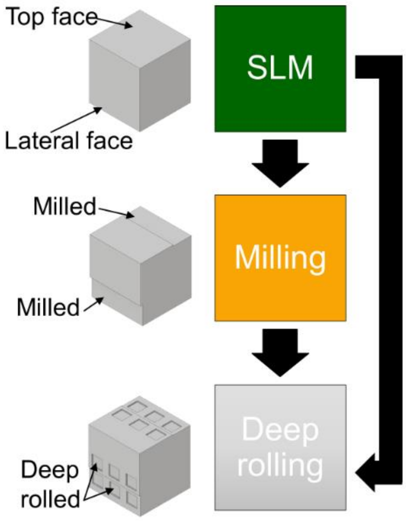

3

Hardness depth profiles

after milling and deep rolling of AM parts

Influence of hatch distance

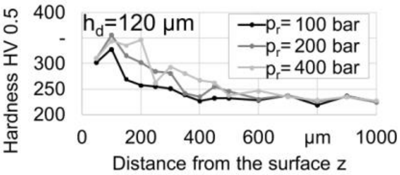

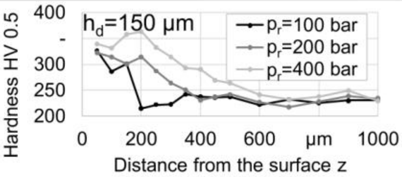

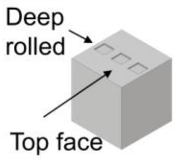

4

Hardness depth profiles

after milling and deep rolling of AM parts

IWT Leibniz-Institut für Werkstofforientierte Technologien

Influence of hatch distance

- Increasing hardness with increasing deep rolling pressure for both hatch distances
- Hatch distance influences the density/prositiy and thus the hardness depth profiles

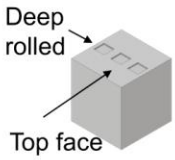

5

Hardness depth profiles

after milling and deep rolling of AM parts

IWT Leibniz-Institut für Werkstofforientierte Technologien

Influence of hatch distance

- Increasing hardness with increasing deep rolling pressure for both hatch distances
- Hatch distance influences the density/prositiy and thus the hardness depth profiles

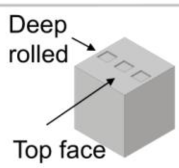

Influence of post-processing

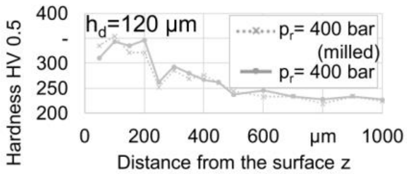

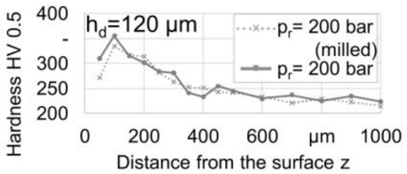

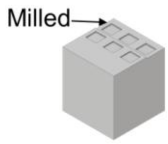

6

Hardness depth profiles

after milling and deep rolling of AM parts

IWT

Influence of hatch distance

- Increasing hardness with increasing deep rolling pressure for both hatch distances
- Hatch distance influences the density/prositiy and thus the hardness depth profiles

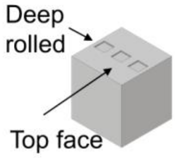

Influence of post-processing

- Hardness values are comparable for both post-processing strategies

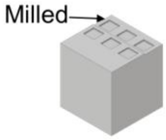

7

Hardness depth profiles

after milling and deep rolling of AM parts

IWT

Influence of hatch distance

- Increasing hardness with increasing deep rolling pressure for both hatch distances
- Hatch distance influences the density/prositiy and thus the hardness depth profiles

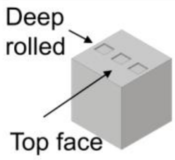

Influence of post-processing

- Hardness values are comparable for both post-processing strategies

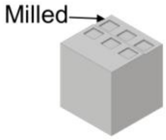

Influence of layer orientation

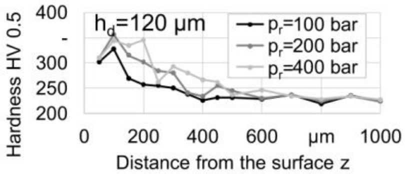

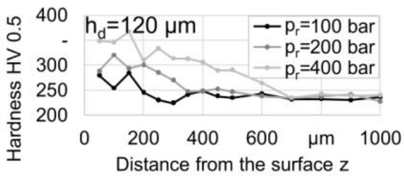

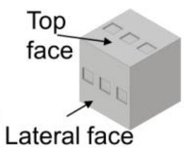

8

Hardness depth profiles

after milling and deep rolling of AM parts

Influence of hatch distance

- Increasing hardness with increasing deep rolling pressure for both hatch distances
- Hatch distance influences the density/prositiy and thus the hardness depth profiles

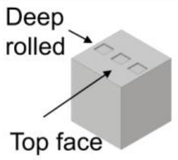

Influence of post-processing

- Hardness values are comparable for both post-processing strategies

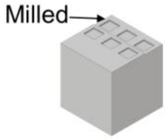

Influence of layer orientation

- Increasing hardness with increasing deep rolling pressure for both faces of the cube
- The courses differ more from each other at the lateral face

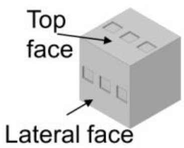

9

Surface topography

after deep rolling of AM parts

Top face

Sa = 6423.0 nm

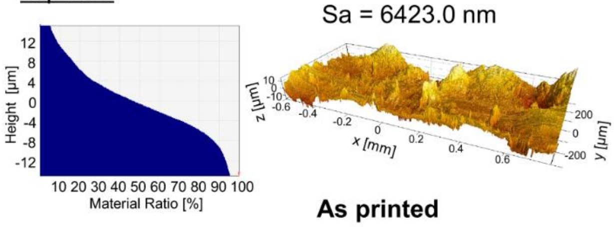

As printed

Sa = 162.7 nm

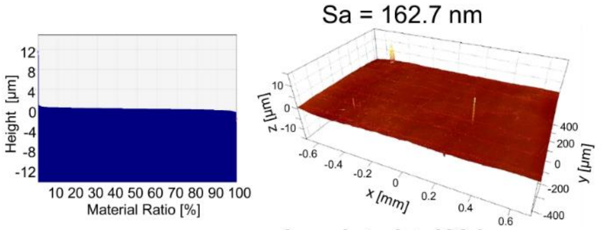

As printed + 400 bar

Lateral face

Sa = 10010.0 nm

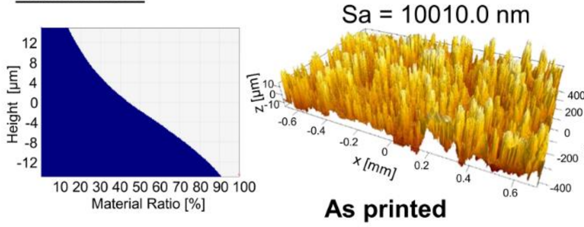

As printed

Sa = 390.2 nm

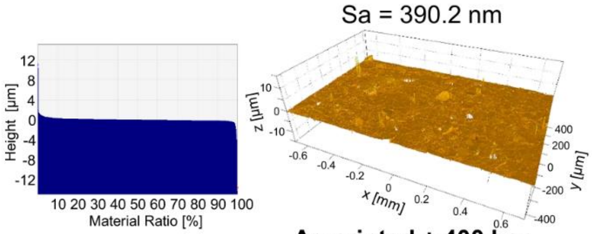

As printed + 400 bar

10

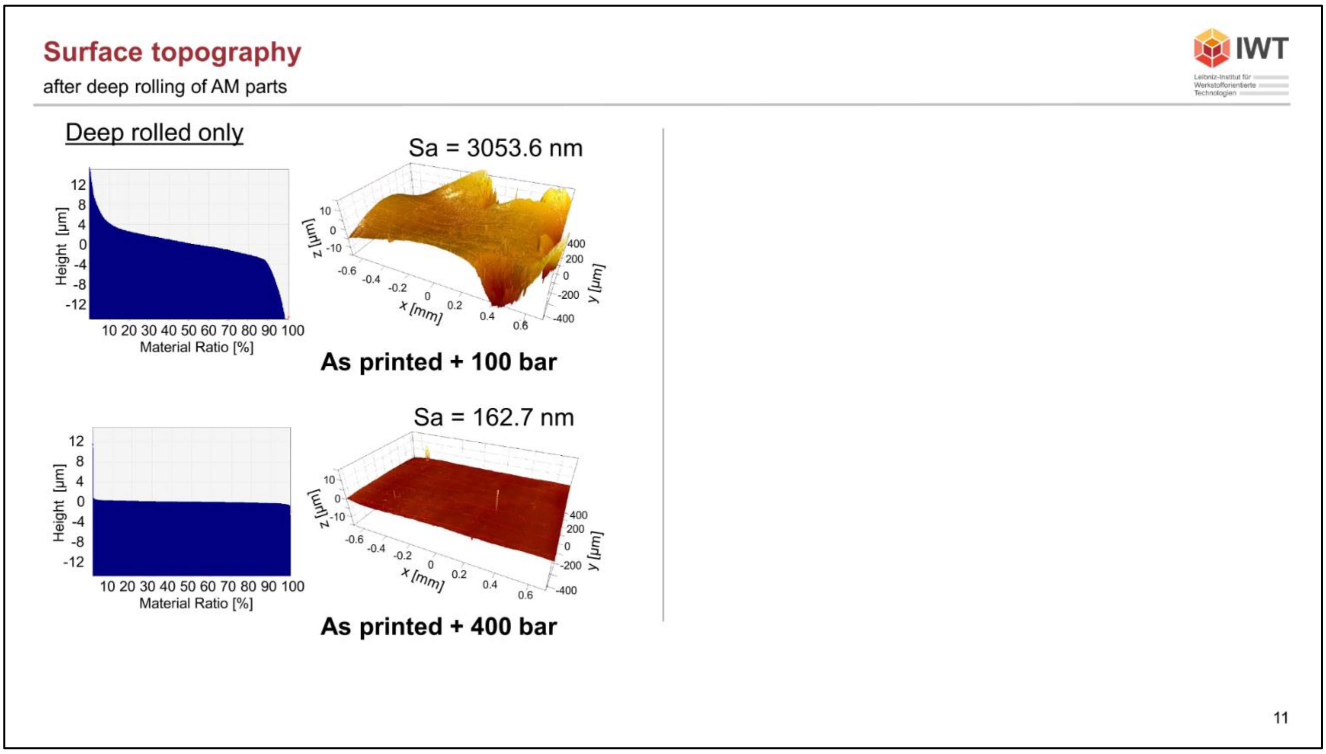
Surface topography
after deep rolling of AM parts
IWT
Deep rolled only
Sa = 3053.6 nm
As printed + 100 bar
Sa = 162.7 nm
As printed + 400 bar
Height [µm]
Material Ratio [%]
x [mm]
y [µm]
z [µm]
11

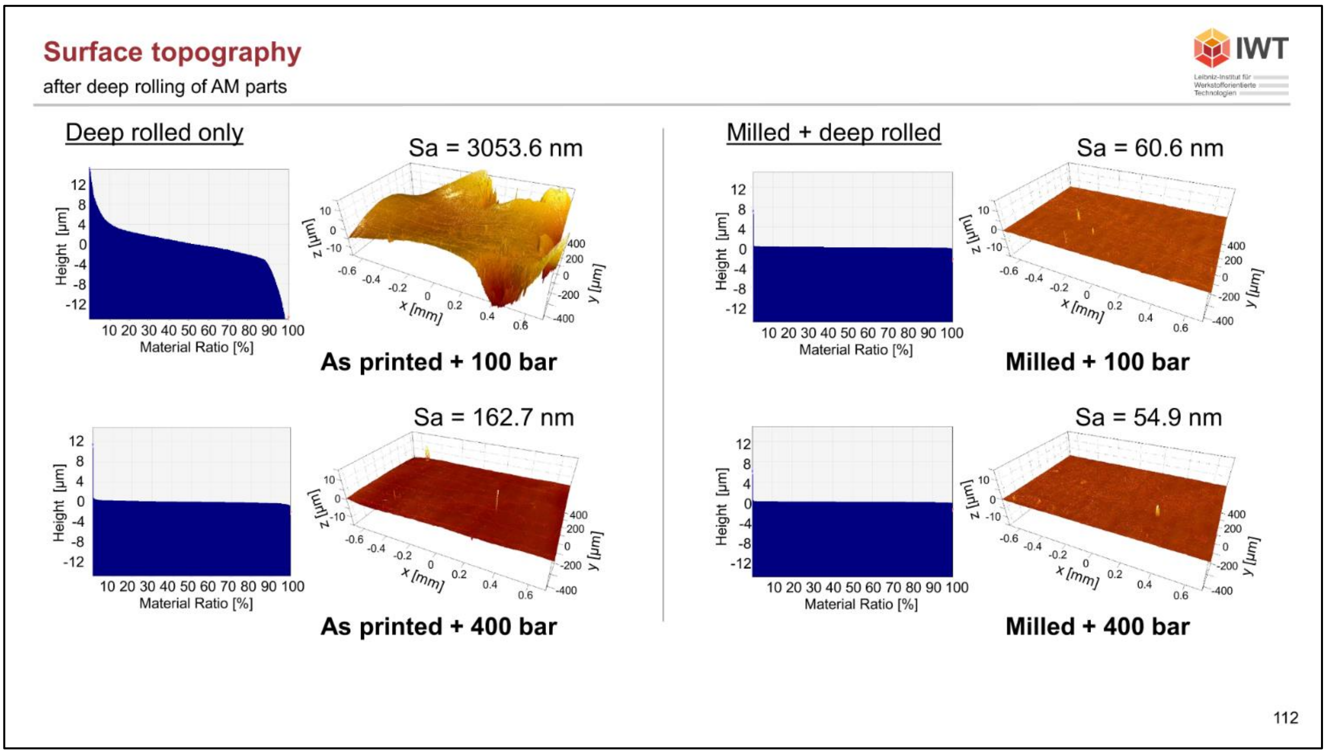
Surface topography
after deep rolling of AM parts
IWT
Deep rolled only
Sa = 3053.6 nm
As printed + 100 bar
Sa = 162.7 nm
As printed + 400 bar
Milled + deep rolled
Sa = 60.6 nm
Milled + 100 bar
Sa = 54.9 nm
Milled + 400 bar
Height [µm]
Material Ratio [%]
x [mm]
y [µm]
z [µm]
112

Scope of this presentation

IWT

Additive Manufacturing

EOS.info

Parts with limited surface quality and complex microstructures

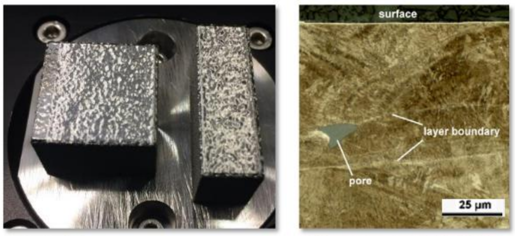

Leibniz-IWT Brinksmeier et al., CIRP 2010

Post-Processing influencing the Surface Integrity

Dmgmori.com Leibniz-IWT

Influence the bulk material or inaccessible areas locally

13

The concept of internal reinforced domains

IWT

- Make use of temporary accessibility of all areas during the build phase in AM
- Perform mechanical surface treatment with high depth effect locally
- Apply additional layers by Additive Manufacturing
- Generate three-dimensional internal reinforced domains with adapted Material Integrity

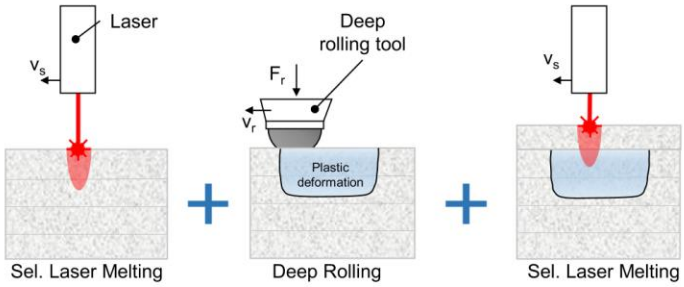

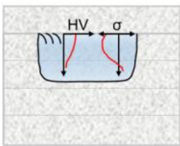

Internal reinforced Domains

14

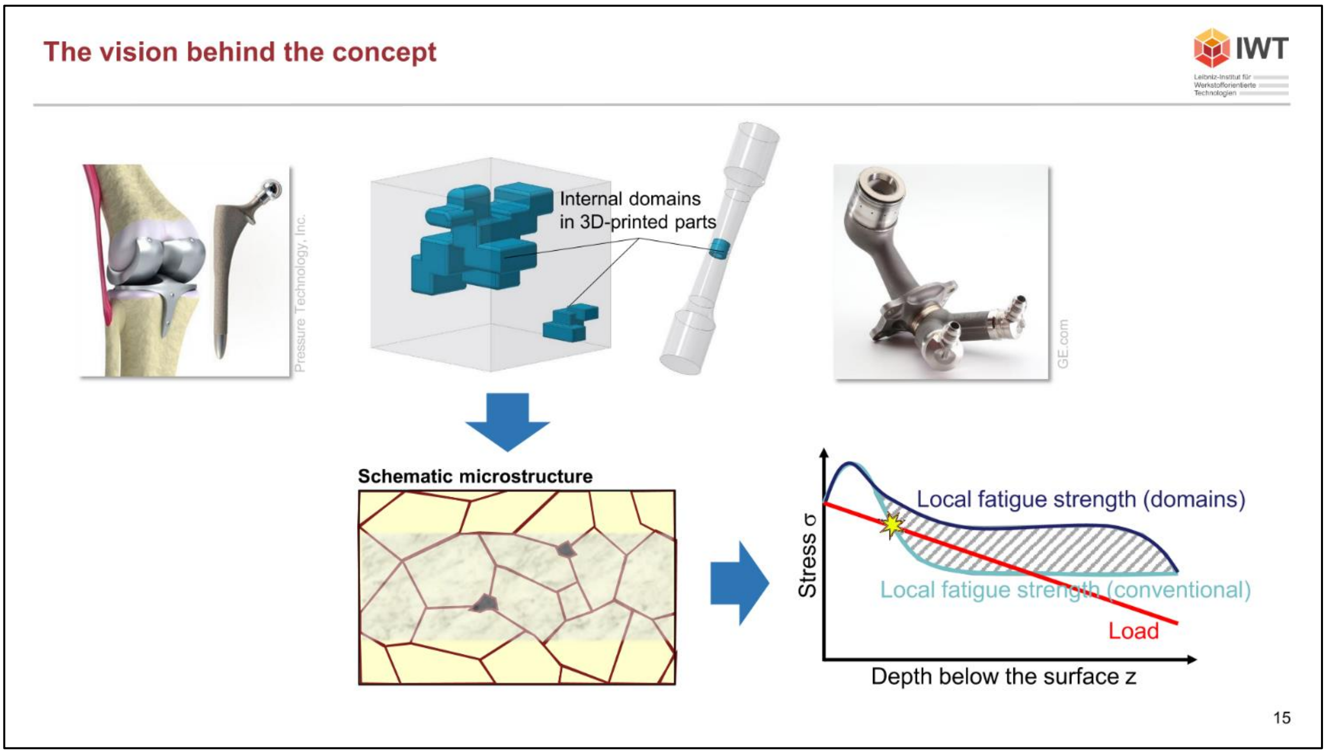
The vision behind the concept
IWT
Pressure Technology, Inc.
Internal domains
in 3D-printed parts
GE.com
Schematic microstructure
Stress σ
Local fatigue strength (domains)
Local fatigue strength (conventional)
Load
Depth below the surface z
15

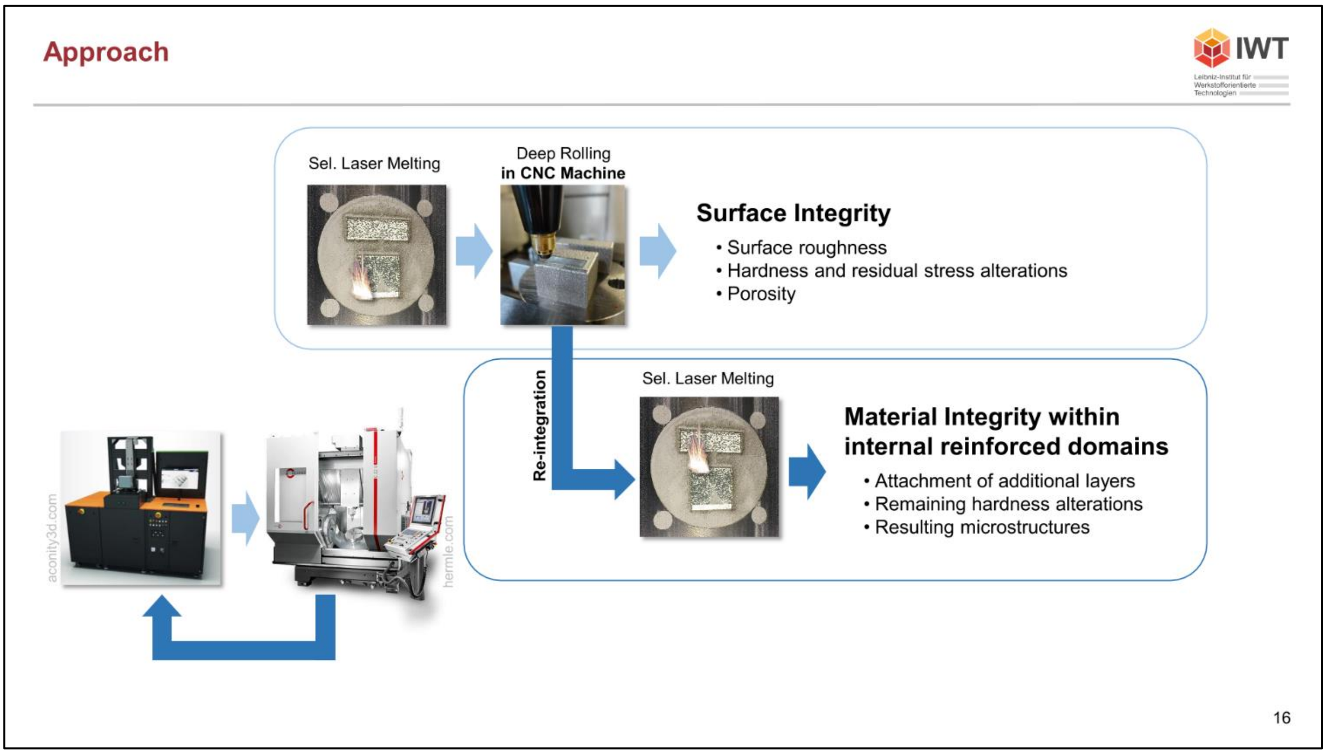
Approach
IWT
Sel. Laser Melting
Deep Rolling
in CNC Machine
Surface Integrity
• Surface roughness
• Hardness and residual stress alterations
• Porosity
Re-integration
Sel. Laser Melting
Material Integrity within
internal reinforced domains
• Attachment of additional layers
• Remaining hardness alterations
• Resulting microstructures
aconity3d.com
hermle.com
16

Surface Integrity after deep rolling of AM-parts

Surface Topography

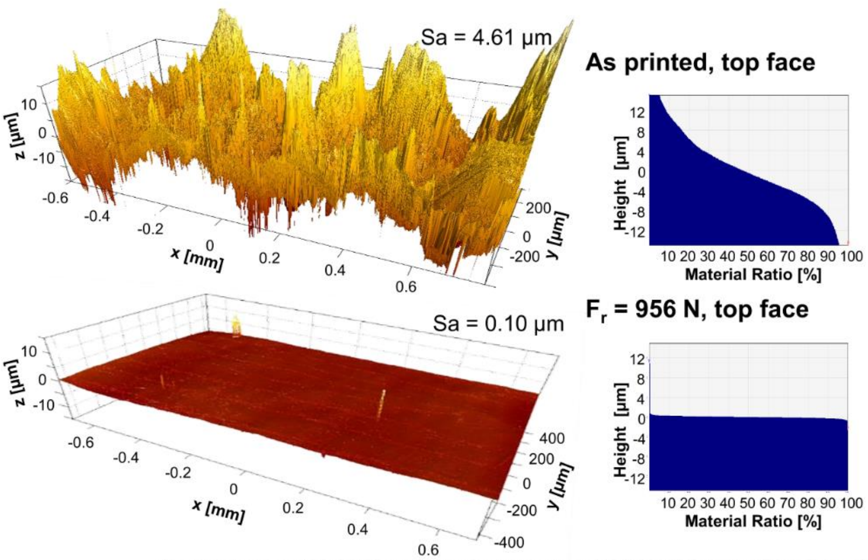

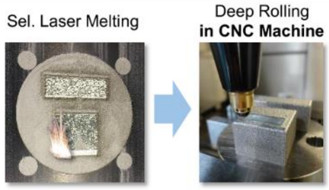

Selective Laser Melting

Material	AISI 316L
Part dimensions	50 x 50 x 50 mm
Laser power P_L	235 W
Layer thickness t_l	50 µm
Hatch distance h	120 µm; 150 µm
Scanning velocity v_s	700 m/s

Deep rolling

Ball diameter d_b	6 mm
Rolling pressure p_r	100 bar; 200 bar; 400 bar
Rolling force F_r	205 N; 441 N; 956 N
Feed f	0.1 mm
Rolling velocity v_r	100 mm/min

Sa-measurements: ISO 25178, applying a form operator and ISO 16610 Gaussian Filter, Talysurf CCI HD+ Software SPIP 6.7.4

17

Attachment of additional SLM-layers

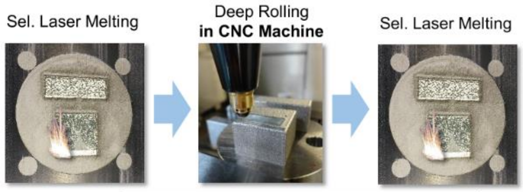

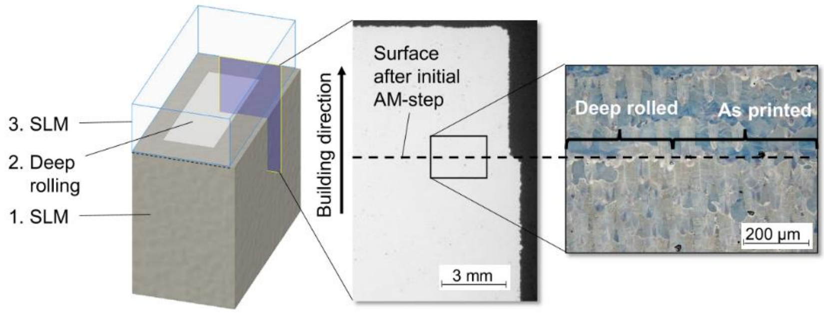

Selective Laser Melting

Material	AISI 316L
Part dimensions	50 x 50 x 50 mm
Laser power P_L	235 W
Layer thickness t_l	50 µm
Hatch distance h	120 µm
Scanning velocity v_s	700 m/s

Deep rolling

Ball diameter d_b	6 mm
Rolling pressure p_r	400 bar
Rolling force F_r	956 N
Feed f	0.1 mm
Rolling velocity v_r	100 mm/min

18

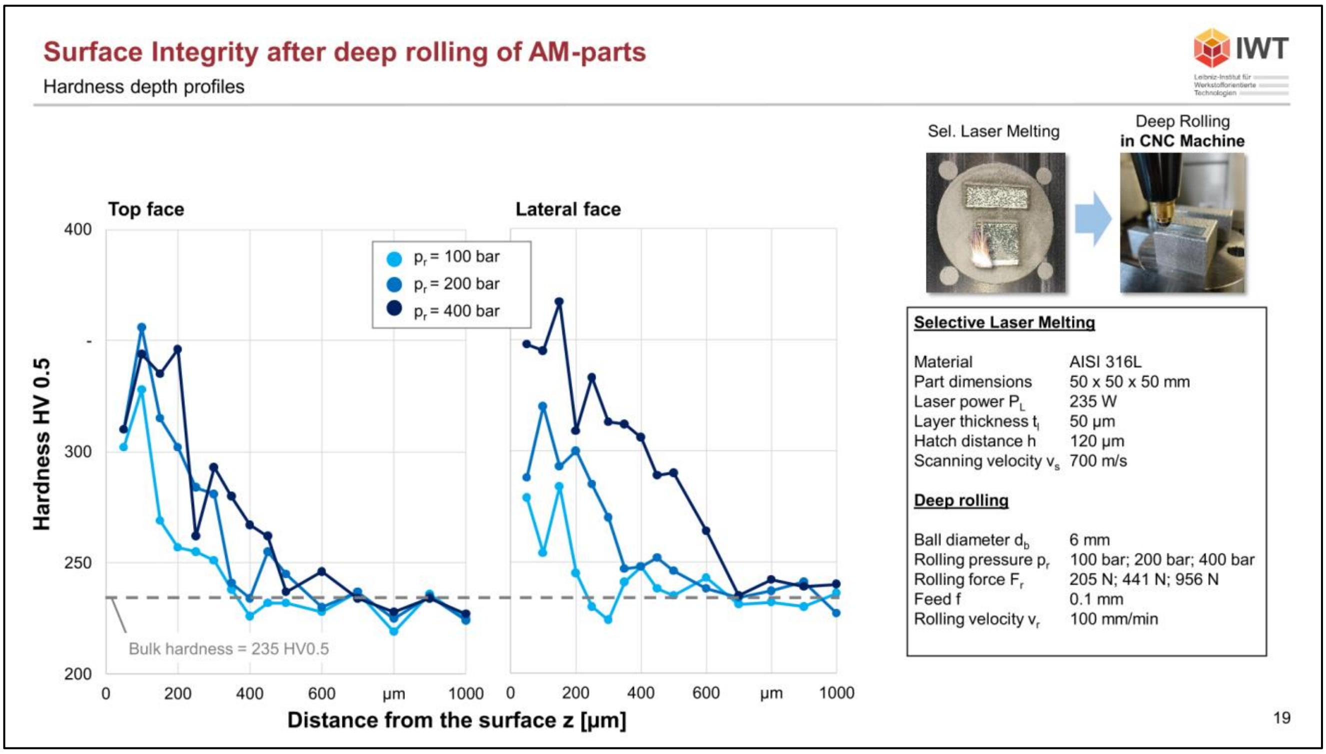
Surface Integrity after deep rolling of AM-parts
Hardness depth profiles
IWT
Sel. Laser Melting
Deep Rolling in CNC Machine
Top face
Lateral face
pr = 100 bar
pr = 200 bar
pr = 400 bar
Hardness HV 0.5
400
300
250
200
Bulk hardness = 235 HV0.5
0
200
400
600
µm
1000
Distance from the surface z [µm]
Selective Laser Melting
Material AISI 316L
Part dimensions 50 x 50 x 50 mm
Laser power PL 235 W
Layer thickness tl 50 µm
Hatch distance h 120 µm
Scanning velocity vs 700 m/s
Deep rolling
Ball diameter db 6 mm
Rolling pressure pr 100 bar; 200 bar; 400 bar
Rolling force Fr 205 N; 441 N; 956 N
Feed f 0.1 mm
Rolling velocity vr 100 mm/min
19

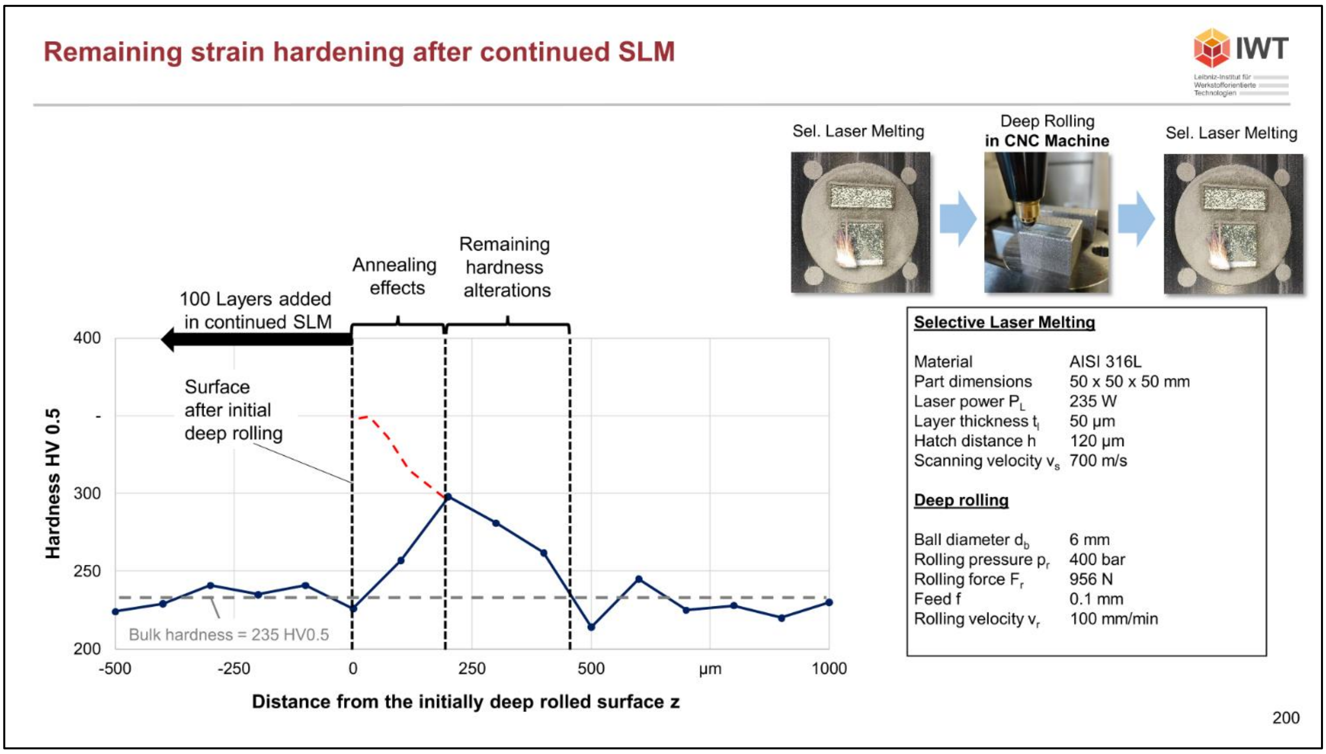
Remaining strain hardening after continued SLM
IWT
Sel. Laser Melting
Deep Rolling in CNC Machine
Sel. Laser Melting
100 Layers added in continued SLM
Annealing effects
Remaining hardness alterations
Surface after initial deep rolling
Hardness HV 0.5
400
300
250
200
Bulk hardness = 235 HV0.5
-500
-250
0
250
500
µm
1000
Distance from the initially deep rolled surface z
Selective Laser Melting
Material AISI 316L
Part dimensions 50 x 50 x 50 mm
Laser power PL 235 W
Layer thickness tl 50 µm
Hatch distance h 120 µm
Scanning velocity vs 700 m/s
Deep rolling
Ball diameter db 6 mm
Rolling pressure pr 400 bar
Rolling force Fr 956 N
Feed f 0.1 mm
Rolling velocity vr 100 mm/min
200

Remaining microstructural effects after continued SLM

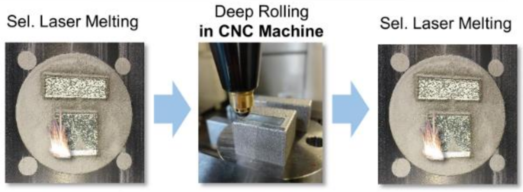

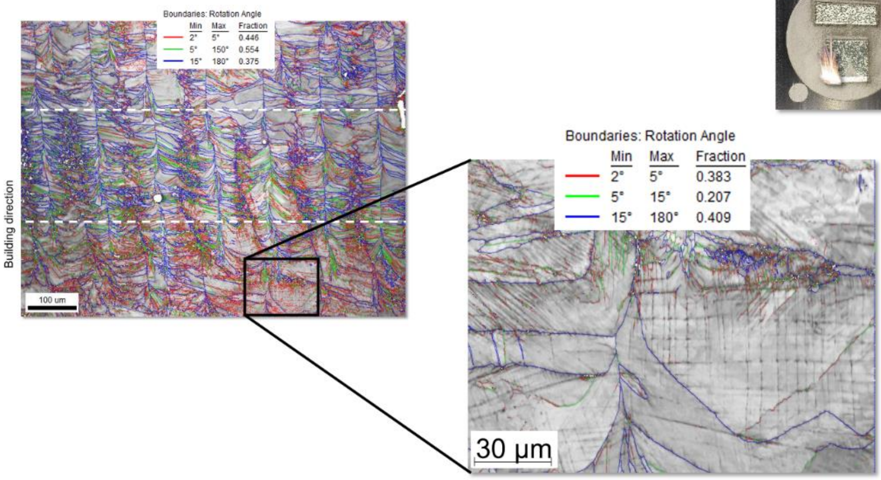

Dislocation slip and twinning effects

Selective Laser Melting

Material	AISI 316L
Part dimensions	50 x 50 x 50 mm
Laser power P_L	235 W
Layer thickness t_l	50 µm
Hatch distance h	120 µm
Scanning velocity v_s	700 m/s

Deep rolling

Ball diameter d_b	6 mm
Rolling pressure p_r	400 bar
Rolling force F_r	956 N
Feed f	0.1 mm
Rolling velocity v_r	100 mm/min

211

Conclusions and Outlook

- Smooth surfaces do not cause issues regarding attachment of additional layers
- Parts of the strain hardening effects after deep rolling are preserved after continuation of SLM
- Recrystallization effects occur due to re-heating effects
- Internal reinforced domains with enhanced Material Integrity can be generated using conventional machines and printers

- Reduce the depth effect of re-heating by adaptation of SLM parameters
- Generate specific hardness profiles in an alternating operation mode
- Consider effects of varying temperature in the building chamber
- Integrate the deep rolling process into the 3D-printer

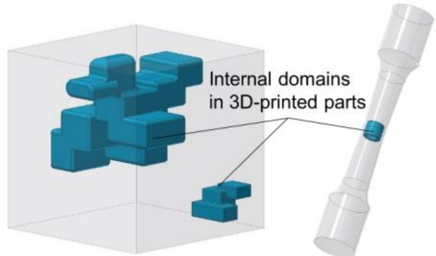

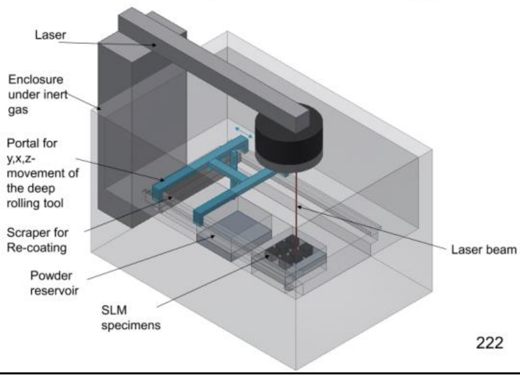

222


IWT
Thank you
for your kind attention!
Interne Verfestigungsdomänen durch mechanische Oberflächenbehandlung während der additiven Fertigung
Contact
Dr.-Ing. Dipl.-Biol. Daniel Meyer
Leibniz Institute for Materials Engineering (IWT)
Badgasteiner Str. 3
28359 Bremen, Germany
Tel.: +49(0) 421 218 51149
Fax: +49(0) 421 218 51101
E-Mail: dmeyer@iwt.uni-bremen.de

Influence of MHP on the material structure of CrNi steels

Markus Prießnitz

Institute of Production Engineering and Photonic Technologies

TU Wien

Agenda

1	**Background**
1.1	Metastable austenitic stainless steels
1.2	Martensitic transformation in stainless steels
2	**Experimental investigation**
2.1	Material selection
2.2	Sensor
2.3	Setup
2.4	Outcomes
3	**Application examples and outlook**

TU Wien | IFT Institute of Production Engineering and Photonic Technologies Page 3

Background of the research

- Previous work
  - Krall S., Reiter M., Bleicher F.. **"Influence of the machine hammer peening technology on the surface near material structure of stainless steel X5CrNi18-10."** Materials Today: Proceedings 5.13 (2018): 26603-26608.
  - Magnetic properties of stainless steel can be affected by MHP
- Interest
  - Materials science behind the process
  - Systematization and application
  - Code material and detect code
- Dissemination
  - Bachelor thesis
  - Patent protection


TECHNISCHE UNIVERSITÄT WIEN

Institut für Fertigungstechnik und Hochleistungslasertechnik

Bachelorarbeit

Einfluss der MHP Bearbeitung auf das Werkstoffgefüge von CrNi Stählen

ausgeführt zum Zwecke der Erlangung des akademischen Grades eines Bachelor of Science unter der Leitung von

Univ.-Prof. Dipl. Ing. Dr. Friedrich Bleicher

(Institut für Fertigungstechnik und Hochleistungslasertechnik)

Projektass. Dipl.-Ing. (FH) Stephan Krall MSc.

(Institut für Fertigungstechnik und Hochleistungslasertechnik)

Verfahren zur Bearbeitung eines einen Informationsbereich aufweisenden Bauteils, Bauteil mit einem Informationsbereich und Messsystem

Beschreibung

Die Erfindung betrifft ein Verfahren zum Ausbilden eines Informationsbereichs eines Bauteils gemäß dem Oberbegriff des Patentanspruchs 1, ein nach einem derartigen Verfahren ausgebildetes Bauteil und ein Messsystem zum Auslesen des Informationsbereichs eines derartigen Bauteils.

TU Wien | IFT Institute of Production Engineering and Photonic Technologies

Page 4

Types of magnetism

Diamagnetism

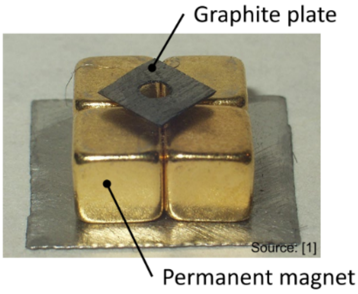

Paramagnetism

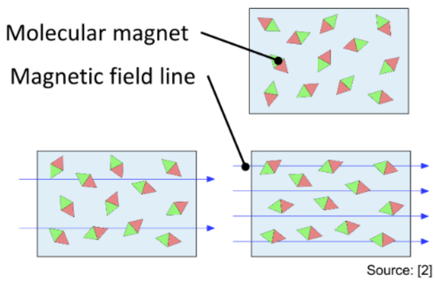

Ferromagnetism

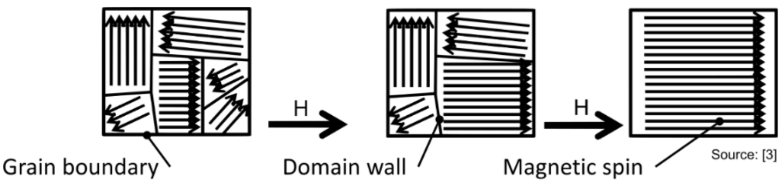

TU Wien | IFT Institute of Production Engineering and Photonic Technologies

Page 5

Magnetic properties of stainless steels

Ferritic stainless steels

- Crystalline structure bcc
- Magnetically soft behaviour
  - Induction
  - Shielding of magnetic fields
- Regulation of magnetic properties through alloying and heat treatment

Austenitic stainless steels

- Crystalline structure cfc
- Diamagnetic behaviour
  - Neutral exposed to magnetic fields
- Paramagnetic properties due to plastic deformation and residual ferrite

Martensitic stainless steels

- Crystalline structure bcc
- Magnetically hard behaviour
- Regulation of magnetic properties through alloying and heat treatment

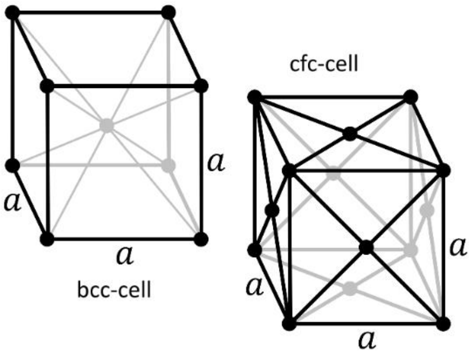

Source: [3]

TU Wien | IFT Institute of Production Engineering and Photonic Technologies

Page 6

Metastable austenitic stainless steels

Stabilisation of austenite

- Mechanically
  - Increase in volume during austenite to martensite transformation
- Chemically
  - Nickel, carbon and cobalt widen austenitic phase field

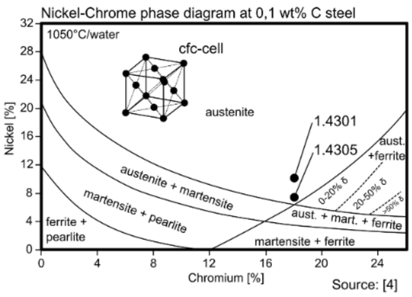

Source: [4]

Avoiding magnetisation

- Ferrite: Heat treatment
- Strain-induced martensite: special alloys with manganese

Relative permeability after cold working

Steel grade	µrel (φ=0)	µrel (φ=0,1)	µrel (φ=0,2)	µrel (φ=0,3)
X8CrNiS18-9 (1.4305)	1,003	1,050	1,620	3,420
X5CrNi18-10 (1.4301)	1,012	1,046	1,626	3,090
X2CrNiMo18-14-3 (1.4435)	1,007	1,008	1,024	1,130
X3CrNiCu18-9-4 (1.4567)	1,005	1,005	1,012	1,082

TU Wien | IFT Institute of Production Engineering and Photonic Technologies

Page 7

Martensite transformation - Initiation

- Thermal initiation
  - Driving force due to supercooling
- Mechanical initiation
  - Deformation induced
  - Strain induced
- Initiating the transformation by introducing the necessary enthalpy difference
- If MS<RT no thermal initiation at RT
- Additional mechanical enthalpy enables transformation at RT
- Martensite quantity dependent on stacking error energy

- Effect in sheet metal working known and undesired
- Targeted control of the introduced enthalpy possible through MHP
- Targeted exploitation of the regionally changed magnetic properties

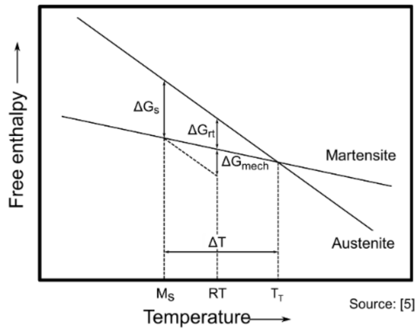

Source: [5]

Agenda

1	**Background**
1.1	Metastable austenitic stainless steels
1.2	Martensitic transformation in stainless steels
2	**Experimental investigation**
2.1	Material selection
2.2	Sensor
2.3	Setup
2.4	Outcomes
3	**Application examples and outlook**

Material selection

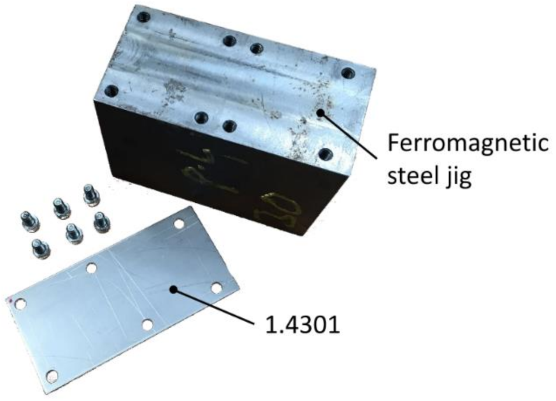

- X5CrNi18-10 (1.4301)
- 125x60x2mm
- E-MHP accurapuls
- Haas VF3

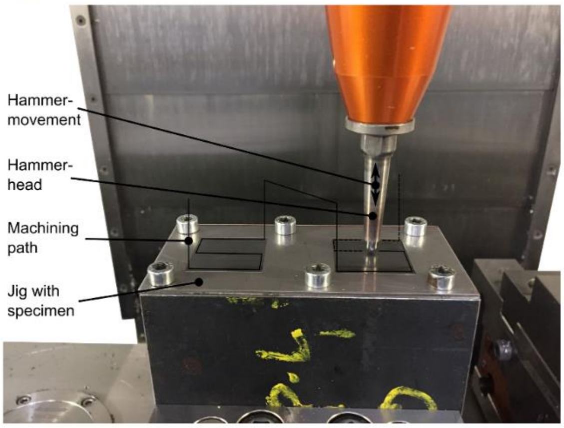

Parameter	Value and Unit
Diameter of hammerhead d	6mm
Hammering frequency f	200Hz
Stroke h	1mm
Feed rate v	1200mm/min
Stepover s	0,1mm
Distance between impressions a	0,1mm

TU Wien | IFT Institute of Production Engineering and Photonic Technologies

Page 10

Detection of magnetic permeability

- Magnetic induction
  - Coil on core
- Magnetic flux density
  - Hall-Effect
  - Magnetoresistance
- Ferromagnetism
  - Magnetic scale

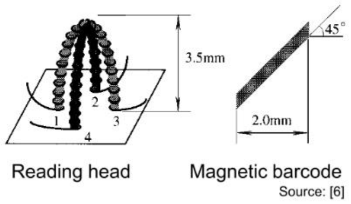

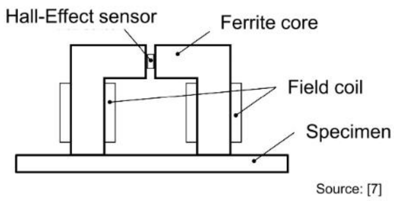

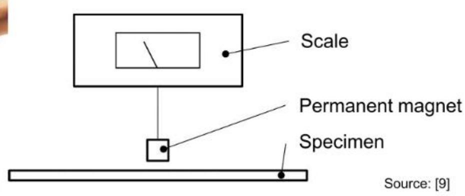

TU Wien | IFT Institute of Production Engineering and Photonic Technologies

Page 11

Sensor design

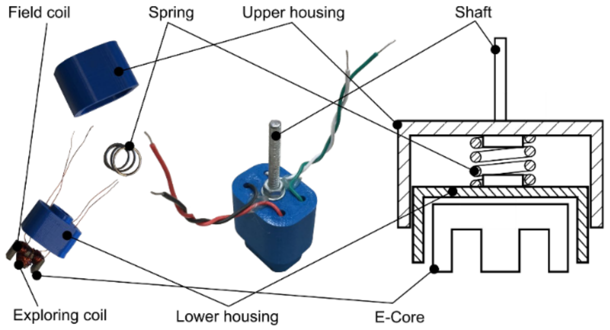

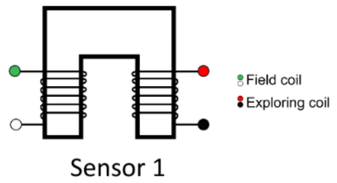

Parameter (Sensor 2)	Value and Unit
Windings of field coil Wire diameter	2x 30 windings 0,25mm
Windings of exploring coil Wire diameter	30 windings 0,25mm
Resistance of field coil	0,3028Ω
Inductance of field coil	27,3µH
Resistance of exploring coil	0,4376Ω
Inductance of exploring coil	106,92µH

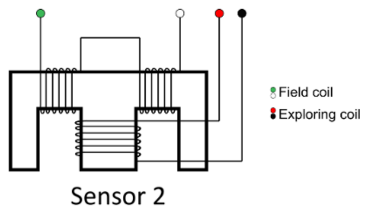

TU Wien | IFT Institute of Production Engineering and Photonic Technologies   Page 12

Experimental setup

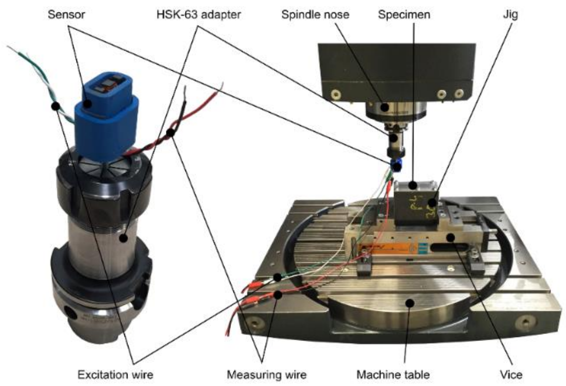

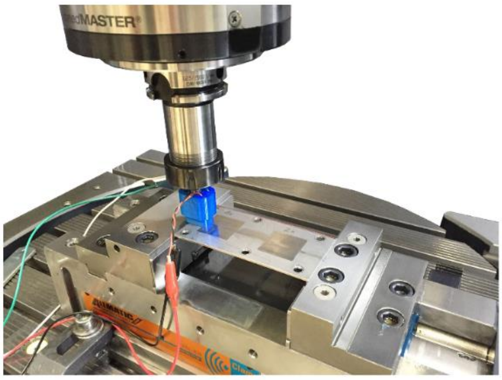

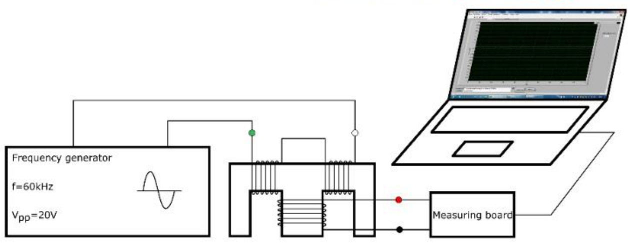

TU Wien | IFT Institute of Production Engineering and Photonic Technologies   Page 13

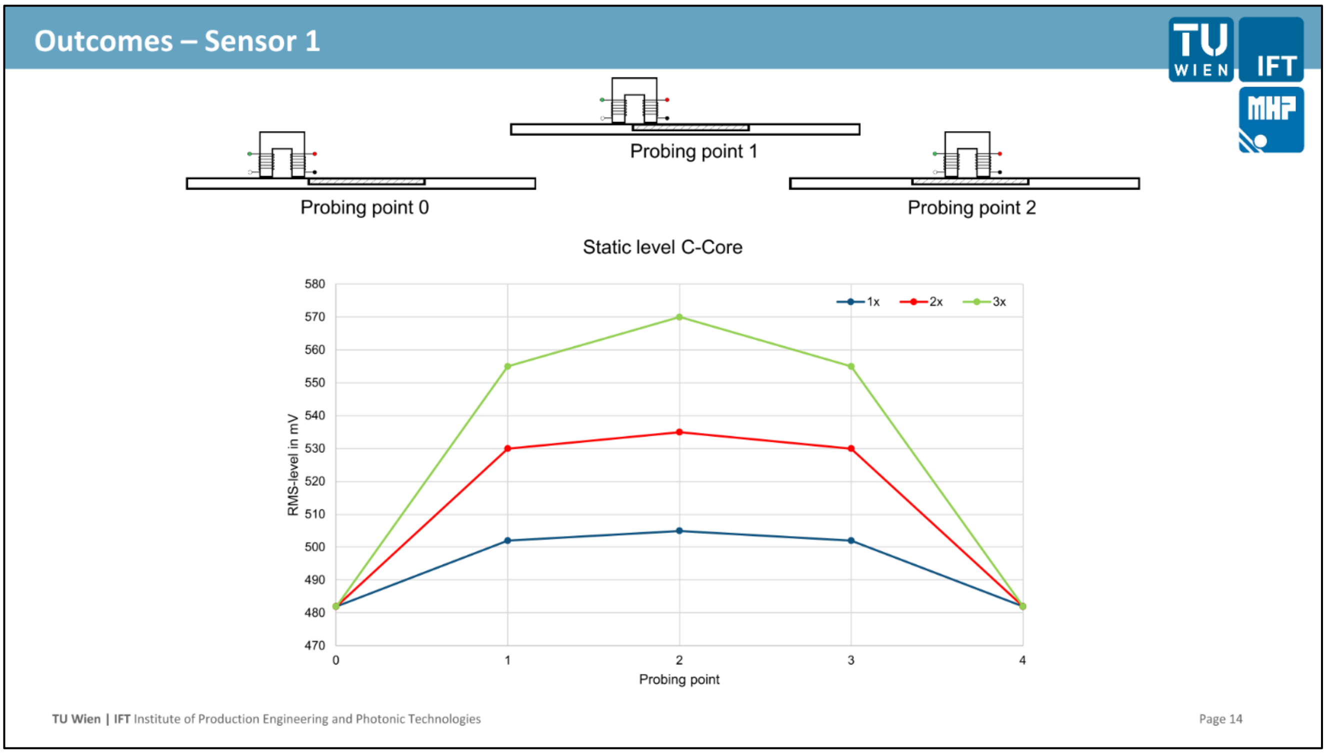
Outcomes – Sensor 1
TU WIEN
IFT
MHP
Probing point 1
Probing point 0
Probing point 2
Static level C-Core
1x
2x
3x
RMS-level in mV
580
570
560
550
540
530
520
510
500
490
480
470
0
1
2
3
4
Probing point
TU Wien | IFT Institute of Production Engineering and Photonic Technologies
Page 14

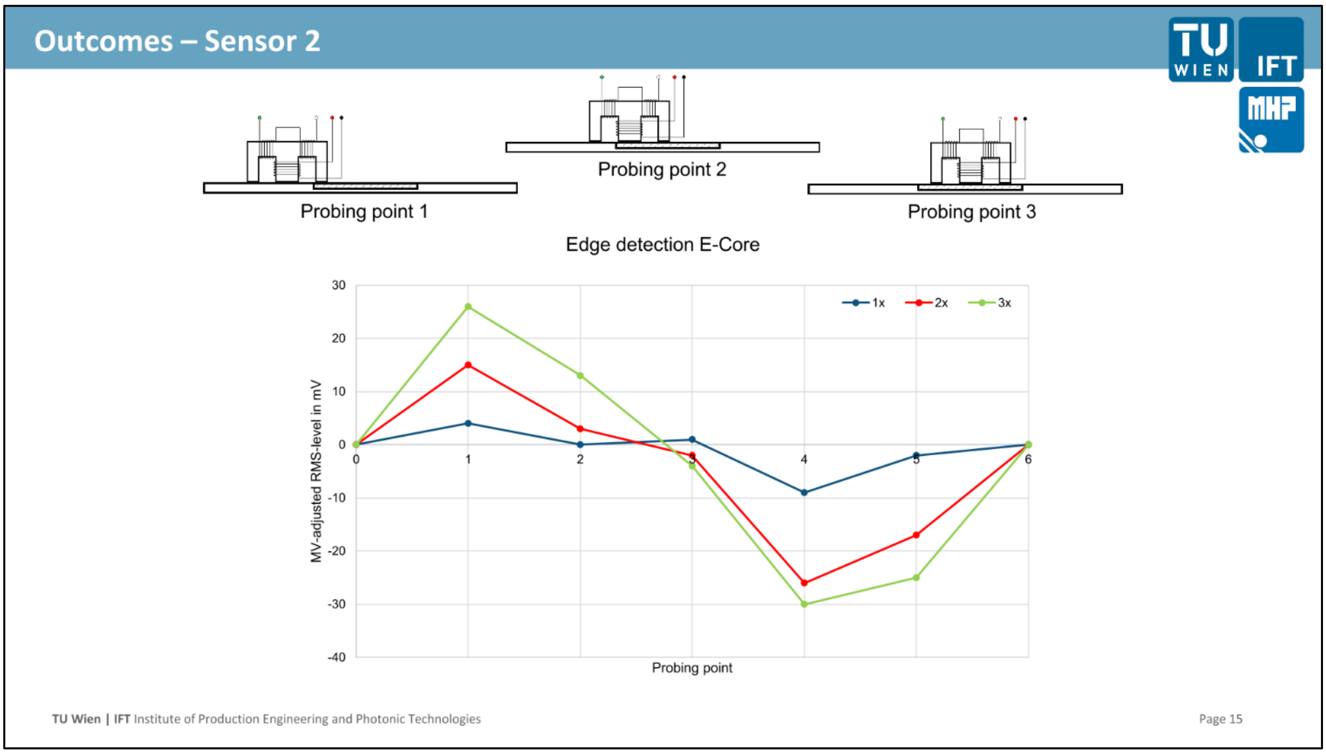
Outcomes – Sensor 2
TU WIEN
IFT
MHP
Probing point 2
Probing point 1
Probing point 3
Edge detection E-Core
1x
2x
3x
MV-adjusted RMS-level in mV
30
20
10
0
-10
-20
-30
-40
0
1
2
3
4
5
6
Probing point
TU Wien | IFT Institute of Production Engineering and Photonic Technologies
Page 15

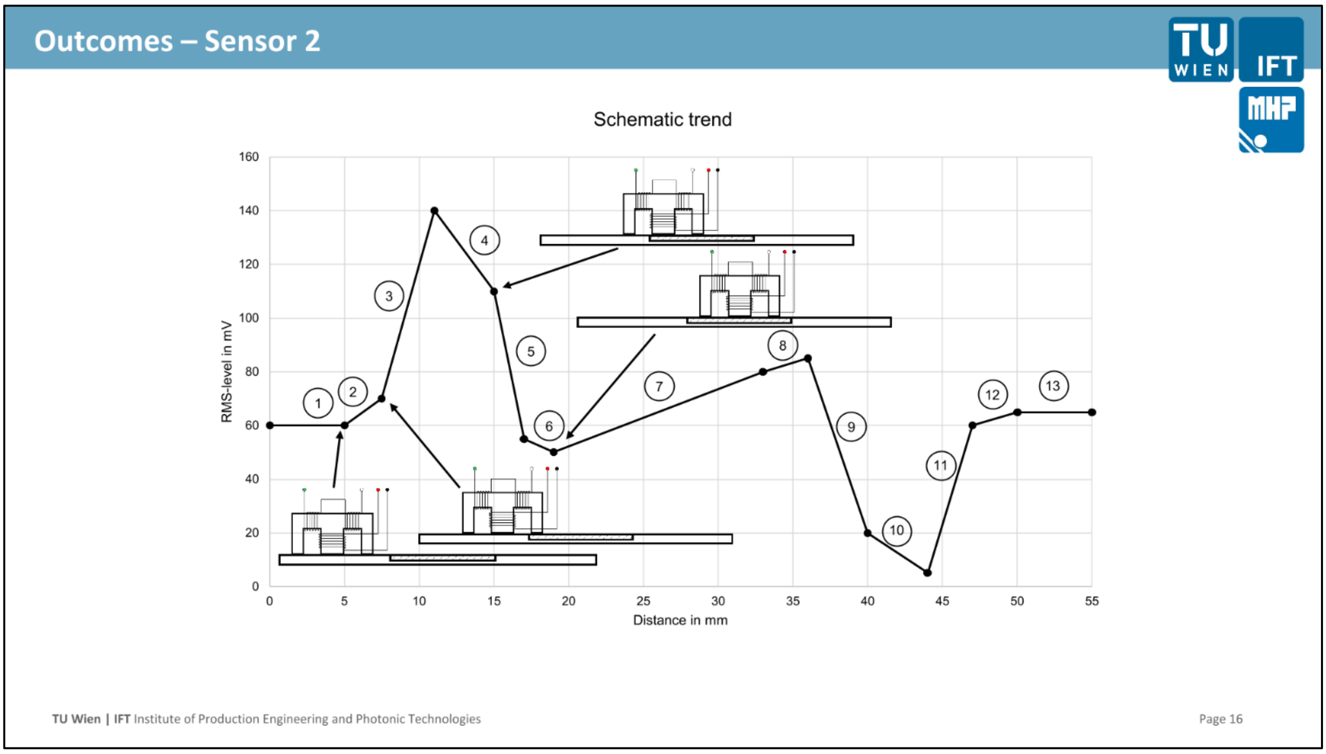
Outcomes – Sensor 2
Schematic trend
RMS-level in mV
Distance in mm
TU Wien | IFT Institute of Production Engineering and Photonic Technologies
Page 16

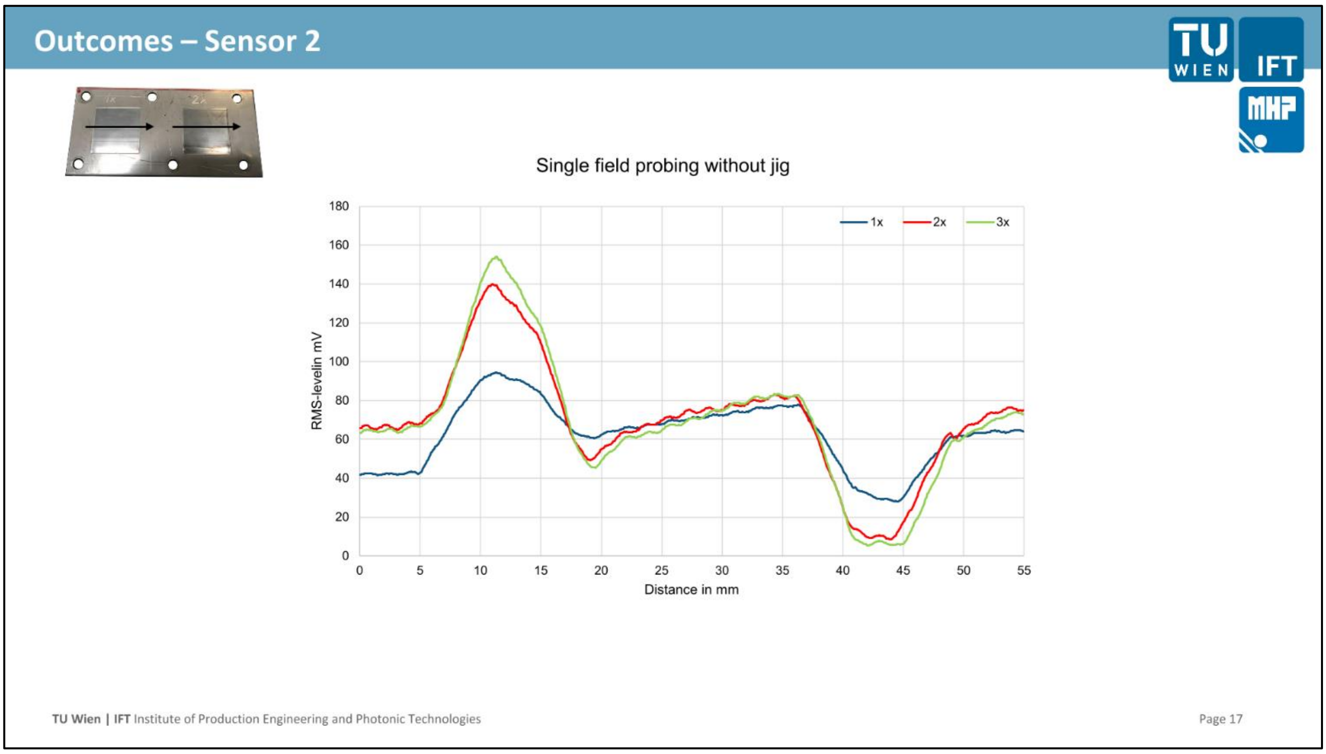
Outcomes – Sensor 2
Single field probing without jig
1x
2x
3x
RMS-levelin mV
Distance in mm
TU Wien | IFT Institute of Production Engineering and Photonic Technologies
Page 17

Outcomes – Sensor 2

Double field probing (1x – 2x)

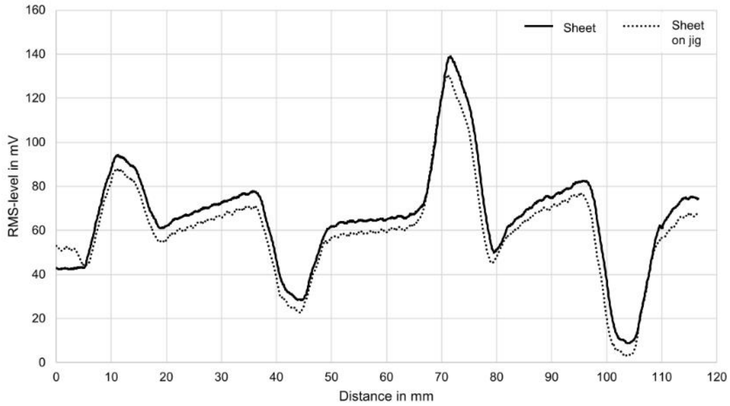

TU Wien | IFT Institute of Production Engineering and Photonic Technologies

Page 18

Agenda

1	**Background**
1.1	Metastable austenitic stainless steels
1.2	Martensitic transformation in stainless steels
2	**Experimental investigation**
2.1	Material selection
2.2	Sensor
2.3	Setup
2.4	Outcomes
3	**Application examples and outlook**

TU Wien | IFT Institute of Production Engineering and Photonic Technologies

Page 19

Application examples

- Treatment with MHP system on conventional NC systems
- Removal of machining marks by surface removal or coating possible
- Codification, marking
- Position measuring systems
- Locking systems
- Protection against operating errors
- OEM parts monitoring

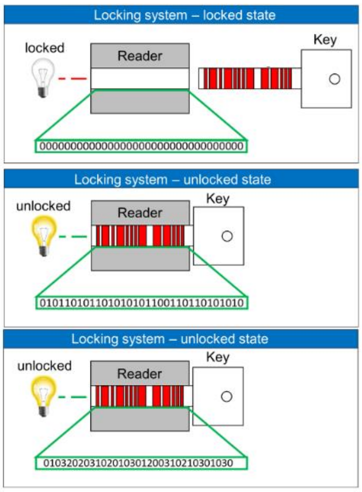

TU Wien | IFT Institute of Production Engineering and Photonic Technologies

Page 20

Intellectual property protection

- Patent application 2018111316194000DE
- "Verfahren zur Bearbeitung eines einen Informationsbereich aufweisenden Bauteils, Bauteil mit einem Informationsbereich und Messsystem"
- Area-wise applied information area on metallic surface with varied intensity
- Application using elastic/plastic forming
- Strain-induced microstructure transformation
- Use of information area
  - Codification, marking
  - Metrology
  - Locking systems
  - …
- Reading head for decoding the workpiece

TU Wien | IFT Institute of Production Engineering and Photonic Technologies

Page 21

Outlook

- Miniaturisation and testing of spatial resolution
  - Sensor
  - MHP-Process
- Combined sensors
  - Static measurements
  - Edge detection
- Contactless detection
- Detection on smooth surfaces
- Alternative approaches for detection
  - Hall-Effect sensor

TU Wien | IFT Institute of Production Engineering and Photonic Technologies Page 22

Discussion

Thank you for your attention!
Questions?

Influence of MHP process on the material structure of CrNi steels
Markus Prießnitz
priessnitz@ift.at

We thank the *Machine Tool Technologies Research Foundation* (MTTRF) for the loaned equipment, on which part of the presented work has been carried out.

MTTRF

TU Wien | IFT Institute of Production Engineering and Photonic Technologies Page 23

Contact

Contact Person
Markus Prießnitz
E priessnitz@ift.at
T +43 1 58801 31182

Vienna University of Technology
Institute of Production Engineering and Photonic Technologies

Laboratory for Production Engineering
Franz-Grill-Strasse 4 Building OA
1030 Vienna
AUSTRIA

T +43 1 58801 31101
E office@ift.at

TU Wien | IFT Institute of Production Engineering and Photonic Technologies   Page 24

Image sources

[1]: Diamagnetic graphite levitation, Author: Splarka, CC0 1.0.

[2]: Paramagnetic probe with varying magnetic fields, Author: Jens Böning, CC0 1.0.

[3]: P. H. Mayrhofer, “Skriptum zur VO Ingenieurwerkstoffe”, TU Wien, 2015.

[4]: M. Zimmermann, Grigorescu, Müller-Bollenhagen, and Christ, “Metastable Austenitic Stainless Steels and the Effect of Deformation-Induced Phase Transformation on the Fatigue Properties”, 2014.

[5]: J. Scheil, “Entwicklung von Austenitisch- Ferritischem Gusseisen (ADI) aus EN-JS2070: Mikrostruktur, mechanische Eigenschaften und deren Auswirkung auf die Oberflächenbearbeitung durch das Maschinelle Oberflächenhämmern”, TU Darmstadt, Darmstadt, 2016.

[6]: N. Watanabe, I. Sasada, and N. Asuke, “A new high density magnetic bar code system”, J. Appl. Phys., Vol. 85, No. 8, P. 5462–5464, Apr. 1999.

[7]: F. Oberhauser, “Measurement Device for Magnetic Permeability of Steel in Production Processes”, TU Graz, Graz, 2014.

[8]: Helmut Fischer GmbH, “Broschüre Feritscope FMP30”

[9]: J. Talonen, P. Aspegren, and H. Hänninen, “Comparison of different methods for measuring strain induced α-martensite content in austenitic steels”, *Mater. Sci. Technol.*, Vol. 20, No. 12, P. 1506–1512, Dec. 2004.

Images without source number: M. Prießnitz, “Einfluss der MHP Bearbeitung auf das Werkstoffgefüge von CrNi Stählen”, TU Wien, Wien, 2018.

TU Wien | IFT Institute of Production Engineering and Photonic Technologies   Page 25

Influence of the hammer head geometry when machining higher strength materials by MHP

Peter Sticht

Institute for Production Engineering and Forming Machines

Technische Universität Darmstadt

Machine hammer peening (MHP) is a dynamic process to smoothen tool surfaces, increase hardness and introduce residual compressive stresses into the surface layer. Additionally, MHP can be used to apply surface textures that act as lubricant pockets onto tools with specifically shaped hammer heads. MHP-treated surfaces have proven to minimize friction and decrease wear and tear of sheet metal forming tools. As of now, the applicability on higher strength materials in the context of bulk metal forming processes has not yet been investigated sufficiently.

The presentation focuses on the application of MHP in the field of cold forging tools. High strength materials as hardened tool steel, powder metallurgical steel and cemented carbide are treated by MHP and the surface characteristics by means of roughness are investigated.

It is shown that MHP allows for a mechanical treatment of higher strength material and that adapted hammerhead geometries can lead to enhanced surface characteristics.

Forming processes and their reliability are heavily affected by the surface integrity of the tools used. Therefore, high effort is put into the finishing of tool surfaces. [1] MHP is commonly used for smoothing technical surfaces [2] and introducing residual compressive stresses [3] as well as causing strain hardening in the surface layer of the components treated [4]. By using specially shaped hammer heads, surface textures, which serve as lubricant pockets, can be applied onto the surface in the same process step [5]. The aforementioned effects are caused by an oscillating hammerhead that is deterministically guided over the surface by an industrial robot or a machining center [6].

Within the modern industrial environment, mainly electro-magnetic [7] or pneumatic [8] systems are used, whereas piezo-electric [9] actuators are used in current research applications. Primarily, MHP is used in the tool and mold making industry to ensure the surface integrity of the tools that will be involved in production processes such as deep drawing. It has been shown that micro textures can lower the friction coefficients by about 30 % compared to manually polished surfaces [5]. Also, wear phenomena and locations change, as particles that would be able to move in process direction are being caught by the micro textures and prevented from causing further abrasive wear on the tool [10]. Not only sheet metal forming processes, but also cold forging processes can benefit from hammer peened surfaces. The tribological loads in these processes are considerably higher and therefore, higher strength materials are selected to meet the criteria regarding durability.

So far, the effect of different hammerhead diameters on the smoothening behavior on tool steel and nodular cast iron has been investigated extensively whereas always spherical hammerheads have been used.

Different tool materials are measured in a variety of conditions. These values define the benchmark for the ongoing surface treatment by machine hammer peening.

In the next step, higher strength materials commonly used in the cold forging industry are treated by machine hammer peening with different parameter settings and an increasing number of repetitions, where necessary. It is shown that, for the most materials, it is possible to reach the desired characteristic surface values.

Following the study an approach to improve the MHP-treatment of higher strength material is presented, taking different hammer head geometries into consideration. The latest developments regarding the MHP treatment of higher strength materials as well as an outlook on further investigations conclude the presentation.

The authors would like to thank all participating industrial partners as well as the funding organizations for their contribution to the MHP technology.

References

1. Schulze, V., Bleicher, F.,Groche, P., Guo, Y.B., Pyun, Y.S.: Surface modification by machine hammer peening and burnishing: CIRP Annals – Manufacturing Technology 65 (2016), pp. 809-832

2. Wied, J.: Oberflächenbehandlung von Umformwerkzeugen durch Festklopfen: PhD-Thesis, Darmstadt (2011)

3. Hacini, L., van Le, N.: Effect of impact energy on residual stresses induced by hammer peening of 304L plates: in Journal of Materials Processing Technology 208 (2008), pp. 542-548

4. Groche, P., Engels, M., Müller: C.: Wear behavior of sheet metal forming tools made from nodular cast iron after mechanical surface treatments: in Transactions of NAMRI of SME (2010), pp. 531 – 538

5. Steitz, M. Stein, P., Groche, P.: Influence of Hammer-Peened Surface Textures on Friction Behavior: Tribology Letters (2015) 58:24

6. Steitz, M. Scheil, J., Müller, C. Groche, P.: Effect of Process Parameters on Surface Roughness in Hammer Peening and Deep Rolling: in Key Eng. Mat., Trans Tech Publications, Switzerland, 554-557 (2013), pp. 1887 – 1901

7. Patent DE 10 2006 033 004 A1: Klopfvorrichtung- und Verfahren, Deutsches Patent- und Markenamt, Germany (2006)

8. Patent 10 2010 019 547 A1: Kaltschmiedevorrichtung und Kaltschmiede-verfahren, Deutsches Patent- und Markenamt, Germany (2010)

9. Lienert, F., Hoffmeister, J., Schulze, V.: Residual Stress Depth Distribution after Piezo Peening of Quenched and Tempered AISI 4140: in Materials Science Forum, Vol. 768 – 769 (2014), pp. 526-533

10. Steitz, M, Klasen, P., Groche, P.: Wear behavior of hammer peened surface textures during strip drawing test: IDDRG 2015 Conference, Shanghai, China (2015)

Optimization of the stream finishing process for mechanical surface treatment by numerical and experimental process analysis

Patrick Neuenfeldt

wbk Institute of Production Science

Karlsruhe Institute of Technology

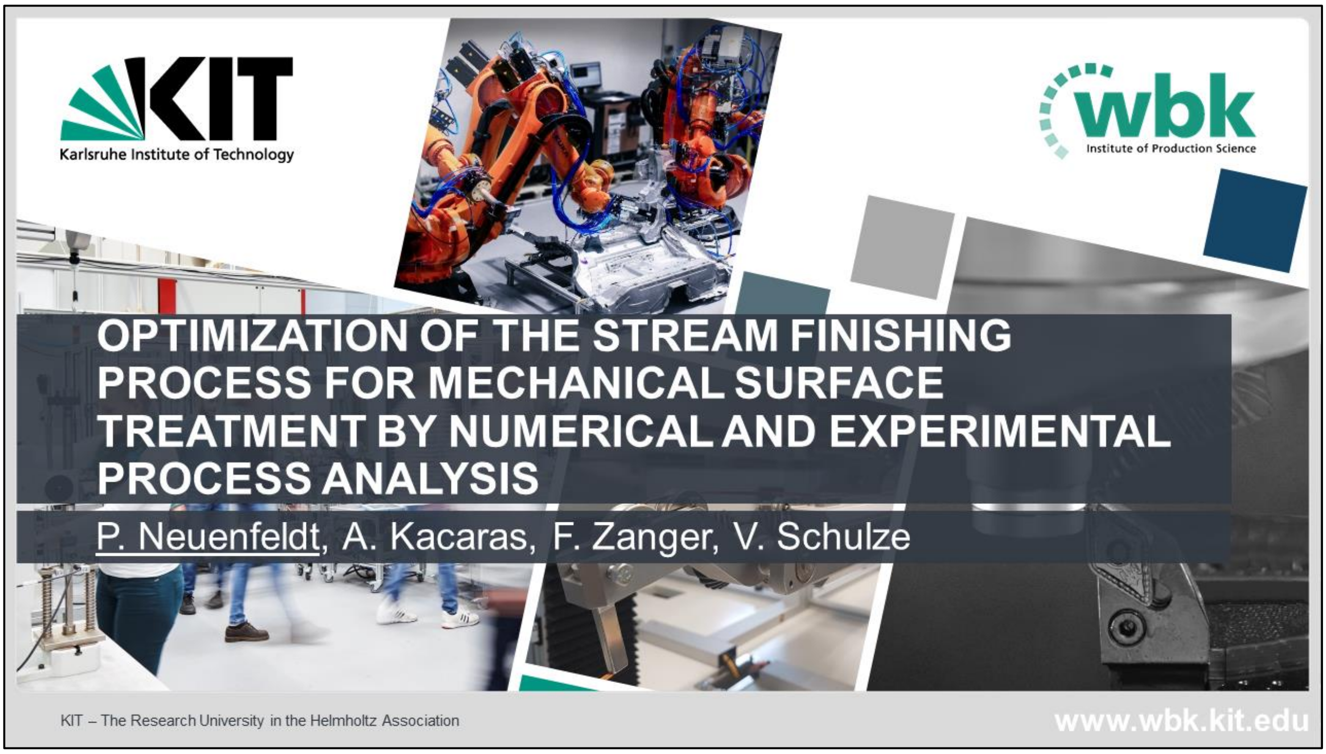
KIT
Karlsruhe Institute of Technology
wbk
Institute of Production Science
OPTIMIZATION OF THE STREAM FINISHING PROCESS FOR MECHANICAL SURFACE TREATMENT BY NUMERICAL AND EXPERIMENTAL PROCESS ANALYSIS
P. Neuenfeldt, A. Kacaras, F. Zanger, V. Schulze
KIT – The Research University in the Helmholtz Association
www.wbk.kit.edu

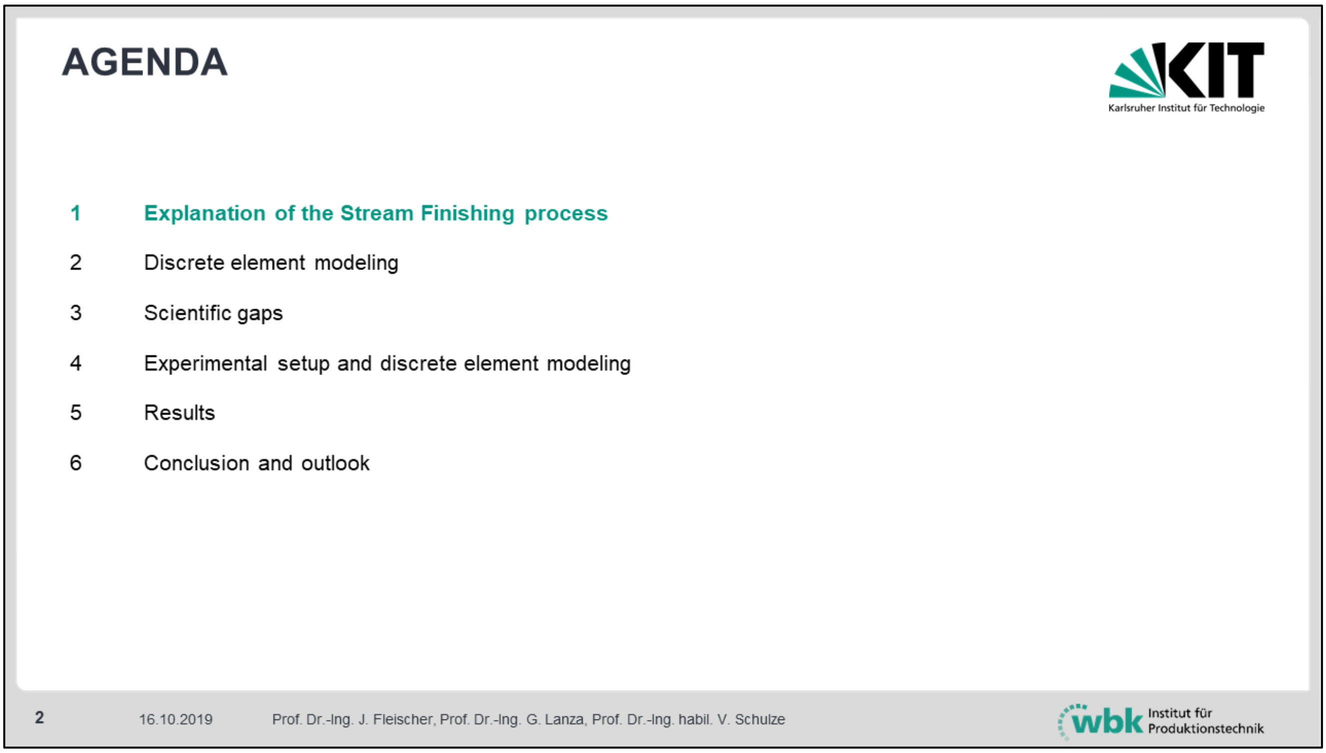
AGENDA
KIT
Karlsruher Institut für Technologie
1 Explanation of the Stream Finishing process
2 Discrete element modeling
3 Scientific gaps
4 Experimental setup and discrete element modeling
5 Results
6 Conclusion and outlook
2
16.10.2019
Prof. Dr.-Ing. J. Fleischer, Prof. Dr.-Ing. G. Lanza, Prof. Dr.-Ing. habil. V. Schulze
wbk Institut für Produktionstechnik

EXPLANATION OF THE STREAM FINISHING PROCESS

Karlsruhe Institute of Technology

Process properties

- Rotating bowl filled with granular material (media)
- Types of media
  - Bonded media: abrasive particles fixed in a matrix
  - Unbonded media
- Defined positioning of workpiece
  → relative velocity between media an workpiece's surface

Different types of bonded media

Stream Finishing of a turbine blade

3 16.10.2019 Prof. Dr.-Ing. J. Fleischer, Prof. Dr.-Ing. G. Lanza, Prof. Dr.-Ing. habil. V. Schulze

wbk Institute of Production Science

AGENDA

Karlsruher Institut für Technologie

1 Explanation of the Stream Finishing process

2 Discrete element modeling

3 Scientific gaps

4 Experimental setup and discrete element modeling

5 Results

6 Conclusion and outlook

4 16.10.2019 Prof. Dr.-Ing. J. Fleischer, Prof. Dr.-Ing. G. Lanza, Prof. Dr.-Ing. habil. V. Schulze

wbk Institut für Produktionstechnik

DISCRETE ELEMENT MODELING

Simulation method
- Numerical method to determine the movement of solids
- No meshing of the computation area needed like e.g. in CFD
- Meshing of solids only
- Different kinds of geometries and properties of solids possible
- DEM-Software Rocky DEM

Simulation procedure in general
- Definition of boundary conditions
- Definition of machine and workpiece kinematics
- Filling of the calculation area by stochastic distribution of solids
- Time-discrete calculation while executing machine and workpiece kinematics
  → transient simulation

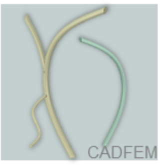

Fiber

Sheet

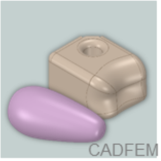

Volume

5 16.10.2019 Prof. Dr.-Ing. J. Fleischer, Prof. Dr.-Ing. G. Lanza, Prof. Dr.-Ing. habil. V. Schulze

DISCRETE ELEMENT MODELING

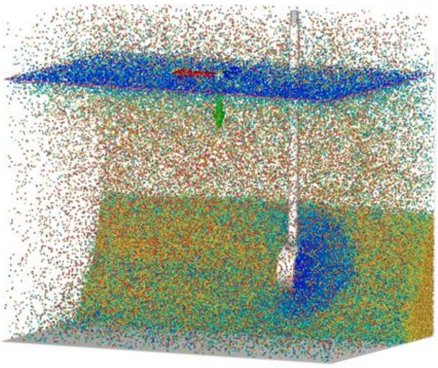
Filling of the calculation area

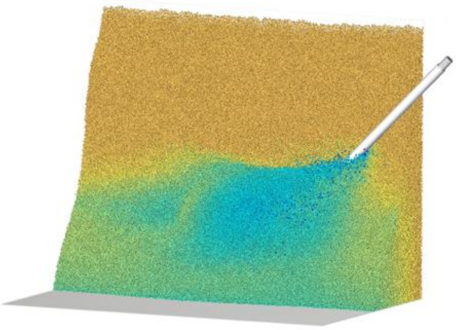
Executing machine and workpiece kinematics

6 16.10.2019 Prof. Dr.-Ing. J. Fleischer, Prof. Dr.-Ing. G. Lanza, Prof. Dr.-Ing. habil. V. Schulze

AGENDA

Karlsruher Institut für Technologie

1 Explanation of the Stream Finishing process

2 Discrete element modeling

3 **Scientific gaps**

4 Experimental setup and discrete element modeling

5 Results

6 Conclusion and outlook

7 16.10.2019 Prof. Dr.-Ing. J. Fleischer, Prof. Dr.-Ing. G. Lanza, Prof. Dr.-Ing. habil. V. Schulze

wbk Institut für Produktionstechnik

INTRODUCTION

Present scientific gaps for mass finishing

Karlsruhe Institute of Technology

Proportional relationship between material removal and the power equivalent is still unproven for mass finishing (Brocker)

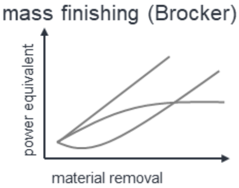

Knowledge of local contact forces and velocities is not available

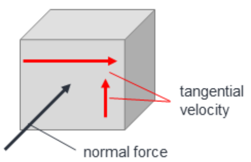

No approach for a realistic description of spatial flow formation is available

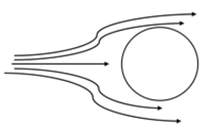

No consideration of surface states besides surface topography and correlation with process parameters

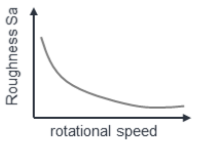

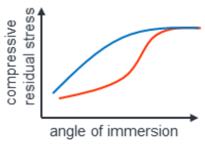

Scientific goal

- Cause-effect relationships between process parameters, contact conditions and surface integrity
- Experiment:
  - Normal force F_N
  - Material removal Δm
  - Roughness Sa
  - Residual stress σ^{RS}
- Simulation:
  - Normal force F_N
  - Tangential velocity v_t
  - → $P = F_N \cdot v_t$

8 16.10.2019 Prof. Dr.-Ing. J. Fleischer, Prof. Dr.-Ing. G. Lanza, Prof. Dr.-Ing. habil. V. Schulze

wbk Institute of Production Science

AGENDA

Karlsruher Institut für Technologie

1 Explanation of the Stream Finishing process

2 Discrete element modeling

3 Scientific gaps

4 **Experimental setup and discrete element modeling**

5 Results

6 Conclusion and outlook

9 16.10.2019 Prof. Dr.-Ing. J. Fleischer, Prof. Dr.-Ing. G. Lanza, Prof. Dr.-Ing. habil. V. Schulze

wbk Institut für Produktionstechnik

EXPERIMENTAL SETUP AND DISCRETE ELEMENT MODELING

Equipment and target values

Karlsruhe Institute of Technology

Experimental equipment

- Stream finishing machine SF1 68
- Alumina media KXMA 16 wetted with water and compound SC15 (grain size 1.7 to 2.4 mm)
- Disc shaped quenched and tempered AISI 4140 specimen
- Piezo resistive normal force sensors

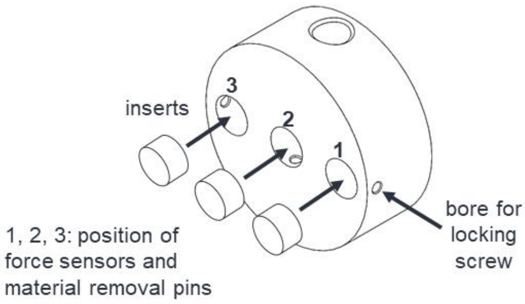

Stream Finishing of a specimen using KXMA 16

10 16.10.2019 Prof. Dr.-Ing. J. Fleischer, Prof. Dr.-Ing. G. Lanza, Prof. Dr.-Ing. habil. V. Schulze

wbk Institute of Production Science

EXPERIMENTAL SETUP AND DISCRETE ELEMENT MODELING

Processing parameters

Constant parameters

- Radius of immersion r = 270 mm
- Media height of 220 mm

Varied parameters

- To evaluate the influence of process parameters a broad parameter range was used

Height above the bowl bottom	z	75 to 150	mm
Rotational speed	n	30 to 90	U/min
Angle of immersion	φ	0° to 45°	
Workpiece orientation	γ	-50° to 50°	

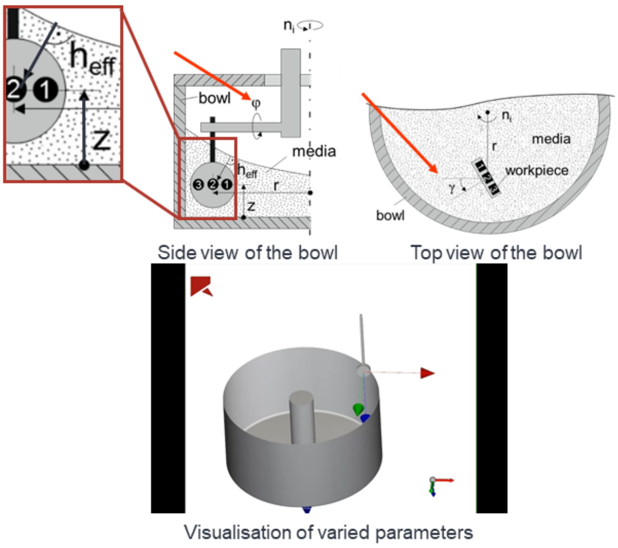

11 16.10.2019 Prof. Dr.-Ing. J. Fleischer, Prof. Dr.-Ing. G. Lanza, Prof. Dr.-Ing. habil. V. Schulze

EXPERIMENTAL SETUP AND DISCRETE ELEMENT MODELING

Simulative approach

- Abstracting trough a linear analogy channel
- Velocity distribution trough discrete path velocities on the ground
- particle distribution trough gravitational acceleration equivalent normal to the outer wall
- Media modelled by spheres (Ø 2 mm)

- Physical media properties according to dry Al_2O_3 [7, 8, 9]
- 1.25 Mio. particles
- Particles Young's modulus reduced by factor 1 E3 [10], [11]

→ **Downscaling provides comparable particle velocity vectors and flow formation [11]**

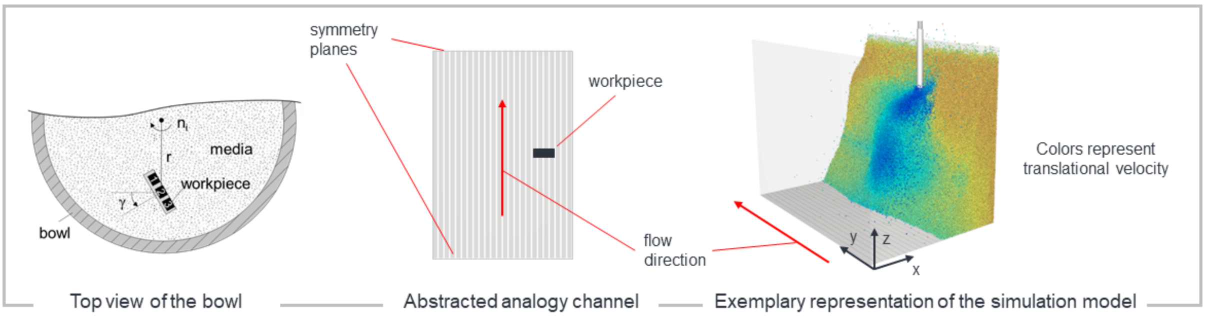

12 16.10.2019 Prof. Dr.-Ing. J. Fleischer, Prof. Dr.-Ing. G. Lanza, Prof. Dr.-Ing. habil. V. Schulze

AGENDA

KIT Karlsruher Institut für Technologie

1 Explanation of the Stream Finishing process

2 Discrete element modeling

3 Scientific gaps

4 Experimental setup and discrete element modeling

5 **Results**

6 Conclusion and outlook

13 16.10.2019 Prof. Dr.-Ing. J. Fleischer, Prof. Dr.-Ing. G. Lanza, Prof. Dr.-Ing. habil. V. Schulze

wbk Institut für Produktionstechnik

RESULTS

Correlation of simulation and experiments

KIT Karlsruhe Institute of Technology

- Vertically oriented groove direction before stream finishing (after surface grinding)
- Range of h_{eff} is largely in accordance to the experimental determined texture directions
- Good correlation of local texture directions (pos. a, 2, b) between experiment and simulation

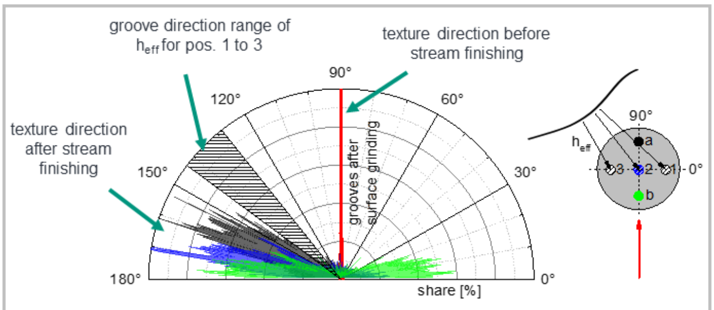

Fast fourier transform of surface topography

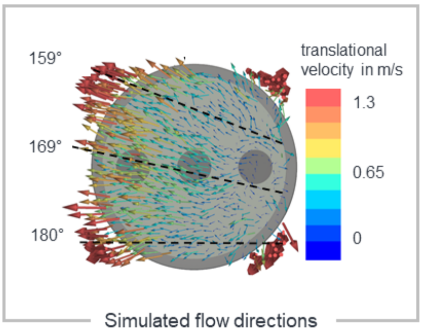

Simulated flow directions

14 16.10.2019 Prof. Dr.-Ing. J. Fleischer, Prof. Dr.-Ing. G. Lanza, Prof. Dr.-Ing. habil. V. Schulze

wbk Institute of Production Science

RESULTS

Normal Force

Karlsruhe Institute of Technology

Variation of process angles

- Variation of γ or φ to higher/lower values than 0 should always lead to reduced normal force F_N due to
  - Vector distribution of forces
  - Reduced impoundment effects due to a reduced projected area

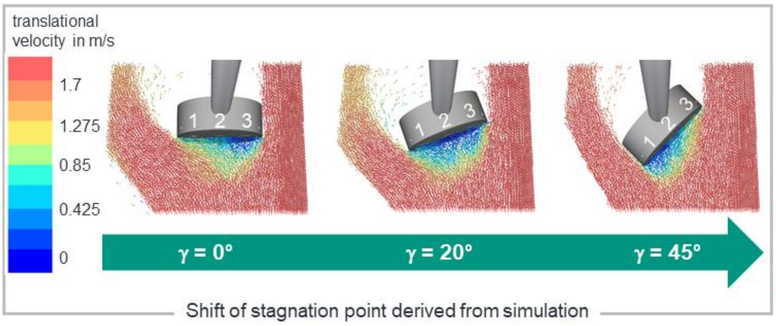

Shift of stagnation point derived from simulation

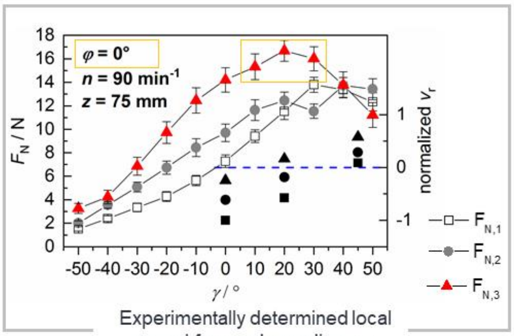

Experimentally determined local normal forces depending on γ

Inverse relation between normal force and tangential velocity is expected

15 16.10.2019 Prof. Dr.-Ing. J. Fleischer, Prof. Dr.-Ing. G. Lanza, Prof. Dr.-Ing. habil. V. Schulze

wbk Institute of Production Science

RESULTS

Simulation results

Karlsruhe Institute of Technology

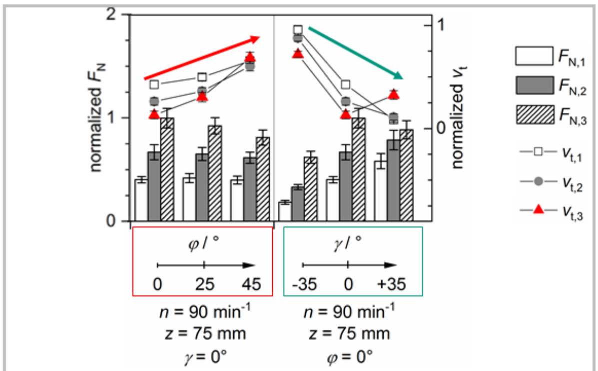

Simulative determined normal forces and tangential velocities

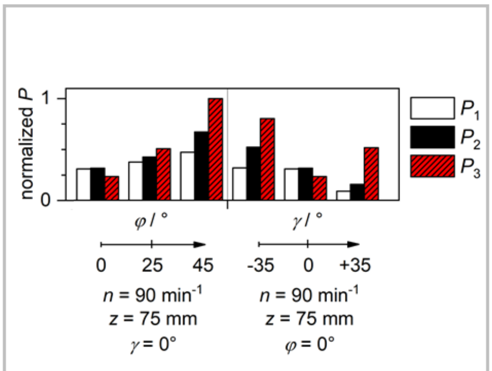

Power equivalent derived from simulation

- Normal force F_N and tangential velocity v_t are inversely influenced by process parameters
  - Increase of v_t leads to a decrease of F_N
  - Decrease of v_t leads to an increase of F_N

Introduction of the power equivalent P is necessary for a holistic process description

16 16.10.2019 Prof. Dr.-Ing. J. Fleischer, Prof. Dr.-Ing. G. Lanza, Prof. Dr.-Ing. habil. V. Schulze

wbk Institute of Production Science

RESULTS
Material removal

KIT – Karlsruhe Institute of Technology

- 20 min of stream finishing for each parameter
- Stationary roughness state despite of highly varying material removal
- P/Δm ratio shows standard deviation of 68 %
- Prestons law is therefore not applicable
- Results by Brocker can be confirmed

→ **No proportional correlation!**

Increase of power equivalent P leads to an increase of material removal Δm (qualitatively)

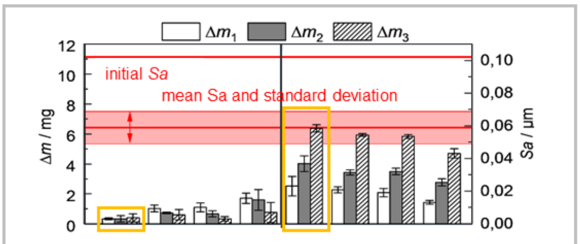

Experimentally determined material removal and roughness Sa

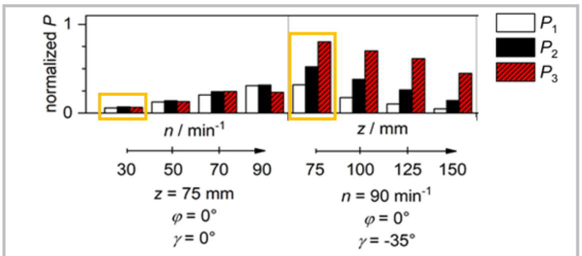

Simulative determined power equivalent P

17 16.10.2019 Prof. Dr.-Ing. J. Fleischer, Prof. Dr.-Ing. G. Lanza, Prof. Dr.-Ing. habil. V. Schulze

wbk Institute of Production Science

RESULTS
Surface integrity

KIT – Karlsruhe Institute of Technology

- Comparison of residual stress σ^{RS} and P
- Residual stress measured at position 2
- Evaluation of depth profiles up to 5 µm is reasonable
- Qualitative correlation of P and σ^{RS}
- Assumption of Kacaras et al. can clearly be confirmed

Increase of power equivalent P leads to an increase of compressive residual stress

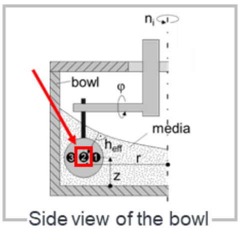

Side view of the bowl

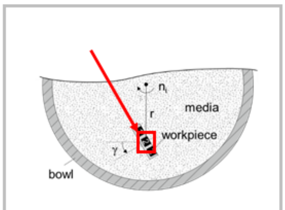

Top view of the bowl

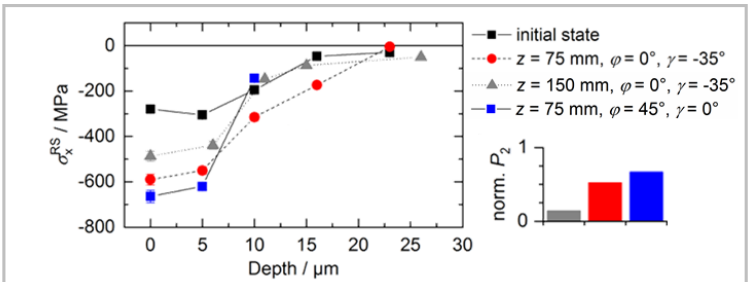

Residual stress states for defined process parameters and corresponding values of P

18 16.10.2019 Prof. Dr.-Ing. J. Fleischer, Prof. Dr.-Ing. G. Lanza, Prof. Dr.-Ing. habil. V. Schulze

wbk Institute of Production Science

AGENDA

Karlsruher Institut für Technologie

1 Explanation of the Stream Finishing process

2 Discrete element modeling

3 Scientific gaps

4 Experimental setup and discrete element modeling

5 Results

6 Conclusion and outlook

19 16.10.2019 Prof. Dr.-Ing. J. Fleischer, Prof. Dr.-Ing. G. Lanza, Prof. Dr.-Ing. habil. V. Schulze

wbk Institut für Produktionstechnik

CONCLUSION AND OUTLOOK

Karlsruhe Institute of Technology

Key findings

- Local consideration of normal force and tangential velocity is mandatory
- Process efficiency can effectively be influenced by the
  - Angle of immersion φ
  - Workpiece orientation γ
- Power equivalent P is a valid qualitative measure for Δm and σ^{RS}

Outlook

- Improve simulative approach to gain quantitative normal force values
- Validate findings using a complex geometry

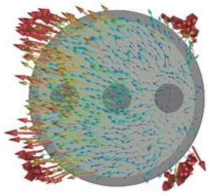

Simulated flow directions

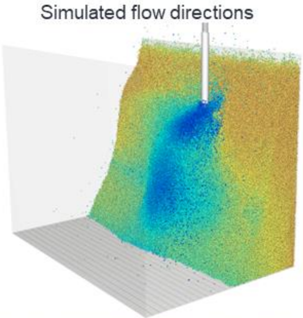

Exemplary representation of the simulation model

20 16.10.2019 Prof. Dr.-Ing. J. Fleischer, Prof. Dr.-Ing. G. Lanza, Prof. Dr.-Ing. habil. V. Schulze

wbk Institute of Production Science

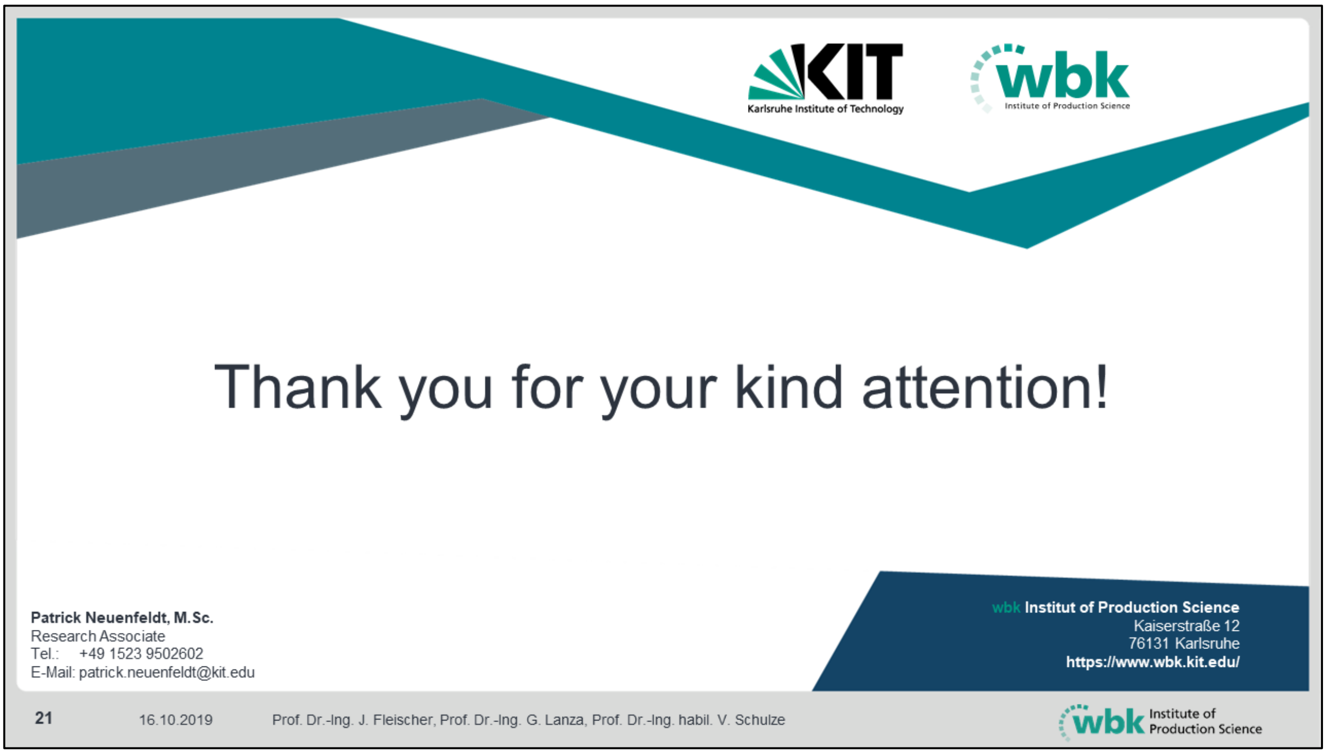

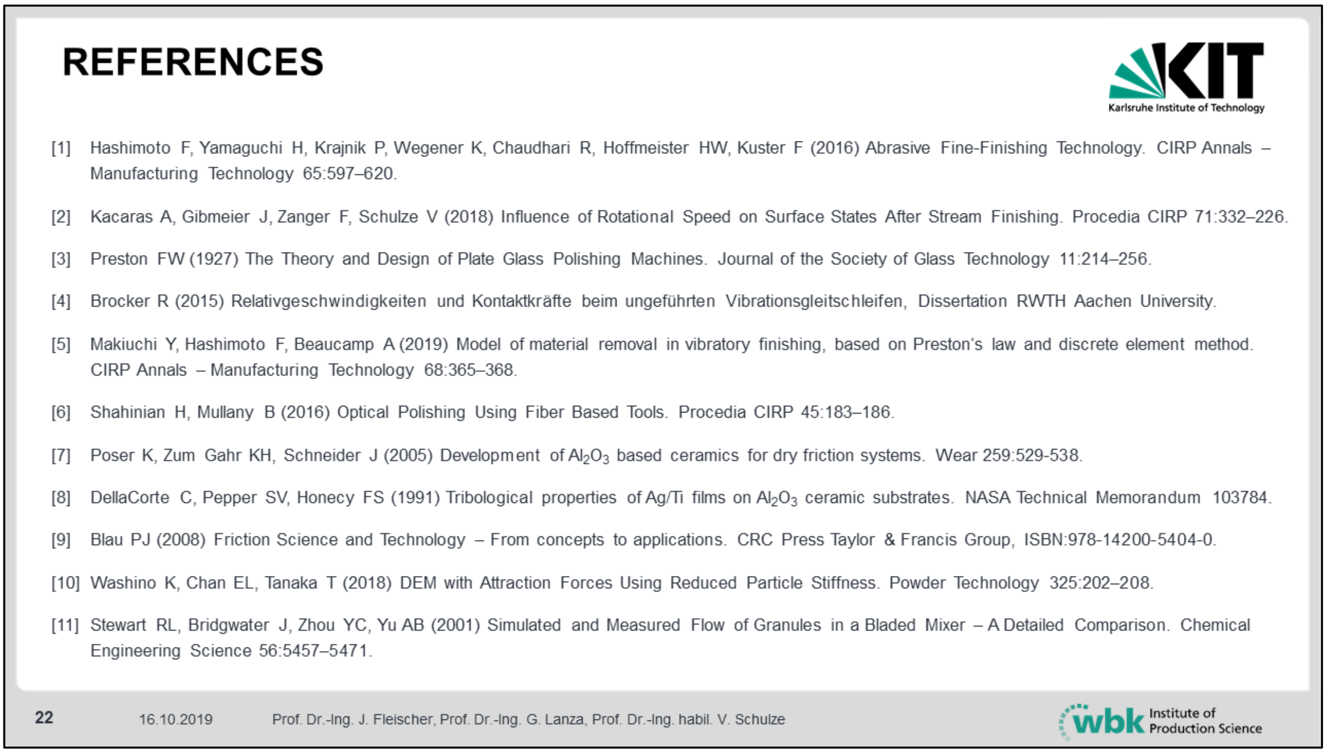

REFERENCES

[1] Hashimoto F, Yamaguchi H, Krajnik P, Wegener K, Chaudhari R, Hoffmeister HW, Kuster F (2016) Abrasive Fine-Finishing Technology. CIRP Annals – Manufacturing Technology 65:597–620.

[2] Kacaras A, Gibmeier J, Zanger F, Schulze V (2018) Influence of Rotational Speed on Surface States After Stream Finishing. Procedia CIRP 71:332–226.

[3] Preston FW (1927) The Theory and Design of Plate Glass Polishing Machines. Journal of the Society of Glass Technology 11:214–256.

[4] Brocker R (2015) Relativgeschwindigkeiten und Kontaktkräfte beim ungeführten Vibrationsgleitschleifen, Dissertation RWTH Aachen University.

[5] Makiuchi Y, Hashimoto F, Beaucamp A (2019) Model of material removal in vibratory finishing, based on Preston's law and discrete element method. CIRP Annals – Manufacturing Technology 68:365–368.

[6] Shahinian H, Mullany B (2016) Optical Polishing Using Fiber Based Tools. Procedia CIRP 45:183–186.

[7] Poser K, Zum Gahr KH, Schneider J (2005) Development of Al_2O_3 based ceramics for dry friction systems. Wear 259:529-538.

[8] DellaCorte C, Pepper SV, Honecy FS (1991) Tribological properties of Ag/Ti films on Al_2O_3 ceramic substrates. NASA Technical Memorandum 103784.

[9] Blau PJ (2008) Friction Science and Technology – From concepts to applications. CRC Press Taylor & Francis Group, ISBN:978-14200-5404-0.

[10] Washino K, Chan EL, Tanaka T (2018) DEM with Attraction Forces Using Reduced Particle Stiffness. Powder Technology 325:202–208.

[11] Stewart RL, Bridgwater J, Zhou YC, Yu AB (2001) Simulated and Measured Flow of Granules in a Bladed Mixer – A Detailed Comparison. Chemical Engineering Science 56:5457–5471.

22 16.10.2019 Prof. Dr.-Ing. J. Fleischer, Prof. Dr.-Ing. G. Lanza, Prof. Dr.-Ing. habil. V. Schulze